UNIVERSITY OF CALIFORNIA, MERCED

The Regulation of Cardiac Nrf2 During an Acute Glucose Challenge and the Impact on Mitochondrial Function During Insulin Resistance and Type II Diabetes Mellitus

A dissertation submitted in partial satisfaction of the requirements

for the degree

Doctor of Philosophy

in

Quantitative and Systems Biology

by

Max Andrew Thorwald

Committee in charge:

Professor Kara E. McCloskey

Professor Frederick W. Wolf

Professor Henry J. Forman

Professor Rudy M. Ortiz, Chair

2018

The Dissertation of Max Andrew Thorwald is approved, and it is acceptable in quality and form for publication on microfilm and electronically.

_____

Kara E. McCloskey PhD

_____

Henry J. Forman PhD

_____

Frederick W. Wolf PhD

_____

Rudy M. Ortiz PhD, Chair

University of California, Merced

2018

Table of Contents

List of Tables

List of Figures

Figure 2. Mean ± SEM values of **A)** Systolic blood pressure starting from 17 weeks until 25 weeks of age, and **B)** plasma angiotensin II levels post glucose challenge in Long Evans Tokushima Otsuka (LETO; n=6), Otsuka Long Evans Tokushima Fatty (OLETF; n=8), OLETF + angiotensin receptor type 1 blocker 8 weeks (ARB; n=8) rats, and OLETF + angiotensin receptor type 1 blocker 4 weeks, then removed (ARBM; n=8) rats.

Figure 3. Mean ± SEM values of **A)** plasma glucose levels, **B)** glucose area under the curve values, **C)** plasma insulin levels, and **D)** insulin under the curve values post glucose challenge in Long Evans Tokushima Otsuka (LETO; n=6), Otsuka Long Evans Tokushima Fatty (OLETF; n=8), OLETF + angiotensin receptor type 1 blocker 8 weeks (ARB; n=8) rats, and OLETF + angiotensin receptor type 1 blocker 4 weeks, then removed (ARBM; n=8) rats. *Significant difference from LETO ($P< 0.05$).

Figure 4. Nrf2 signaling pathway. Mean ± SEM values of **A)** nrf2 transcripts, **B)** cytosolic nrf2 protein, **C)** nuclear nrf2 protein, **D)** acetylated-nrf2 protein, **E)** GSK3β mRNA, **F)** GSK3β protein, **G)** keap1 mRNA, **H)** keap1 protein, **I)** bach1 mRNA, and **J)** c-Myc mRNA values post glucose challenge in Long Evans Tokushima Otsuka (LETO; n=6), Otsuka Long Evans Tokushima Fatty (OLETF; n=8), OLETF + angiotensin receptor type 1 blocker 8 weeks (ARB; n=8) rats, and OLETF + angiotensin receptor type 1 blocker 4 weeks, then removed (ARBM; n=8) rats.

Figure 5. Nrf2 related transcript levels. Mean ± SEM values of **A)** GCLC mRNA, **B)** GCLM mRNA, **C)** G6PD mRNA, and **D)** PGD mRNA values post glucose challenge in Long Evans Tokushima Otsuka (LETO; n=6), Otsuka Long Evans Tokushima Fatty (OLETF; n=8), OLETF + angiotensin receptor type 1 blocker 8 weeks (ARB; n=8) rats, and OLETF + angiotensin receptor type 1 blocker 4 weeks, then removed (ARBM; n=8) rats.

Figure 6. GSH production and cellular redox potential. Mean ± SEM values of **A)** total GSH levels, **B)** GCLM protein, **C)** GCLC protein, **D)** plasma GGT activity **E)** NADP+/NADPH ratio, and **F)** NAD+/NADH ratio values post glucose challenge in Long Evans Tokushima Otsuka (LETO; n=6), Otsuka Long Evans Tokushima Fatty (OLETF; n=8), OLETF + angiotensin receptor type 1 blocker 8 weeks (ARB; n=8) rats, and OLETF + angiotensin receptor type 1 blocker 4 weeks, then removed (ARBM; n=8) rats.

Figure 7. Mitochondrial function and cellular damage. Mean ± SEM values of **A)** aconitase activity, **B)** complex I activity, **C)** complex II activity, **D)** parkin protein levels, and **E)** nitrated protein level values post glucose challenge in Long Evans Tokushima Otsuka (LETO; n=6), Otsuka Long Evans Tokushima Fatty (OLETF; n=8), OLETF + angiotensin receptor type 1 blocker 8 weeks (ARB; n=8) rats, and OLETF + angiotensin receptor type 1 blocker 4 weeks, then removed (ARBM; n=8) rats.

Figure 8. Mitochondrial antioxidant activities. Mean ± SEM values of **A)** superoxide dismutase activity, **B)** catalase activity, **C)** glutathione peroxidase activity, **D)** glutathione reductase activity, **E)** glutathione s-transferase activity values post glucose challenge in Long Evans Tokushima Otsuka (LETO; n=6), Otsuka Long Evans Tokushima Fatty (OLETF; n=8), OLETF + angiotensin receptor type 1 blocker 8 weeks (ARB; n=8) rats,

and OLETF + angiotensin receptor type 1 blocker 4 weeks, then removed (ARBM; n=8) rats.

Figure 9. Cytosolic antioxidant activities. Mean ± SEM values of **A)** superoxide dismutase activity, **B)** catalase activity, **C)** glutathione peroxidase activity, **D)** glutathione reductase activity, **E)** glutathione s-transferase activity values post glucose challenge in Long Evans Tokushima Otsuka (LETO; n=6), Otsuka Long Evans Tokushima Fatty (OLETF; n=8), OLETF + angiotensin receptor type 1 blocker 8 weeks (ARB; n=8) rats, and OLETF + angiotensin receptor type 1 blocker 4 weeks, then removed (ARBM; n=8) rats.

Chapter 3

Figure 1. NF-κB signaling during the progression of T2DM. Mean ± SEM values of **A)** NF-κB mRNA, **B)** cytosolic NF-κB protein, **C)** nuclear NF-κB protein, **D)** acetylated-NF-κB protein, **E)** IκBα mRNA, and **F)** p-IκBα/IκBα ratio in Sprague Dawley's (SD; n=7), pre-diabetic UCD-T2DM (Pre; n=9), 2-week diabetic UCD (2Wk; n=9), 3-month diabetic UCD-T2DM (3Mo; n=13), and 6-month diabetic UCD-T2DM (6Mo; n=9) rats.

Figure 2. Nrf2 signaling during the progression of T2DM. Mean ± SEM values of **A)** Nrf2 mRNA, **B)** cytosolic Nrf2 protein, **C)** nuclear Nrf2 protein, **D)** acetylated-Nrf2 protein, **E)** Keap1 mRNA, **F)** Keap1 protein, **G)** GSK3β mRNA, **H)** GSK3β protein, **I)** C-Myc mRNA, and **J)** Bach1 mRNA in Sprague Dawley's (SD; n=7), pre-diabetic UCD-T2DM (Pre; n=9), 2-week diabetic UCD (2Wk; n=9), 3-month diabetic UCD-T2DM (3Mo; n=13), and 6-month diabetic UCD-T2DM (6Mo; n=9) rats.

Figure 3. Downstream targets of NF-κB activation. Mean ± SEM values of **A)** TNFα mRNA, **B)** TNFα plasma levels, **C)** Nox4 mRNA, **D)** Nox4 protein, and **E)** Nox2 protein in Sprague Dawley's (SD; n=7), pre-diabetic UCD-T2DM (Pre; n=9), 2-week diabetic UCD (2Wk; n=9), 3-month diabetic UCD-T2DM (3Mo; n=13), and 6-month diabetic UCD-T2DM (6Mo; n=9) rats.

Figure 4. Downstream targets of Nrf2 activation. Mean ± SEM values of **A)** HO-1 mRNA, **B)** GCLC mRNA, **C)** GCLC protein, **D)** GCLM mRNA, and **E)** GCLM protein, in Sprague Dawley's (SD; n=7), pre-diabetic UCD-T2DM (Pre; n=9), 2-week diabetic UCD (2Wk; n=9), 3-month diabetic UCD-T2DM (3Mo; n=13), and 6-month diabetic UCD-T2DM (6Mo; n=9) rats. * Significant difference from SD ($P < 0.05$).

Figure 5. Mitochondrial Function during the progression of T2DM. Mean ± SEM values of **A)** aconitase activity, **B)** complex I activity, **C)** complex II activity, **D)** mitochondrial Parkin content, and **E)** mitochondrial 4HNE adducts in Sprague Dawley's (SD; n=7), pre-diabetic UCD-T2DM (Pre; n=9), 2-week diabetic UCD (2Wk; n=9), 3-month diabetic UCD-T2DM (3Mo; n=13), and 6-month diabetic UCD-T2DM (6Mo; n=9) rats.

Acknowledgements

The text of this dissertation in the first chapter is a reprint as it appears in publication. Max Thorwald was supported by the Minority Health and Disparities International Research (MHIRT) and UC Merced (Graduate Dean's Dissertation Fellowship 2018). This research was also funded by a grant (R01-HL091767) awarded from The National Heart, Lung and Blood institute to Dr. Rudy Ortiz.

Several people participated in monitoring the animals and harvesting tissue at the times of dissections at Kagawa Medical University in 2012 and 2015. Thanks to Andrew Lee, Bridget Martinez, Gema Rodriguez, and Marco Rodriguez, and Ruben Rodriguez for their assistance in working with the animals. All animal procedures were approved by the Institutional Animal Care and Use Committee at The University of California, Merced and Kagawa Medical University. Thanks to Jose Arquimides Godoy-Lugo, Pablo Juarez, Andrew Lee, and Ruben Rodriguez for their laboratory assistance. Special thanks to Dr. Henry Forman and Dr. Jose Pablo Vazquez-Medina for your discussions of redox biology and aid with experimental design.

I want to thank my advisors, Dr. Rudy Ortiz and Dr. Henry Forman, for their unequivocal support through this process, for always encouraging me to pursue what I was interested in, and for taking an interest in my future career. Thank you to my committee members Dr. Kara McCloskey and Dr. Frederick Wolf for providing insight and advice on these projects and aiding me in the completion of this process.

I would also like to thank my parents Louise Foggia and Robert Thorwald for providing me with unconditional support and for always encouraging me to do what was right rather than what was easy. Thank you to my friends who have shown me immense support through this process. I thank Luyen Hoang for her patience and her support of all of my goals present and future.

Curriculum Vitae

Education

2013 B.S. Human Biology. University of California Merced, Merced, CA.

2018 PhD. Quantitative Systems Biology. University of California Merced, Merced, CA.

Advisors: Rudy M. Ortiz & Henry J. Forman

Publications

1. Rodriguez R, Lee A, Mathis KW, Broome HJ, **Thorwald M**, Martinez M, Nakano D, Nishiyama A, Ryan M, Rudy M. Ortiz. Angiotensin Receptor and TNF-α Activation Contribute to Glucose Intolerance Independent of Systolic Blood Pressure in OLETF Rats. *Am J Physiol Renal Physiol*. 2018 Jul 11. doi: 10.1152/ajprenal.00156.2018
2. Dhillon J, **Thorwald M**, De La Cruz N, Vu E, Asad Asghar S, Kuse Q, Diaz-Rios K, RM Ortiz. Almond snacking for 8 weeks improved glucose tolerance and postprandial insulin sensitivity compared to an isocaloric graham cracker snack in young adults. Nutrients. *Accepted.*
3. **Thorwald M**, Rodriguez R, Lee A, Martinez B, Peti-Peterdi J, Nakano D, Nishiyama A, Ortiz RM. Angiotensin receptor blockade improves cardiac mitochondrial activity in response to an acute glucose load in obese insulin resistant rats. Redox Biol. 2018 Apr; 14: 371–378.
4. Jacqueline N. Minas, **Max A. Thorwald**, Debra Conte, Jose-Pablo Vázquez-Medina, Akira Nishiyama, and Rudy M. Ortiz. Angiotensin and Mineralocorticoid Receptor Antagonism Attenuates Cardiac Oxidative Stress in Angiotensin II-Infused Rats. *Clin Exp Pharmacol Physiol. 2015 Nov; 42(11): 1178–1188.*
5. Vazquez-Medina JP, I Popovich, **M Thorwald**, JA Viscarra, R Rodriguez, JG Sonanez-Organis, L Lam, J Peti-Peterdi, D Nakano, A Nishiyama, RM Ortiz. Angiotensin receptor mediated oxidative stress is associated with impaired cardiac redox signaling and mitochondrial function in insulin resistant rats. *American Journal of Physiology-Heart and Circulatory Physiology*. 2013. PMID: 23771688
6. Montez P, JP Vazquez-Medina, R Rodriguez, **MA Thorwald**, JA Viscarra, L Lam, J Peti-Peterdi, D Nakano, A Nishiyama, and RM Ortiz. Angiotensin Receptor-Mediated Suppression of Hepatic UCP2 Expression and Aconitase Activity Is Associated with Increased Hepatic Lipid Peroxidation in a Model of Metabolic Syndrome. *Endocrinology.* 153(12): 5746-5759, 2012. PMCID: PMC3512060

Abstract

The Regulation of Cardiac Nrf2 During an Acute Glucose Challenge and the impact on the Mitochondria During Insulin Resistance and Type II Diabetes Mellitus

Max Andrew Thorwald

Doctor of Philosophy

University of California, Merced, 2018

Committee Chair: Dr. Rudy M. Ortiz

During the progression of Type II diabetes hearts are under stress due to increases in oxidant production and contractile force from elevated blood pressure. Pre-diabetic and diabetic individuals undergo periods of hyperglycemia which contribute significantly to oxidant production while elevated blood pressure also contributes to the influx of oxidant production. The renin angiotensin system is responsible for blood pressure homeostasis and becomes chronically elevated during metabolic derangements. Furthermore, chronic low-grade inflammation mediated through NF-κB is present during the disease manifestation which has been reported to be antagonistic of Nrf2, a transcription factor with a wide array of cellular detoxifying genes. The objectives of these projects were to elucidate the impact a hyperglycemic event has on insulin resistant and diabetic hearts, the role of AT1 activation of mitochondrial function and antioxidant capacity, and the changes in NF-kB and Nrf2 signaling as type II diabetes progresses. In the first chapter we demonstrate that insulin resistant hearts experience mitochondrial dysfunction and increases in damage, while blocking the AT1 receptor increases Nrf2 binding to the electrophile response element during an acute glucose challenge. In the second chapter we demonstrate that diabetic hearts increase glutathione content in response to glucose and that antagonism of the AT1 receptor has beneficial impacts on Nrf2 related gene expression. We also demonstrate that non-diabetic animals increase Nrf2 related genes after a glucose bolus indicating that Nrf2 increases in response to glucose. The third chapter examines the relationship between cardiac Nrf2 and NF-κB during the progression of diabetes. Here we demonstrate that nuclear NF-κB content and acetylation increases rapidly as type II diabetes progresses and that nuclear Nrf2 content and acetylation is blunted. This is the first time that acute glucose challenges have been performed in in vivo during both insulin resistant and type II diabetic animals where blockade of the AT1 has been incorporated. Our findings contribute to the understanding of antioxidant defense during hyperglycemic events through the progression of type II diabetes. These studies illustrate the importance of antioxidant defense during even the early stages of insulin resistance and bolster the idea that antioxidant defense is impaired during hyperglycemic events.

Introduction. Regulation of Nrf2 during the progression of Type II diabetes

Type II diabetes mellitus (T2DM) has become a rising epidemic with the CDC stating that more than 29 million people afflicted as of 2015. T2DM starts as an issue processing glucose primarily through defects in insulin signaling known as insulin resistance [1]. Beta cells secrete more insulin to help overcome the impairment in insulin action causing beta cell exhaustion, accompanied by inflammation and eventual apoptosis of beta cells [2,3]. This leads to frank diabetes where insulin is relied upon with every meal. Insulin resistance originates as a disease of the pancreas and develops into a systemic disease. Here, we will primarily focus on the heart as over 70% of individuals with T2DM die of cardiovascular related complications such as stroke or myocardial infarction [4]. Furthermore, insulin resistant and diabetic individuals undergo acute phases of hyperglycemia, burdening their hearts as they have difficulty efficiently processing glucose resulting in increases in oxidant production [5–8]. Antioxidant defense primarily mediated through Nuclear factor (erythroid-derived 2)-like 2 (Nrf2) is generally impaired during the progression of insulin resistance or T2DM which proves problematic for the heart due to its oxidative nature [9,10].

The renin angiotensin-aldosterone system (RAAS) is a cardiorenal network in which blood pressure is regulated to ensure proper filtration within the kidneys [11]. The kidneys play a large role in diabetic complications, as their regulation is very intricate involving many organ systems. RAAS works by secreting angiotensinogen from the liver which is then cleaved by renin secreted by the kidneys and put into circulation [11]. Angiotensinogen is then converted to angiotensin I which is then converted to angiotensin II (Ang II) in the lungs and can be further converted to angiotensin III-VII [11–13]. Angiotensin II is then free to activate the angiotensin II type 1 receptor (AT1) which signals for an increase in blood pressure as well as increases in sodium retention through aldosterone's action [14]. These effects are generally short lived and act as a rheostat as many systems within the body to in order to maintain homeostasis. However, during insulin resistance, AT1 activation increases and remains elevated into T2DM [15]. This chronic elevation in systolic blood pressure leads to signaling events such as NADPH oxidase 2 (Nox2) formation in the heart [16]. Nox2 is a protein most notably known for xenobiotic elimination through macrophages, but also exists in vasculature [16–19]. While its role is not specifically known, it's thought to produce oxidants as secondary messengers to initiate redox signaling cascades. However, during T2DM, Nox2 is increased leading to increases in oxidant production under chronic inappropriate AT1 activation [16]. In order to deal with overactivation of RAAS, a wide variety of angiotensin receptor blockers (ARB) have been administered to patients [13,20]. ARB's have been shown to effectively normalize blood pressure in hypertensive individuals, but more recently have shown other benefits such as improvements in mitochondrial function and antioxidant activities in insulin resistant rats [21–25]. While these benefits may direct or indirect consequences of blood pressure regulation, it's possible they exert other hermetic effects on the insulin resistant or diabetic cell.

Nrf2 is a cap-n-collar leucine zipper transcription factor which regulates over 200 genes responsible for several processes not limited to antioxidant defense, xenobiotic detoxification, and energy homeostasis [26]. Nrf2 is most notable recognized for its involvement in the

upregulation of imperative genes for antioxidant cycling such as glutathione (GSH). Nrf2 is sequestered in the cytosol by kelch-like ECH-associated protein 1(Keap1) which ubiquitinates Nrf2 for degradation with the aid of a Cullen3ligase complex [27]. Keap1 contains several reactive cysteine residues which upon oxidation undergo a conformational shift, releasing Nrf2, allowing to translocate into the nucleus [27]. A non-conical known method of Nrf2 activation occurs when Nrf2 is phosphorylated in the cytosol by protein kinase c (PKC) [28,29], which can also liberate Nrf2 from Keap1, allowing for its entry into the nucleus. Once inside, Nrf2 binds with small maf proteins, f, g and k [30], which help facilitate it's binding to the electrophile response element (EpRE) where Nrf2 initiates transcription. Several other modes of regulation exist. Glycogen synthase kinase 3β (GSK3β) resides in both the cytosol and the nucleus and facilitates degradation of Nrf2 through the β-TrCP complex [31,32]. BTB Domain And CNC Homolog 1 (Bach1) and oncogene c-Myc are also known nuclear repressors of Nrf2 which either block binding Nrf2 to the EpRE or block expression of specific genes [33–35]. Nrf2's role during insulin resistance and diabetes has been shown to be impaired where translocation does not function as it should. The exact misstep in the mechanism has not been elucidated, however some reports have claimed that NF-κB simply outcompetes Nrf2 for transcription machinery [36–39].

GSH is the most abundant non-enzymatic antioxidant in the body [40]. Glutathione is tightly regulated and exists in different pools dependent on the tissue and sub-cellular location within that cell. GSH conjugates itself to many different xenobiotics, initiating their degradation through the use of glutathione s-transferase (GST) or through reduction of hydroperoxides with glutathione peroxidases (GPx) [41]. GSH relies heavily on the use of NADPH as the processes listed above require reduction of GSSG back to GSH using NADPH through glutathione reductase (GR). In order for more NADPH to be generated, Nrf2 up-regulated genes involved in the pentose phosphate pathways: glucose-6 phosphogluconate dehydrogenase (G6PD) and phosphogluconate dehydrogenase (PGD) [26]. GSH's regulation occurs either through import of cysteine from GSH broken down in the bloodstream through the use of gamma glutamyl transpeptidase (GGT) or through manufacture by glutamate cysteine ligase (GCL) [40]. Nrf2 is the transcription factor primarily responsible for the production of subunits glutamate cysteine ligase catalytic (GCLC) and glutamate cysteine ligase modifier (GCLM). GCLM regulates the activity of GCLC and therefore is the rate limiting step in GSH synthesis [42]. Once GCLC creates gamma-glutamylcycteine, glycine is coupled to the product through glutathione synthetase producing GSH. The role of GSH during diabetes is not well characterized but has been thought to be lowered due to the impaired antioxidant capacity seen during the disease progression. This would be detrimental to the heart due to its highly oxidative nature, lowering endogenous antioxidant protection.

The mitochondria has been long implicated as the largest source of oxidant production due to oxygen's role has the final acceptor of electrons in the electron transport chain (ETC) [43–45]. Mitochondrial oxidant production occurs from multiple enzymes, but most notable from aconitase in the citric acid cycle and from the complexes in the ETC. Aconitase contains iron-sulfur clusters which upon oxidation render the enzyme inactive [46–48]. Iron in particular has been proven to undergo changes in transition state. These iron-sulfur clusters can also be sites of oxidant generation through Fenton reactions. The complex proteins have also been implicated as

producers of increased oxidant production primarily during times of high nutrient influxes [7,8]. Since these oxidants are in close vicinity to mitochondrial membranes and mitochondrial enzymes they create damaging products such as nitrotyrosine or 4-HNE adducts with the lipid bilayer. These increases in oxidant production and damage can lead to increases in mitochondrial turnover called mitophagy. In this process, a protein called PINK1 becomes activated in the cytosol and acts as an activator on the outside of the mitochondrial membrane where it causes the opening on channels allowing another protein, parkin to translocate inside [49,50]. This then initiates mitophagy which has been shown to occur more in mitochondria who have accrued damage.

Inflammation has been characterized as a component of T2DM where individuals undergo chronic low-grade inflammation [51]. This is problematic because Nrf2 has been suggested to have an opposing role of NF-κB which potentiates the inflammatory response [39]. It's been suggested that if NF-κB and Nrf2 are both in the nucleus they may compete for molecular machinery needed to initiate their target genes [36–38]. Since inflammation is one of the characteristics of T2DM, the heart may be at risk for cellular detoxification if NF-κB is suppressing antioxidant response. Furthermore, glucose and AT1 activation have been shown to increase TNFα mediated inflammation which would likely dampen Nrf2 activation further [52,53]. TNFα, while a strong inducer of NF-κB is also one of its target genes, perpetuating the inflammatory effect. Furthermore, TNFα has been implicated in increasing activation of Nox proteins further increasing oxidant generation and disrupting insulin's action during periods of hyperglycemia [51].

In summary, T2DM hearts are at an increased risk of oxidant production which is exacerbated by increased activation of the AT1 receptor, mitochondrial dysfunction, impaired Nrf2 nuclear activation and increased chronic inflammation. Frequent bouts of hyperglycemia occur often in diabetics particularly in Western civilization. Blockade of the renin angiotensin system has been shown to be beneficial in treating hypertension by normalizing systolic blood pressure. However, large amounts of evidence has been gathered suggesting that AT1 antagonism improves other impairments accrued during T2DM such as glucose intolerance, insulin insensitivity, and mitochondrial dysfunction [13,21,22,25].

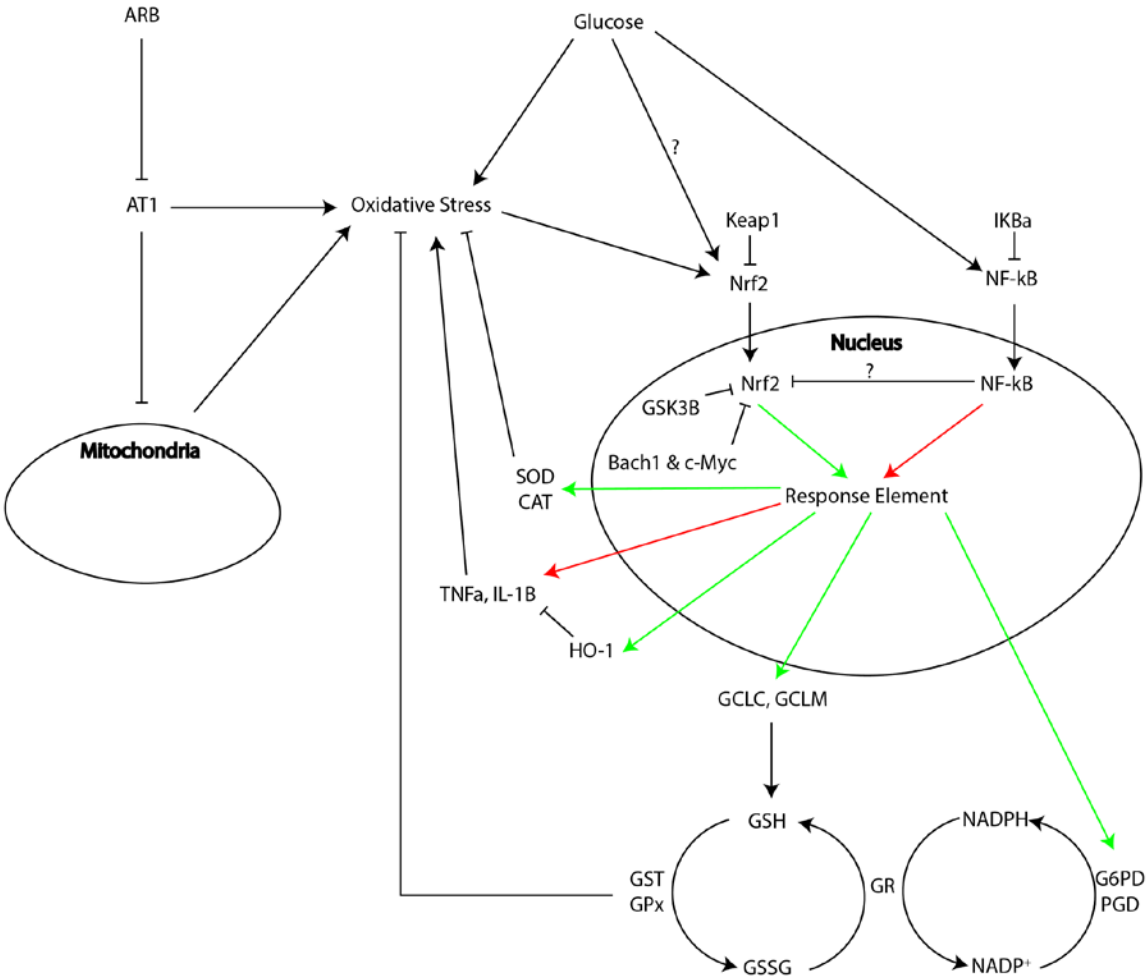

Figure 1. Schematic representation of the connection between AT1 activation, Nrf2, mitochondrial dysfunction, and NF-κB during Type II diabetes in the heart. Green Arrows indicate genes produced by Nrf2. Red arrows indicate genes produced by NF-κB. Abbreviations: ARB = angiotensin receptor blocker, AT1 = angiotensin II type 1 receptor, Bach1= BTB Domain And CNC Homolog 1, CAT = catalase, G6PD = glucose 6-phosphate dehydrogenase, GCLC = glutathione cysteine ligase catalytic subunit, GCLM = glutathione cysteine ligase modifier subunit, GGT = gamma-glutamyl transferase, GPx = glutathione peroxidase, GR = glutathione reductase, GSH = reduced glutathione, GSK3B = glycogen synthase kinase 3 beta, GSSG = oxidized glutathione, GST = glutathione s-transferase, HO-1 = heme oxygenase 1, IKBa = nuclear factor kappa beta inhibitor alpha, IL-1B = interleukin 1 beta, NF-kB = nuclear factor kappa beta, Nrf2 = Nuclear factor erythriod-2- related factor 2, PGD = phosphogluconate dehydrogenase, and SOD = superoxide dismutase, TNFa = tumor necrosis factor alpha.

References

[1] A.B. Bikhazi, S.T. Azar, A.E. Birbari, G.N. El-Zein, G.E. Haddad, R.E. Haddad, K.M. Bitar, Characterization of insulin-resistance: role of receptor alteration in insulin-dependent diabetes mellitus, essential hypertension and cardiac hypertrophy, Eur. J. Pharm. Sci. 11 (2000) 299–306. doi:10.1016/S0928-0987(00)00110-X.

[2] A.E. Butler, J. Janson, S. Bonner-Weir, R. Ritzel, R.A. Rizza, P.C. Butler, Beta-cell deficit and increased beta-cell apoptosis in humans with type 2 diabetes, Diabetes. 52 (2003) 102–110.
[3] M.Y. Donath, D.M. Schumann, M. Faulenbach, H. Ellingsgaard, A. Perren, J.A. Ehses, Islet inflammation in type 2 diabetes: from metabolic stress to therapy, Diabetes Care. 31 Suppl 2 (2008) S161-164. doi:10.2337/dc08-s243.
[4] M. Laakso, Cardiovascular Disease in Type 2 Diabetes From Population to Man to Mechanisms, Diabetes Care. 33 (2010) 442–449. doi:10.2337/dc09-0749.
[5] M. Dunlop, Aldose reductase and the role of the polyol pathway in diabetic nephropathy, Kidney Int. Suppl. 77 (2000) S3-12.
[6] G. Giacchetti, L.A. Sechi, S. Rilli, R.M. Carey, The renin-angiotensin-aldosterone system, glucose metabolism and diabetes, Trends Endocrinol. Metab. TEM. 16 (2005) 120–126. doi:10.1016/j.tem.2005.02.003.
[7] K.R. Pryde, J. Hirst, Superoxide Is Produced by the Reduced Flavin in Mitochondrial Complex I A SINGLE, UNIFIED MECHANISM THAT APPLIES DURING BOTH FORWARD AND REVERSE ELECTRON TRANSFER, J. Biol. Chem. 286 (2011) 18056–18065. doi:10.1074/jbc.M110.186841.
[8] C.L. Quinlan, A.L. Orr, I.V. Perevoshchikova, J.R. Treberg, B.A. Ackrell, M.D. Brand, Mitochondrial Complex II Can Generate Reactive Oxygen Species at High Rates in Both the Forward and Reverse Reactions, J. Biol. Chem. 287 (2012) 27255–27264. doi:10.1074/jbc.M112.374629.
[9] G.V. Velmurugan, N.R. Sundaresan, M.P. Gupta, C. White, Defective Nrf2-dependent redox signalling contributes to microvascular dysfunction in type 2 diabetes, Cardiovasc. Res. 100 (2013) 143–150. doi:10.1093/cvr/cvt125.
[10] A.S. Jiménez-Osorio, A. Picazo, S. González-Reyes, D. Barrera-Oviedo, M.E. Rodríguez-Arellano, J. Pedraza-Chaverri, Nrf2 and Redox Status in Prediabetic and Diabetic Patients, Int. J. Mol. Sci. 15 (2014) 20290–20305. doi:10.3390/ijms151120290.
[11] M.A. Sparks, S.D. Crowley, S.B. Gurley, M. Mirotsou, T.M. Coffman, Classical Renin-Angiotensin System in Kidney Physiology, Compr. Physiol. 4 (2014) 1201–1228. doi:10.1002/cphy.c130040.
[12] S.A. Atlas, The renin-angiotensin aldosterone system: pathophysiological role and pharmacologic inhibition, J. Manag. Care Pharm. JMCP. 13 (2007) 9–20. doi:10.18553/jmcp.2007.13.s8-b.9.
[13] M.A. Zaman, S. Oparil, D.A. Calhoun, Drugs targeting the renin-angiotensin-aldosterone system, Nat. Rev. Drug Discov. 1 (2002) 621–636. doi:10.1038/nrd873.
[14] B.J. He, M.E. Anderson, Aldosterone and cardiovascular disease: the heart of the matter, Trends Endocrinol. Metab. TEM. 24 (2013) 21–30. doi:10.1016/j.tem.2012.09.004.
[15] K. Kawano, T. Hirashima, S. Mori, Y. Saitoh, M. Kurosumi, T. Natori, Spontaneous long-term hyperglycemic rat with diabetic complications. Otsuka Long-Evans Tokushima Fatty (OLETF) strain, Diabetes. 41 (1992) 1422–1428.
[16] K.K. Griendling, C.A. Minieri, J.D. Ollerenshaw, R.W. Alexander, Angiotensin II stimulates NADH and NADPH oxidase activity in cultured vascular smooth muscle cells., Circ. Res. 74 (1994) 1141–1148. doi:10.1161/01.RES.74.6.1141.

[17] A.M. Garrido, K.K. Griendling, NADPH oxidases and angiotensin II receptor signaling, Mol. Cell. Endocrinol. 302 (2009) 148–158. doi:10.1016/j.mce.2008.11.003.
[18] B. Rada, T.L. Leto, Oxidative innate immune defenses by Nox/Duox family NADPH Oxidases, Contrib. Microbiol. 15 (2008) 164–187. doi:10.1159/000136357.
[19] T.L. Leto, M. Geiszt, Role of Nox Family NADPH Oxidases in Host Defense, Antioxid. Redox Signal. 8 (2006) 1549–1561. doi:10.1089/ars.2006.8.1549.
[20] H.M.A. Abraham, C.M. White, W.B. White, The Comparative Efficacy and Safety of the Angiotensin Receptor Blockers in the Management of Hypertension and Other Cardiovascular Diseases, Drug Saf. 38 (2015) 33–54. doi:10.1007/s40264-014-0239-7.
[21] M. Thorwald, R. Rodriguez, A. Lee, B. Martinez, J. Peti-Peterdi, D. Nakano, A. Nishiyama, R.M. Ortiz, Angiotensin receptor blockade improves cardiac mitochondrial activity in response to an acute glucose load in obese insulin resistant rats, Redox Biol. 14 (2018) 371–378. doi:10.1016/j.redox.2017.10.005.
[22] J.P. Vázquez-Medina, I. Popovich, M.A. Thorwald, J.A. Viscarra, R. Rodriguez, J.G. Sonanez-Organis, L. Lam, J. Peti-Peterdi, D. Nakano, A. Nishiyama, R.M. Ortiz, Angiotensin receptor-mediated oxidative stress is associated with impaired cardiac redox signaling and mitochondrial function in insulin-resistant rats, Am. J. Physiol. - Heart Circ. Physiol. 305 (2013) H599–H607. doi:10.1152/ajpheart.00101.2013.
[23] P. Montez, J.P. Vázquez-Medina, R. Rodríguez, M.A. Thorwald, J.A. Viscarra, L. Lam, J. Peti-Peterdi, D. Nakano, A. Nishiyama, R.M. Ortiz, Angiotensin Receptor Blockade Recovers Hepatic UCP2 Expression and Aconitase and SDH Activities and Ameliorates Hepatic Oxidative Damage in Insulin Resistant Rats, Endocrinology. 153 (2012) 5746–5759. doi:10.1210/en.2012-1390.
[24] R. Rodriguez, J.A. Viscarra, J.N. Minas, D. Nakano, A. Nishiyama, R.M. Ortiz, Angiotensin Receptor Blockade Increases Pancreatic Insulin Secretion and Decreases Glucose Intolerance during Glucose Supplementation in a Model of Metabolic Syndrome, Endocrinology. 153 (2012) 1684–1695. doi:10.1210/en.2011-1885.
[25] R. Rodriguez, J.N. Minas, J.P. Vazquez-Medina, D. Nakano, D.G. Parkes, A. Nishiyama, R.M. Ortiz, Chronic AT1 blockade improves glucose homeostasis in obese OLETF rats, J. Endocrinol. 237 (2018) 271–284. doi:10.1530/JOE-17-0678.
[26] J.D. Hayes, A.T. Dinkova-Kostova, The Nrf2 regulatory network provides an interface between redox and intermediary metabolism, Trends Biochem. Sci. 39 (2014) 199–218. doi:10.1016/j.tibs.2014.02.002.
[27] J.W. Kaspar, S.K. Niture, A.K. Jaiswal, Nrf2:INrf2 (Keap1) signaling in oxidative stress, Free Radic. Biol. Med. 47 (2009) 1304–1309. doi:10.1016/j.freeradbiomed.2009.07.035.
[28] D.A. Bloom, A.K. Jaiswal, Phosphorylation of Nrf2 at Ser40 by protein kinase C in response to antioxidants leads to the release of Nrf2 from INrf2, but is not required for Nrf2 stabilization/accumulation in the nucleus and transcriptional activation of

antioxidant response element-mediated NAD(P)H:quinone oxidoreductase-1 gene expression, J. Biol. Chem. 278 (2003) 44675–44682. doi:10.1074/jbc.M307633200.
[29] H.-C. Huang, T. Nguyen, C.B. Pickett, Phosphorylation of Nrf2 at Ser-40 by protein kinase C regulates antioxidant response element-mediated transcription, J. Biol. Chem. 277 (2002) 42769–42774. doi:10.1074/jbc.M206911200.
[30] M.B. Kannan, V. Solovieva, V. Blank, The small MAF transcription factors MAFF, MAFG and MAFK: current knowledge and perspectives, Biochim. Biophys. Acta. 1823 (2012) 1841–1846. doi:10.1016/j.bbamcr.2012.06.012.
[31] P. Rada, A.I. Rojo, S. Chowdhry, M. McMahon, J.D. Hayes, A. Cuadrado, SCF/β-TrCP Promotes Glycogen Synthase Kinase 3-Dependent Degradation of the Nrf2 Transcription Factor in a Keap1-Independent Manner, Mol. Cell. Biol. 31 (2011) 1121–1133. doi:10.1128/MCB.01204-10.
[32] S. Chowdhry, Y. Zhang, M. McMahon, C. Sutherland, A. Cuadrado, J.D. Hayes, Nrf2 is controlled by two distinct β-TrCP recognition motifs in its Neh6 domain, one of which can be modulated by GSK-3 activity, Oncogene. 32 (2013) 3765–3781. doi:10.1038/onc.2012.388.
[33] S. Dhakshinamoorthy, A.K. Jain, D.A. Bloom, A.K. Jaiswal, Bach1 competes with Nrf2 leading to negative regulation of the antioxidant response element (ARE)-mediated NAD(P)H:quinone oxidoreductase 1 gene expression and induction in response to antioxidants, J. Biol. Chem. 280 (2005) 16891–16900. doi:10.1074/jbc.M500166200.
[34] S. Levy, H.J. Forman, C-Myc is a Nrf2-interacting protein that negatively regulates phase II genes through their electrophile responsive elements, IUBMB Life. 62 (2010) 237–246. doi:10.1002/iub.314.
[35] L. Zhou, H. Zhang, K.J.A. Davies, H.J. Forman, Aging-related decline in the induction of Nrf2-regulated antioxidant genes in human bronchial epithelial cells, Redox Biol. 14 (2018) 35–40. doi:10.1016/j.redox.2017.08.014.
[36] H. Chen, Y. Fang, W. Li, R.C. Orlando, N. Shaheen, X.L. Chen, NFkB and Nrf2 in esophageal epithelial barrier function, Tissue Barriers. 1 (2013) e27463. doi:10.4161/tisb.27463.
[37] W. Li, T.O. Khor, C. Xu, G. Shen, W.-S. Jeong, S. Yu, A.-N. Kong, Activation of Nrf2-antioxidant signaling attenuates NF-κB-inflammatory response and elicits apoptosis, Biochem. Pharmacol. 76 (2008) 1485–1489. doi:10.1016/j.bcp.2008.07.017.
[38] J.D. Wardyn, A.H. Ponsford, C.M. Sanderson, Dissecting molecular cross-talk between Nrf2 and NF-κB response pathways, Biochem. Soc. Trans. 43 (2015) 621–626. doi:10.1042/BST20150014.
[39] G.-H. Liu, J. Qu, X. Shen, NF-kappaB/p65 antagonizes Nrf2-ARE pathway by depriving CBP from Nrf2 and facilitating recruitment of HDAC3 to MafK, Biochim. Biophys. Acta. 1783 (2008) 713–727. doi:10.1016/j.bbamcr.2008.01.002.
[40] H. Zhang, H.J. Forman, J. Choi, Gamma-glutamyl transpeptidase in glutathione biosynthesis, Methods Enzymol. 401 (2005) 468–483. doi:10.1016/S0076-6879(05)01028-1.
[41] S.C. Lu, GLUTATHIONE SYNTHESIS, Biochim. Biophys. Acta. 1830 (2013) 3143–3153. doi:10.1016/j.bbagen.2012.09.008.

[42] C.C. Franklin, D.S. Backos, I. Mohar, C.C. White, H.J. Forman, T.J. Kavanagh, Structure, function, and post-translational regulation of the catalytic and modifier subunits of glutamate cysteine ligase, Mol. Aspects Med. 30 (2009) 86–98. doi:10.1016/j.mam.2008.08.009.
[43] H. Van Remmen, A. Richardson, Oxidative damage to mitochondria and aging, Exp. Gerontol. 36 (2001) 957–968.
[44] S.S. Korshunov, V.P. Skulachev, A.A. Starkov, High protonic potential actuates a mechanism of production of reactive oxygen species in mitochondria, FEBS Lett. 416 (1997) 15–18.
[45] P. Newsholme, E.P. Haber, S.M. Hirabara, E.L.O. Rebelato, J. Procopio, D. Morgan, H.C. Oliveira-Emilio, A.R. Carpinelli, R. Curi, Diabetes associated cell stress and dysfunction: role of mitochondrial and non-mitochondrial ROS production and activity, J. Physiol. 583 (2007) 9–24. doi:10.1113/jphysiol.2007.135871.
[46] P.R. Gardner, I. Fridovich, Superoxide sensitivity of the Escherichia coli aconitase, J. Biol. Chem. 266 (1991) 19328–19333.
[47] J. Vásquez-Vivar, B. Kalyanaraman, M.C. Kennedy, Mitochondrial Aconitase Is a Source of Hydroxyl Radical AN ELECTRON SPIN RESONANCE INVESTIGATION, J. Biol. Chem. 275 (2000) 14064–14069. doi:10.1074/jbc.275.19.14064.
[48] M.C. Kennedy, M.H. Emptage, J.L. Dreyer, H. Beinert, The role of iron in the activation-inactivation of aconitase., J. Biol. Chem. 258 (1983) 11098–11105.
[49] A.M. Pickrell, R.J. Youle, The roles of PINK1, parkin, and mitochondrial fidelity in Parkinson's disease, Neuron. 85 (2015) 257–273. doi:10.1016/j.neuron.2014.12.007.
[50] X. Zheng, T. Hunter, Parkin mitochondrial translocation is achieved through a novel catalytic activity coupled mechanism, Cell Res. 23 (2013) 886–897. doi:10.1038/cr.2013.66.
[51] G.S. Hotamisligil, N.S. Shargill, B.M. Spiegelman, Adipose expression of tumor necrosis factor-alpha: direct role in obesity-linked insulin resistance, Science. 259 (1993) 87–91.
[52] Y. Hattori, S. Hattori, N. Sato, K. Kasai, High-glucose-induced nuclear factor kappaB activation in vascular smooth muscle cells, Cardiovasc. Res. 46 (2000) 188–197.
[53] M. Suzuki, J.P. Vázquez-Medina, J.A. Viscarra, J.G. Soñanez-Organis, D.E. Crocker, R.M. Ortiz, Activation of systemic, but not local, renin–angiotensin system is associated with upregulation of TNF-α during prolonged fasting in northern elephant seal pups, J. Exp. Biol. 216 (2013) 3215–3221. doi:10.1242/jeb.085225.

Chapter 1. Angiotensin receptor blockade improves cardiac mitochondrial activity in response to an acute glucose load in obese insulin resistant rats*

Abstract

Hyperglycemia increases the risk of oxidant overproduction in the heart through activation of a multitude of pathways. Oxidation of mitochondrial enzymes may impair their function resulting in accumulation of intermediates and reverse electron transfer, contributing to mitochondrial dysfunction. Furthermore, the renin-angiotensin system (RAS) becomes inappropriately activated during metabolic syndrome, increasing oxidant production. To combat excess oxidant production, the transcription factor, nuclear factor erythriod-2- related factor 2 (Nrf2), induces expression of many antioxidant genes. We hypothesized that angiotensin II receptor type 1 (AT1) blockade improves mitochondrial function in response to an acute glucose load via upregulation of Nrf2. To address this hypothesis, an oral glucose challenge was performed in three groups prior to dissection (n= 5-8 animals/group/time point) of adult male rats: 1) Long Evans Tokushima Otsuka (LETO; lean strain-control), 2) insulin resistant, obese Otsuka Long Evans Tokushima Fatty (OLETF), and 3) OLETF + angiotensin receptor blocker (ARB; 10 mg olmesartan/kg/d x 6 weeks). Hearts were collected at T0, T60, and T120 minutes post-glucose infusion. ARB increased Nrf2 binding 32% compared to OLETF at T60. Total superoxide dismutase (SOD) and catalase (CAT) activities were increased 45% and 66% respectively in ARB treated animals compared to OLETF. Mitochondrial enzyme activities of aconitase, complex I, and complex II increased by 135%, 33% and 66%, respectively in ARB compared to OLETF. These data demonstrate the protective effects of AT1 blockade on mitochondrial function during the manifestation of insulin resistance suggesting that the inappropriate activation of AT1 during insulin resistance may impair Nrf2 translocation and subsequent antioxidant activities and mitochondrial function.

* Thorwald M, Rodriguez R, Lee A, Martinez B, Peti-Peterdi J, Nakano D, Nishiyama N, Ortiz RM. Redox Biol. 2018 Apr;14:371-378

Introduction

Metabolic syndrome is a rising epidemic in the western world and is characterized by the simultaneous presence of hypertension, dyslipidemia, elevated fasting plasma glucose levels, abdominal obesity, and insulin resistance (11). Insulin resistance (IR) is a hallmark for the progression of type II diabetes and causes an incomplete uptake of circulating plasma glucose due to impaired insulin secretion and/or receptor signaling (1). Inappropriate activation of the renin-angiotensin system (RAS) through the angiotensin II type I (AT1) receptor occurs during insulin resistance and has been implicated in contributing to cardiovascular derangements not limited to vasoconstriction, thrombosis, and cardiovascular remodeling (9). Mitochondrial dysfunction contributes to heart disease, and may contribute disproportionately to the accumulation of oxidative damage during diabetes (2, 19). Furthermore, cardiomyocytes contain larger amounts of mitochondria compared to other tissues (27), while the heart as a whole contains a lower antioxidant capacity (33) which increases its susceptibility to mitochondria-derived oxidation. In turn, mitochondrial oxidation increases oxidant generation further burdening antioxidant enzymes, which may lessen their ability to correct the oxidant imbalance (14). Furthermore, mitochondrial and antioxidant dysfunctions may be exacerbated by post-prandial glucose mediated oxidant production in insulin resistant individuals (3, 34). Among the enzymes that are altered by oxidized conditions are aconitase, and in the citric acid cycle, NADH dehydrogenase (complex I), succinate dehydrogenase (complex II), and cytochrome c reductase (complex III) (4, 22).

Cellular detoxification is an important process that helps remove excess oxidants from the cellular environment through endogenous antioxidants or other molecules capable of reduction. One of the key regulators of antioxidant production is the transcription factor, nuclear factor (erythroid-derived 2)-like 2 (Nrf2), which regulates the production of genes responsible for cellular detoxification among other functions (13). Nrf2 controls production of several antioxidants such as catalase (CAT), glutathione peroxidase (GPx), and superoxide dismutase (SOD), which together aid in neutralizing excess oxidant production (35). In order for Nrf2 to translocate to the nucleus, it must dissociate from Kelch-like ECH-associated protein 1 (Keap1) in the cytosol usually by oxidation of Keap1's thiols (7).

The impacts of insulin resistance on the acute changes that glucose imposes on cellular metabolism in the heart are not well described. Evaluation of the heart's mitochondrial response to an acute challenge provides insight on its adaptability and potential to recover from such a constant and frequent insult. This study provides novel information on how cardiac mitochondria respond to a large influx of glucose within two hours post ingestion and the effects of angiotensin receptor blockade (ARB) treatment on the insulin resisitant heart. We hypothesized that AT1 receptor blockade improves cardiac mitochondrial function in response to a glucose load via upregulation of Nrf2.

Methods

All experimental procedures were reviewed and approved by the institutional animal care and use committees of Kagawa Medical University (Kagawa, Japan), and the University of California, Merced.

Animals

Male, age matched, 10-week-old, lean strain-control Long Evans Tokushima Otsuka (LETO; 279 ± 7g) and obese Otsuka Long Evans Tokushima Fatty (OLETF; 359 ± 3g) rats (Japan SLC Inc., Hamamatsu, Japan) were chosen because OLETF rats were previously shown to be insulin resistant at the timeframe chosen for this study (24). LETO and OLETF rats were assigned to the following groups (n = 5-8 animals/group/time point): 1) untreated LETO, 2) untreated OLETF, and 3) OLETF + angiotensin receptor blocker (ARB; 10 mg olmesartan/kg/d x 6 wk). ARB (Daiichi-Sankyo, Tokyo, Japan) was administered by oral gavage suspended in carboxymethyl cellulose (CMC) to conscious rats. Untreated LETO and OLETF rats were gavaged with CMC only. All animals were maintained in groups of three or four animals per cage in a specific pathogen-free facility under controlled temperature (23 C) and humidity (55%) with a 12-h light, 12-h dark cycle. All animals were given free access to water and standard laboratory rat chow (MF; Oriental Yeast Corp., Tokyo, Japan).

Body Mass (BM)

BM was measured on a daily basis to calculate the appropriate amount of ARB to gavage.

Blood Pressure

Systolic blood pressure (SBP) was measured at 16 weeks of age in conscious rats by tail-cuff plethysmography (BP-98A; Softron Co., Tokyo, Japan).

Dissections

After 6 weeks of ARB treatment, animals were randomly assigned to 3 different subgroups within each group. Following the subgroup assignment animals were fasted overnight (12 hours). The first subgroup of animals was taken following the overnight fast (T0), the second and third subgroups of animals were taken 1 hour (T60) and 2 hours (T120), following a glucose load (2 g/kg). This protocol allowed us to ascertain the cellular events that transpired in the heart for 2 hours post-glucose load. At dissection, animals were decapitated, and trunk blood was collected into chilled vials containing 50 mM EDTA and protease inhibitor cocktail (sigma), and kept on ice until they could be centrifuged. Thereafter the hearts were rapidly removed, weighed, and snap frozen in liquid nitrogen. Frozen samples were kept at −80 C until analyzed.

Western Blot Analyses

A 35mg piece of frozen heart was homogenized in 250 µl of Tris-buffered saline containing Triton X-100, SDS, and protease and phosphatase inhibitor cocktail (Sigma). Tissue homogenate

was centrifuged (13,200 × g, 10 min), and the aqueous layer was transferred to a separate tube and stored at −80 C for later analyses. Membrane fractions were obtained for p47phox translocation using a Minute Plasma Membrane Protein Isolation Kit (Invent Biotechnologies, Plymouth, MN). Membrane fractions were cross-probed with Na+/K+ ATPase and GAPDH (Santa Cruz Biotechnology, Santa Cruz, CA) antibodies to ensure fraction purity. Total protein content was measured by the Bradford assay (Bio-Rad Laboratories, Hercules, CA). Equal loading of five to forty micrograms of total protein were resolved in 4–15% Tris-HCl SDS gradient gels. Proteins were electroblotted by 2hour wet transfer onto 0.45-µm polyvinyl difluoride membranes. Membranes were blocked with LI-COR Odyssey blocking buffer and incubated for 16 hours with primary antibodies (diluted 1:200 to 1:2000) against Keap1 (Santa Cruz Biotechnology, Santa Cruz, CA), AMPK, phosphorylated (p) AMPK at Thr172, Nitrotyrosine (Cell Signaling, Danvers, MA), MnSOD, Cu/ZnSOD (Stressgen, Farmingdale, NY), P47phox and 4HNE (Milipore, Bedford, MA). Membranes were washed, incubated with IRDye 800CW and/or 700CW donkey anti-goat, donkey anti-mouse, or donkey anti-rabbit (LI-COR Biosciences, Lincoln, NE), and rewashed. Blots were visualized using an Odyssey system (LI-COR Biosciences) and quantified using ImageJ. In addition to consistently loading the same amount of total protein per well, the densitometry values were further normalized by correcting with the densitometry values of Ponceau S staining (28).

Biochemical Analyses

Nrf2 (Active Motif, Carlsbad, CA), antioxidant enzymes and (CAT, GPx, and SOD) and aconitase (Cayman Chemical, Ann Arbor, MI) activities, and other mitochondrial activities (Succinate Dehydrogenase, and NADH Dehydrogenase) (Abcam, Cambridge, MA) were measured using commercially available kits as previously described (32). Nrf2 binding was measured using this kit to best assess its binding to the electrophile response element (EpRE). Nuclear fractions were prepared for Nrf2 activity using a NE-PER Nuclear cytosolic extraction kit (Thermo Fisher Scientific, Waltham, MA). Nuclear purity was cross probed with GAPDH and H3 (Cell Signaling, Danvers, MA). Mitochondrial fractions were obtained according to the Aconitase assay instructions. Mitochondrial purity was cross probed using GAPDH and VDAC1 (Abcam, Cambridge, MA). All samples were analyzed in duplicate and run in a single assay with intra-assay and percent coefficients of variability of less than 10% for all assays.

Statistics

Means (±SEM) were compared by two-way ANOVA adjusted for repeated measures to group and time interactions. Pairwise comparisons were made for individual time points. Means were considered significantly different at $P < 0.05$ using Fisher's PLSD. Statistical analyses were performed with the SPSS version 24 software (IBM, Armonk, NY).

Results

SBP, BM, Heart Mass, Relative Heart Mass, and Glucose Tolerance Tests

Systolic blood pressure and body mass measurements were taken at the end of the study to observe the status of metabolic syndrome in OLETF rats and to confirm the effectiveness of the ARB. At the end of the study SBP was greater in OLETF compared to LETO by 25% and ARB treatment normalized systolic blood pressure (Table 1). Body mass was greater in OLETF compared to LETO by 37%. ARB treatment had no detectable effect on body mass (Table 1). OLETF heart mass was greater than in LETO by 27%. ARB treatment lowered heart mass in the OLETF rats 13% (Table 1). Relative heart mass was 14% lower in OLETF rats compared to LETO. No detectable differences in relative heart mass was seen with ARB treatment (Table 1). Plasma glucose measurements were taken at dissection to ascertain the degree of insulin intolerance. Fasting plasma glucose was greater in OLETF compared to LETO (106±3 vs. 139±5 mg/dL; $p < 0.001$) and ARB treatment decreased it compared to OLETF (139±5 vs. 120±2 mg/dL; $p < 0.002$). At T60 plasma glucose was two-fold in OLETF compared to LETO (154±3 vs. 321±14 mg/dL; $p < 0.001$) and ARB treatment decreased it compared to OLETF (139±5 vs. 120±2 mg/dL; $p < 0.024$). At T120 plasma glucose was greater in OLETF compared to LETO (116±1 vs. 168±7 mg/dL; $p < 0.001$) and ARB treatment decreased it compared to OLETF (168±7 vs. 141±7 mg/dL; $p < 0.006$).

Table 1: Means ± SE SBP, BM, heart mass and relative heart mass. † Significant difference from LETO ($P < 0.05$). * Significant difference from OLETF ($P < 0.05$).

	LETO	OLETF	OLETF+ARB
Systolic Blood Pressure (mmHg)	114±3	142±2 †	120±2 *
Body Mass (g)	366±15	503±9 †	481±4
Heart Mass (g)	1.03±0.01	1.31±0.02 †	1.14±0.02 †,*
Relative Heart Mass (g/ 100 g BM)	0.28±0.01	0.24±0.01 †	0.23±0.01 †,*

P47phox Translocation

P47phox was measured to assess the contribution of angiotensin II to oxidant production through Nox2 assemblage. Glucose infusion increased the translocation of p47phox 29% over 120 minutes in OLETF rats. ARB treatment decreased P47phox translocation to the membrane by 22% at 120 min (Figure 1).

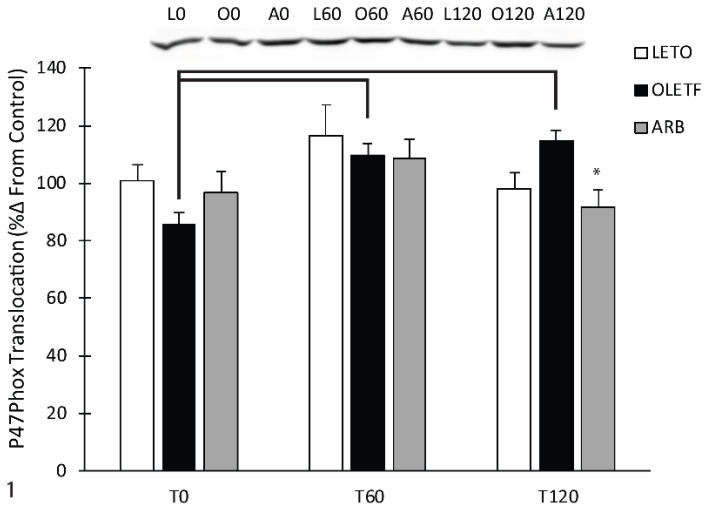

Figure 1: Representative western blot of P47Phox translocation. Means ± SEM values of P47Phox protein expression from Long Evans Tokushima Otsuka (LETO; n=5), Otsuka Long Evans Tokushima Fatty (OLETF; n=8), and OLETF + angiotensin receptor type 1 blocker (ARB; n=8) rats. *Significant difference from OLETF (P< 0.05). Brackets indicate significant differences among respective time points (P<0.05).

Keap1 & Nrf2

Keap1 expression levels decreased 54% in ARB compared to OLETF at T0 (Figure 2A). Glucose had no detectable impact on Keap1 expression in LETO or OLETF over the 2 hr measurement period; however, Keap1 levels were elevated at T120 by 190% compared to baseline with ARB treatment (Figure 2A). Mean nuclear Nrf2 binding to the EpRE increased 21% at T0 in ARB compared to OLETF, while no change was observed between LETO and OLETF rats (Figure 2B). Glucose infusion increased Nrf2 binding 24% in ARB compared to OLETF at T60 (Figure 2B). Nrf2 levels increased 19% in OLETF rats over the two-hour time frame in response to glucose. Glucose increased Nrf2 binding 22% at T60, while binding decreased 39% at T120 in ARB (Figure 2B).

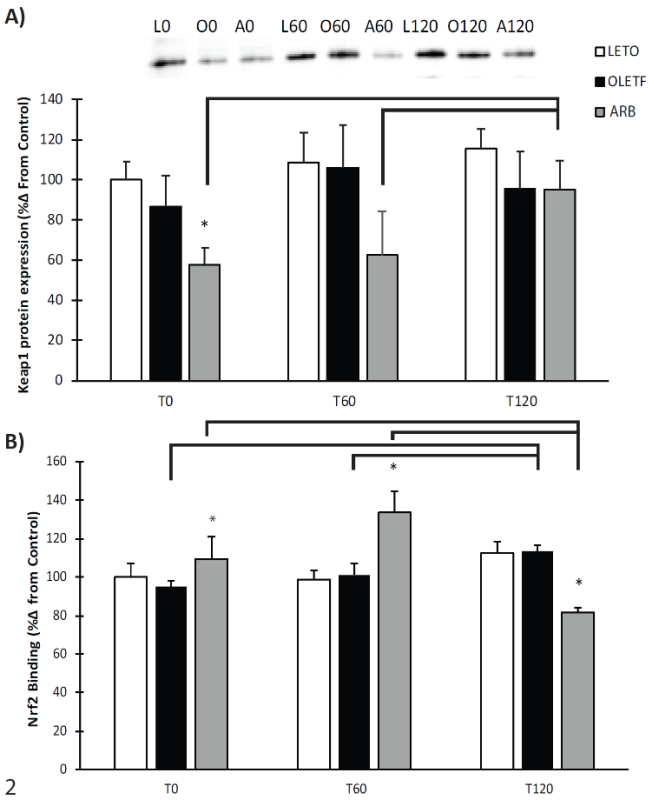

Figure 2: Representative western blot of Kelch-like ECH-associated protein 1 and nuclear Nrf2 activity. Means ± SEM values of Keap1 protein expression and nuclear Nrf2 binding from Long Evans Tokushima Otsuka (LETO; n=5), Otsuka Long Evans Tokushima Fatty (OLETF; n=8), and OLETF + angiotensin receptor type 1 blocker (ARB; n=8) rats. *Significant difference from OLETF ($P< 0.05$). Brackets indicate significant differences among respective time points ($P<0.05$). Keap1 had significant independent group and time interactions. Nrf2 has a significant group time interaction.

Mitochondrial Protein Damage

Indicators of mitochondrial cellular damage were measured to ascertain the amount of damage accumulated in the mitochondria during the progression of insulin resistance, therefore, we measured damage in T0 hearts only. The accumulation of 4-hydroxynonenal (4HNE) adducts increased 30% in OLETF compared to LETO rats (Figure 3A). ARB treated rats had 35% less 4HNE adduct formation compared to OLETF (Figure 3A). The amount of protein nitration increased 28% in OLETF compared to LETO (Figure 3B). ARB treated rats had 14% lower levels of nitrated protein compared to OLETF (Figure 3B).

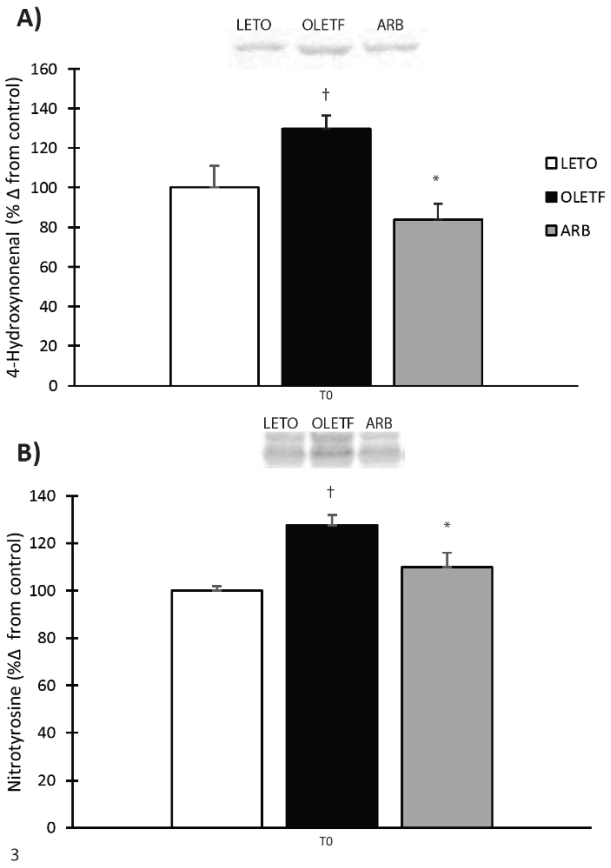

Figure 3: Mitochondrial 4-Hydroxynonenal and Nitrotyrosine measured by western blot. Means ±SEM values of 4HNE protein adducts and nitrated protein from Long Evans Tokushima Otsuka (LETO; n=5), Otsuka Long Evans Tokushima Fatty (OLETF; n=8), and OLETF + angiotensin receptor type 1 blocker (ARB; n=8) rats. †Significant difference from LETO (P<0.05). *Significant difference from OLETF (P< 0.05).

Antioxidant Protein Expression and Activities

Protein expression of MnSOD and Cu/ZnSOD were measured at T0 to differentiate which isoform changed in response to ARB treatment. OLETF MnSOD expression decreased 22% compared to LETO (Figure 4A). ARB treated animals increased Cu/ZnSOD expression 31% and 35% compared to LETO and OLETF rats, respectively (Figure 4B). Enzymatic activity of total SOD, Cat, and GPx were assayed to determine the status of various antioxidant enzymes under Nrf2 control during the early stages of insulin resistance and the impact that AT1 receptor blockade has on activity. Glucose suppressed total SOD activity by 36% one hour after administration in LETO rats (Figure 4C). Glucose infusion increased total SOD 31% at T60, in ARB compared to OLETF (Figure 4C). Total CAT activity decreased 19% in OLETF compared to LETO at T0, and levels increased by 44% in ARB compared to OLETF (Figure 4D). No difference occurred at T60 between LETO or OLETF rats, but ARB treatment caused a 40% increase in total CAT activity. Total CAT activity increased 37% in OLETF compared to LETO

at T120 and was lowered 17% from OLETF in the ARB treatment group (Figure 4D). Glucose infusion suppressed total CAT activity in LETO by 31% at T60 and 23% at T120 (Figure 4D). Glucose also suppressed total CAT activity in OLETF by 20% at T60 but increased activity by 63% at T120 from T60. Glucose suppressed CAT activity in ARB, but to a much lesser extent (25% by T120 from T0) (Figure 4D). Total GPx activity was 15% lower in OLETF rats compared to LETO at T0. Total GPx activity increased 17% at T120 in ARB compared to OLETF (Figure 4E). Total GPx activity decreased 35% in ARB from LETO at T0 (Figure 4E). Glucose infusion suppressed total GPx activity in LETO and OLETF by 41% and 33%, respectively, at T60, with levels remaining similarly suppressed at T120 (Figure 4E).

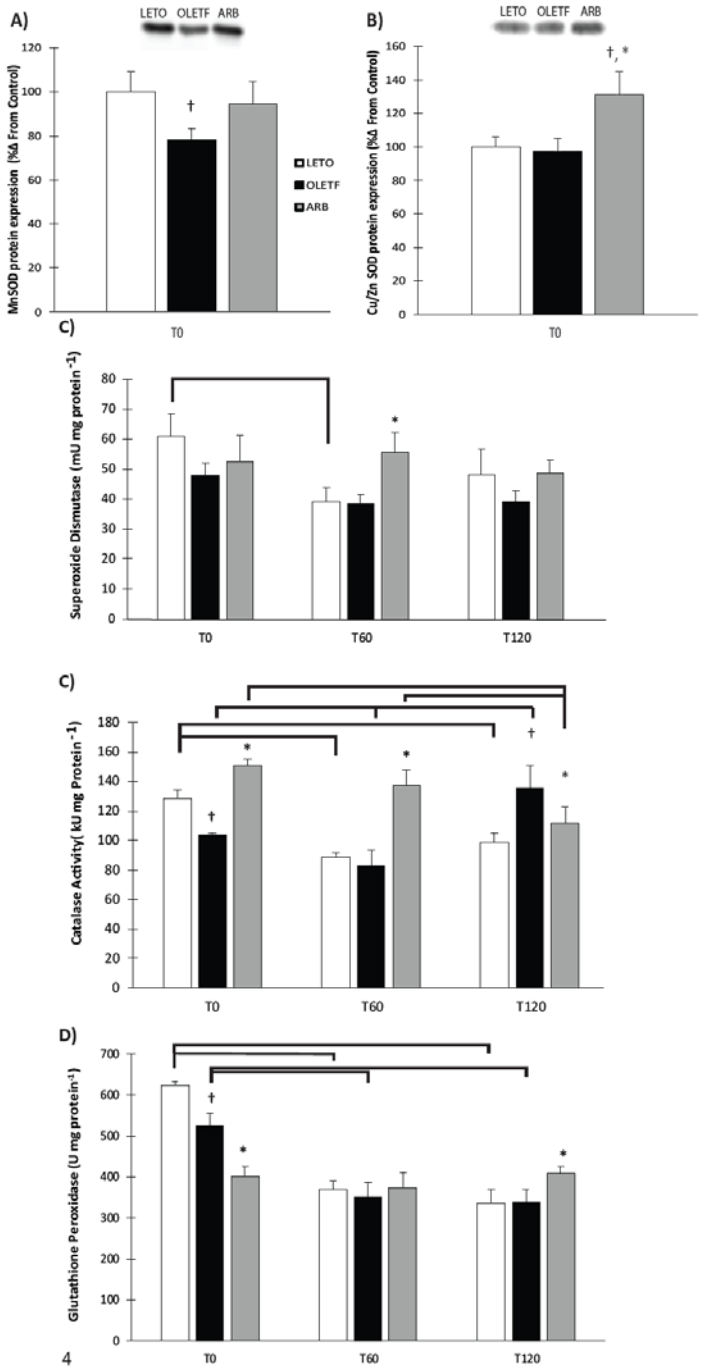

Figure 4: Total cardiac antioxidant protein expression for A) MnSOD B) Cu/ZnSOD and total antioxidant activities for C) superoxide dismutase, D) catalase, and E) glutathione peroxidase. Means ±SEM values of antioxidant activities from Long Evans Tokushima Otsuka (LETO; n=5), Otsuka Long Evans Tokushima Fatty (OLETF; n=8), and OLETF + angiotensin receptor type 1 blocker (ARB; n=8) rats. †Significant difference from LETO ($P<0.05$). *Significant difference from OLETF ($P< 0.05$). Brackets indicate significant differences among respective time points

($P<0.05$). Catalase and glutathione peroxidase had significant group time interactions. A significant time interaction as seen with superoxide dismutase.

Mitochondrial Enzyme Activities & Tissue Succinate Levels

Enzymatic activities of aconitase, complex I, and complex II were measured to assess mitochondrial function in the early stages of insulin resistance. Aconitase activity increased 4-fold over LETO and OLETF at T0 (Figure 5A). At T60 aconitase activity decreased 69% in OLETF compared to LETO. ARB treatment increased levels nearly 6-fold compared to OLETF (Figure 5A). Aconitase activity in OLETF increased 42% compared to LETO at T120. At T60, glucose suppressed aconitase levels in all three groups by 70%, 90% and 87%, respectively, compared to baseline (Figure 5A). By T120 glucose still suppressed aconitase levels by 55%, 14%, and 85%, respectively, compared to baseline (Figure 5A). Complex I exhibited significant group and time interactions independently, but not a group X time interaction. There were no significant differences at baseline; however, ARB treatment increased complex I activity 25% at T60 and 49% at T120 compared to OLETF (Figure 5B). Glucose suppressed complex I activity in both LETO and OLETF rats by 29% and 23%, respectively, at T60 with levels remaining similarly suppressed at T120 (Figure 5B). ARB treatment stabilized complex I activity levels and prevented the suppression at both periods (Figure 5B). Succinate content exhibited a significant group X time interaction with levels increased 22% in OLETF compared to LETO at T0, and ARB was not different from either LETO or OLETF (Figure 5C). Glucose had little effect on succinate content over the two hour period in LETO and OLETF, but did reduce levels in ARB rats by 79% at T120 (Figure 5C). Complex II levels did not differ at baseline; however, glucose suppressed levels in OLETF by 33% at T60 (Figure 5D). ARB treatment increased complex II activity by 76% at T60 (Figure 5D). Complex II levels did not differ between LETO and OLETF at T120, but levels remained 68% higher in ARB compared to OLETF (Figure 5D).

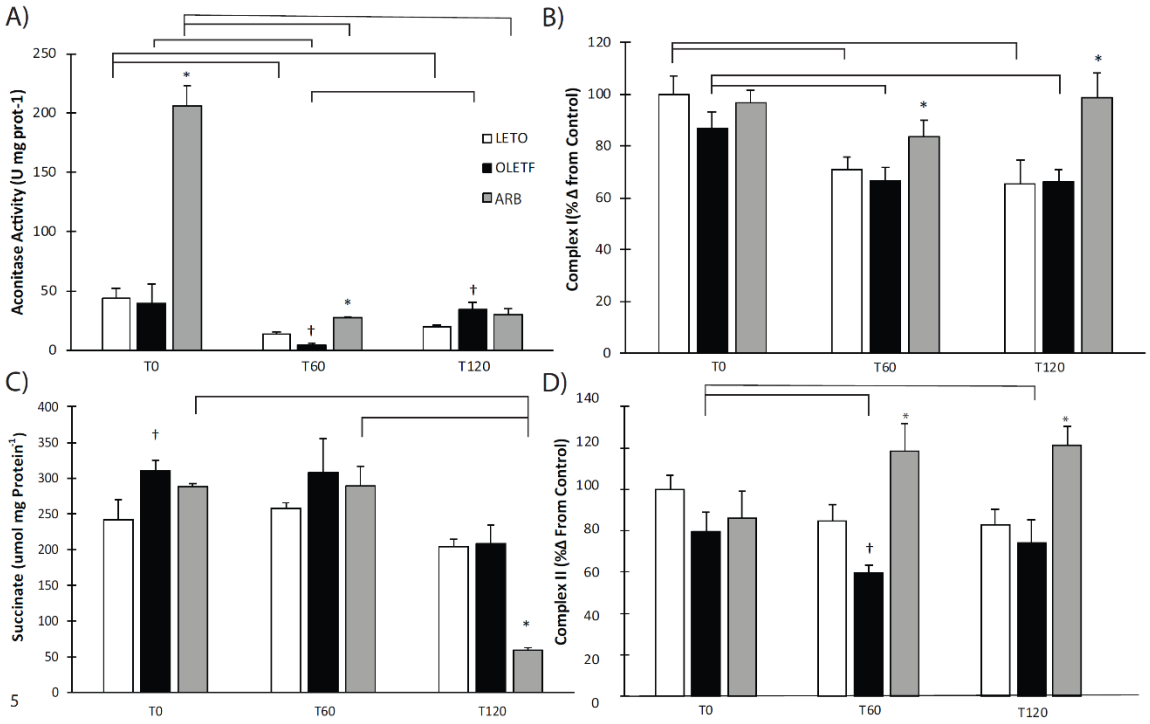

Figure 5: Cardiac mitochondrial activities and succinate tissue content. A) aconitase activity, B) complex I activity, C) tissue succinate content and D) complex II activity. Means ± SEM values of antioxidant activities from Long Evans Tokushima Otsuka (LETO; n=5), Otsuka Long Evans Tokushima Fatty (OLETF; n=8), and OLETF + angiotensin receptor type 1 blocker (ARB; n=8) rats. †Significant difference from LETO (P< 0.05). *Significant difference from OLETF (P< 0.05). Brackets indicate significant differences among respective time points (P<0.05). Aconitase and succinate had a significant group time interaction. Complex I had significant independent group and time interactions. Complex II had a significant group interaction.

AMPK Activation

AMPK expression and phosphorylation (activation) was measured to better assess the impacts of the changes in the mitochondrial enzymes on the energy status of the cell. Activation of AMPK exhibited a significant time interaction with mean AMPK phosphorylation increased two-fold in OLETF at T0 compared to both LETO and ARB (Figure 6). Glucose suppressed AMPK activation by nearly 80% in LETO and nearly 50% in OLETF at T60, while AMPK phosphorylation remained stable in ARB at both T60 and T120 (Figure 6). Activation of AMPK returned to baseline levels in LETO at T120, while levels remained the same in OLETF at T120 (Figure 6).

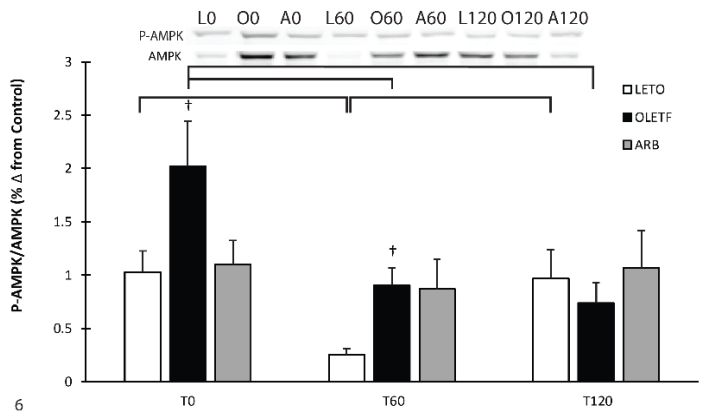

Figure 6: Representative western blot of AMPK and phosphorylated AMPK. Means± SEM values of P-AMPK/AMPK ratio from Long Evans Tokushima Otsuka (LETO; n=5), Otsuka Long Evans Tokushima Fatty (OLETF; n=8), and OLETF + angiotensin receptor type 1 blocker (ARB; n=8) rats. †Significant difference from LETO ($P< 0.05$). Brackets indicate significant differences among respective time points ($P<0.05$). Significant time interaction.

Discussion

Some metabolic syndrome features include impaired insulin signaling (insulin resistance), elevated systolic blood pressure, dyslipidemia, and increased adiposity (6, 18). The factors contributing to the development of insulin resistance are not well known nor is the impact that insulin resistance has on mitochondrial function. However, the inappropriate activation of AT1 has been implicated as a contributor to insulin resistance and mitochondrial dysfunction making it a primary target for study. Furthermore, individuals afflicted with insulin resistance undergo multiple daily bouts of hyperglycemia because of impaired glucose uptake, which may cause cellular damage via oxidant generation from a variety of sources (10). The aim of this study was to determine the impact of ARB treatment on mitochondrial function and antioxidant activity in the hearts of insulin resistant rats. We found that chronic blockade of AT1 protects and stabilizes mitochondrial enzyme activity in the hearts of insulin resistant rats during an acute glucose challenge.

Inappropriate AT1 activation is a known consequence of metabolic syndrome and increases p47phox translocation, which initiates the assemblage of NADPH oxidase (8, 21). Exposure to an acute glucose challenge increased p47phox translocation over two hours in OLETF rats, while translocation was stabilized in LETO and ARB with levels decreasing in both groups at the 2-hour time point. This indicates that insulin resistance is associated with susceptibility of the heart to abrupt increases in glucose-mediated oxidant production through p47phox translocation which has been implicated in diabetic nephropathy and vascular disease (15, 17). The ability of chronic AT1 blockade to ameliorate the glucose-induced increase in translocation suggests that this glucose effect is partially AT1 mediated.

Keap1 facilitates degradation of Nrf2 through a Cul3 ring-box ligase (12) and is susceptible to oxidation on its cysteine switches. Oxidation of Keap1 causes liberation of Nrf2

and subsequent translocation in the nucleus. Nrf2, free of Keap1, can regulate phase II gene transcription by binding to the EpRE (26). Thus, lower Keap1 levels may be indicative of a greater potential of Nrf2 to induced phase II gene transcription, including CAT, GPx, and SOD (29, 35). The lower Keap1 protein levels in ARB after 6 wks of treatment suggests that the ability of ARB to ameliorate the insulin resistance-associated oxidative damage observed in OLETF rats and other models of diabetes and metabolic syndrome may be achieved by decreasing cytosolic Keap1. Glucose infusion tended to increase Keap1 protein levels in LETO and OLETF over the 2 hours; however, levels remained similarly suppressed in ARB at the first measurement hour suggesting that chronic blockade of AT1 protects the heart from any potential glucose-induced increases. Keap1 levels in ARB increased at T120 suggesting that chronic blockade of AT1 desensitizes the heart from abrupt increases in plasma glucose and delays the onset of increasing Keap1. The lack of robust changes in Keap1 protein in LETO and OLETF was associated with similarly unaltered Nrf2 binding to the EpRE. Conversely, the reduced Keap1 levels in ARB were associated with profoundly increased Nrf2 binding, corroborating the impact of AT1 signaling in the Keap1-Nrf2 pathway. Similarly, the increasing trend in Keap1 was associated with decreased Nrf2 binding at T120 in the LETO and OLETF groups. This is important because it demonstrates that Nrf2 activity is not impaired in the early stages of insulin resistance and is not diminished by acutely elevated glucose. This increase in binding is associated with the relative amount of Nrf2 in the nucleus at the respective time points (20).

Aconitase clusters are prone to oxidations and are among the first to undergo a change in transition state during stages of electrophilic stress rendering them inactive (31). Aconitase activity in LETO and OLETF did not differ at T0 suggesting that the early onset of insulin resistance may not be attributed to robust differences in aconitase activity. However, the decreased activity in OLETF at T60 indicates that the early onset of insulin resistance is associated with impaired glucose handling and likely making the mitochondria susceptible to glucose-induced oxidation and damage. The substantial increase in aconitase activity at T0 in ARB is indicative of the protective effects of chronic AT1 blockade and of a strong association between aconitase activity and AT1 signaling. Despite the dramatic reduction in aconitase activity in ARB following the acute glucose challenge, this level remained substantially greater than those in LETO and OLETF, and was equivalent to their levels at baseline (T0) suggesting that chronic blockade of AT1 helped stabilize the response to a glucose insult.

Enzymes within the electron transport chain such as NADH dehydrogenase (complex I) and succinate dehydrogenase (complex II) are also susceptible to oxidative modification, and it has been proposed that electrons under some circumstances may flow backwards liberating a superoxide radical in the process (22, 23). Furthermore, succinate levels may increase in metabolically compromised hearts resulting from complex II no longer processing reactions in a forward direction or from oxidation (5). Furthermore, increased succinate levels in the kidney have been attributed to increasing renin levels, which is the rate limiting enzyme in the formation of Ang II (30). Chronic AT1 blockade helped stabilize these complex-mediated mitochondrial functions by: 1) ameliorating the susceptibility of complex I activity to an acute glucose insult, and 2) increasing complex II activity. While corresponding changes in heart succinate content and complex II activity levels did not align at the measurement time points, the increased activity in

ARB at T60 was followed by substantially reduced succinate content at T120 suggesting that the effects of the changes in enzyme activity on substrate availability are not imparted for at least the following hour in vivo. This suite of mitochondrial measurements demonstrates: 1) the consequences of inappropriate AT1 activation on mitochondrial activity and succinate clearance in the early stages of insulin resistance and metabolic syndrome, and 2) the benefits of chronic AT1 blockade on ameliorating the glucose-induced impairments on mitochondrial function.

SOD, CAT, and GPx are key enzymes responsible for detoxifying oxidants in the cellular environment. Manganese SOD, found in the mitochondria was decreased in OLETF rats while no differences between LETO and OLETF were observed with copper-zinc SOD in the cytosol. However, ARB treatment increased Cu/ZnSOD in the cytosol. In addition to lower expression of MnSOD, increases in mitochondrial 4HNE and NT content was also observed confirming an increase in mitochondrial damage. This suggests that the mitochondria may not be as well equipped to deal with the rapid dismutation of superoxide to hydrogen peroxide during insulin resistance. CAT and GPx are important for removing cellular H2O2, and thus, detoxifying cells with an oxidizing environment, the decreased activity levels of both in insulin resistant OLETF rats at T0 suggests that the oxidative damage associated with insulin resistance and other metabolic disorders is a consequence of an impaired ability to reduce excess free radical production. Conversely, chronic blockade of AT1 prevented the insulin resistance-associated decrease in CAT activity indicating the impact of activated AT1 signaling on catalase activity in the heart during insulin resistance. Interestingly, the greatest reduction in GPx activity was observed in ARB treated rats; however, we propose that the maintenance of catalase activity may be sufficiently efficient at removing excess H2O2 to minimize the need for elevated GPx levels. Thus, the increased catalase activity levels may compensate for the reduced GPx levels. Furthermore, glucose either suppressed or tended to suppress antioxidant enzyme activities in LETO and OLETF, but chronic blockade of AT1 consistently prevented this glucose effect highlighting the detriments of inappropriately activated AT1 on redox balance during the manifestation of insulin resistance, and ultimately, metabolic syndrome. Overall, these effects on antioxidant activities imparted by an acute glucose challenge demonstrate how insulin resistance incapacitates the heart from appropriately responding to oxidant generation caused by hyperglycemia, with the consequences being magnified by frequent bouts of exposure to acutely elevated plasma glucose as with a Western diet.

AMPK is a cellular energy sensor that is phosphorylated in response to high intracellular ADP levels to increase GLUT4 translocation into the cell, and subsequently, increase intracellular glucose levels to provide substrate to replenish ATP levels (25). In metabolic syndrome, sequestration of plasma glucose is impaired through typical insulin signaling, making AMPK-mediated signaling of particular interest as an alternate route for cellular glucose entry (16, 36). The statically and robustly elevated levels of AMPK phosphorylation (activation) in insulin resistant OLETF rats suggests that increased AMPK phosphorylation may try to compensate for the impaired insulin signaling pathway, and further indication of the metabolic derangement associated with OLETF rats. As expected, the acute glucose challenge suppressed AMPK phosphorylation in LETO and OLETF in the first hour; however, ARB treatment stabilized

AMPK activation in response to the glucose, which is a unique observation and demonstrates the importance of stable AT1 signaling in the maintenance of proper glucose regulation.

Hyperglycemia may pose a great deal of stress to the cardiovascular system and these effects may be confounded by preexisting elevations in AT1 activation. In this study, we used an acute glucose challenge in insulin resistant rats with or without ARB treatment to delineate the contributions of AT1 on mitochondrial function in the insulin resistant heart. AT1 activation basally lowered antioxidant activity and increased succinate content. More importantly, AT1 activation when coupled with a surge in glucose levels increased p47phox translocation and decreased mitochondrial enzyme activities including aconitase, complex I, and complex II, which are critical for the proper metabolism of glucose, and when impaired may detrimentally alter substrate metabolism in the insulin resistant heart that may lead to further injury.

References

1. Bikhazi AB, Azar ST, Birbari AE, El-zein GN, Haddad GE, Haddad RE, Bitar KM. Characterization of insulin-resistance : role of receptor alteration in insulin- dependent diabetes mellitus , essential hypertension and cardiac hypertrophy. 11: 299–306, 2000.

2. Boudina S, Abel ED. Diabetic Cardiomyopathy Revisited. Circulation 115: 3213–3223, 2007.

3. Ceriello A, Quagliaro L, Catone B, Pascon R, Piazzola M, Bais B, Marra G, Tonutti L, Taboga C, Motz E. Role of hyperglycemia in nitrotyrosine postprandial generation. Diabetes Care 25: 1439–1443, 2002.

4. Chen Y-R, Zweier JL. Cardiac mitochondria and reactive oxygen species generation. Circ Res 114: 524–537, 2014.

5. Chouchani ET, Pell VR, Gaude E, Aksentijević D, Sundier SY, Robb EL, Logan A, Nadtochiy SM, Ord ENJ, Smith AC, Eyassu F, Shirley R, Hu C-H, Dare AJ, James AM, Rogatti S, Hartley RC, Eaton S, Costa ASH, Brookes PS, Davidson SM, Duchen MR, Saeb-Parsy K, Shattock MJ, Robinson AJ, Work LM, Frezza C, Krieg T, Murphy MP. Ischaemic accumulation of succinate controls reperfusion injury through mitochondrial ROS. Nature 515: 431–435, 2014.

6. DeFina LF, Vega GL, Leonard D, Grundy SM. Fasting glucose, obesity, and metabolic syndrome as predictors of type 2 diabetes: the Cooper Center Longitudinal Study. J Investig Med Off Publ Am Fed Clin Res 60: 1164–1168, 2012.

7. Fourquet S, Guerois R, Biard D, Toledano MB. Activation of NRF2 by Nitrosative Agents and H2O2 Involves KEAP1 Disulfide Formation. J Biol Chem 285: 8463–8471, 2010.

8. Garrido AM, Griendling KK. NADPH oxidases and angiotensin II receptor signaling. Mol Cell Endocrinol 302: 148–158, 2009.

9. Giacchetti G, Sechi LA, Rilli S, Carey RM. The renin-angiotensin-aldosterone system, glucose metabolism and diabetes. Trends Endocrinol Metab TEM 16: 120–126, 2005.

10. Giacco F, Brownlee M. Oxidative stress and diabetic complications. Circ Res 107: 1058–1070, 2010.

11. Grundy SM, Cleeman JI, Daniels SR, Donato KA, Eckel RH, Franklin BA, Gordon DJ, Krauss RM, Savage PJ, Smith SC, Spertus JA, Costa F. Diagnosis and Management of the Metabolic Syndrome. Circulation 112: 2735–2752, 2005.

12. Itoh K, Ye P, Matsumiya T, Tanji K, Ozaki T. Emerging functional cross-talk between the Keap1-Nrf2 system and mitochondria. J Clin Biochem Nutr 56: 91–97, 2015.

13. Kaspar JW, Niture SK, Jaiswal AK. Nrf2:INrf2 (Keap1) signaling in oxidative stress. Free Radic Biol Med 47: 1304–1309, 2009.

14. Kim J, Wei Y, Sowers JR. Role of Mitochondrial Dysfunction in Insulin Resistance. Circ Res 102: 401–414, 2008.

15. Kitada M, Koya D, Sugimoto T, Isono M, Araki S -i., Kashiwagi A, Haneda M. Translocation of Glomerular p47phox and p67phox by Protein Kinase C- Activation Is Required for Oxidative Stress in Diabetic Nephropathy. Diabetes 52: 2603–2614, 2003.

16. Kukidome D, Nishikawa T, Sonoda K, Imoto K, Fujisawa K, Yano M, Motoshima H, Taguchi T, Matsumura T, Araki E. Activation of AMP-activated protein kinase reduces hyperglycemia-induced mitochondrial reactive oxygen species production and promotes mitochondrial biogenesis in human umbilical vein endothelial cells. Diabetes 55: 120–127, 2006.

17. Landmesser U, Cai H, Dikalov S, McCann L, Hwang J, Jo H, Holland SM, Harrison DG. Role of p47phox in Vascular Oxidative Stress and Hypertension Caused by Angiotensin II. Hypertension 40: 511–515, 2002.

18. Lehnen AM, Rodrigues B, Irigoyen MC, De Angelis K, Schaan BD. Cardiovascular Changes in Animal Models of Metabolic Syndrome. J Diabetes Res 2013, 2013.

19. Lorenzi R, Andrades ME, Bortolin RC, Nagai R, Dal-Pizzol F, Moreira JCF. Glycolaldehyde induces oxidative stress in the heart: a clue to diabetic cardiomyopathy? Cardiovasc Toxicol 10: 244–249, 2010.

20. Nguyen T, Sherratt PJ, Pickett CB. Regulatory mechanisms controlling gene expression mediated by the antioxidant response element. Annu Rev Pharmacol Toxicol 43: 233–260, 2003.

21. Papparella I, Ceolotto G, Lenzini L, Mazzoni M, Franco L, Sartori M, Ciccariello L, Semplicini A. Angiotensin II-induced over-activation of p47phox in fibroblasts from hypertensives: which role in the enhanced ERK1/2 responsiveness to angiotensin II? J Hypertens 23: 793–800, 2005.

22. Pryde KR, Hirst J. Superoxide Is Produced by the Reduced Flavin in Mitochondrial Complex I A SINGLE, UNIFIED MECHANISM THAT APPLIES DURING BOTH FORWARD AND REVERSE ELECTRON TRANSFER. J Biol Chem 286: 18056–18065, 2011.

23. Quinlan CL, Orr AL, Perevoshchikova IV, Treberg JR, Ackrell BA, Brand MD. Mitochondrial Complex II Can Generate Reactive Oxygen Species at High Rates in Both the Forward and Reverse Reactions. J Biol Chem 287: 27255–27264, 2012.

24. Rodriguez R, Viscarra JA, Minas JN, Nakano D, Nishiyama A, Ortiz RM. Angiotensin receptor blockade increases pancreatic insulin secretion and decreases glucose intolerance during glucose supplementation in a model of metabolic syndrome. Endocrinology 153: 1684–1695, 2012.

25. Russell RR, Bergeron R, Shulman GI, Young LH. Translocation of myocardial GLUT-4 and increased glucose uptake through activation of AMPK by AICAR. Am J Physiol - Heart Circ Physiol 277: H643–H649, 1999.

26. Stefanson AL, Bakovic M. Dietary regulation of Keap1/Nrf2/ARE pathway: focus on plant-derived compounds and trace minerals. Nutrients 6: 3777–3801, 2014.

27. Strom J, Xu B, Tian X, Chen QM. Nrf2 protects mitochondrial decay by oxidative stress. FASEB J Off Publ Fed Am Soc Exp Biol 30: 66–80, 2016.

28. Thacker JS, Yeung DH, Staines WR, Mielke JG. Total protein or high-abundance protein: Which offers the best loading control for Western blotting? Anal Biochem 496: 76–78, 2016.

29. Thimmulappa RK, Mai KH, Srisuma S, Kensler TW, Yamamoto M, Biswal S. Identification of Nrf2-regulated genes induced by the chemopreventive agent sulforaphane by oligonucleotide microarray. Cancer Res 62: 5196–5203, 2002.

30. Toma I, Kang JJ, Sipos A, Vargas S, Bansal E, Hanner F, Meer E, Peti-Peterdi J. Succinate receptor GPR91 provides a direct link between high glucose levels and renin release in murine and rabbit kidney. J Clin Invest 118: 2526–2534, 2008.

31. Vásquez-Vivar J, Kalyanaraman B, Kennedy MC. Mitochondrial Aconitase Is a Source of Hydroxyl Radical AN ELECTRON SPIN RESONANCE INVESTIGATION. J Biol Chem 275: 14064–14069, 2000.

32. Vázquez-Medina JP, Popovich I, Thorwald MA, Viscarra JA, Rodriguez R, Sonanez-Organis JG, Lam L, Peti-Peterdi J, Nakano D, Nishiyama A, Ortiz RM. Angiotensin receptor-mediated oxidative stress is associated with impaired cardiac redox signaling and mitochondrial function in insulin-resistant rats. Am J Physiol - Heart Circ Physiol 305: H599–H607, 2013.

33. Whaley-Connell A, Govindarajan G, Habibi J, Hayden MR, Cooper SA, Wei Y, Ma L, Qazi M, Link D, Karuparthi PR, Stump C, Ferrario C, Sowers JR. Angiotensin II-mediated

oxidative stress promotes myocardial tissue remodeling in the transgenic (mRen2) 27 Ren2 rat. Am J Physiol - Endocrinol Metab 293: E355–E363, 2007.

34. Wright E, Scism-Bacon J, Glass L. Oxidative stress in type 2 diabetes: the role of fasting and postprandial glycaemia. Int J Clin Pract 60: 308–314, 2006.

35. Zhu H, Itoh K, Yamamoto M, Zweier JL, Li Y. Role of Nrf2 signaling in regulation of antioxidants and phase 2 enzymes in cardiac fibroblasts: protection against reactive oxygen and nitrogen species-induced cell injury. FEBS Lett 579: 3029–3036, 2005.

36. Zou M-H, Wu Y. AMP-ACTIVATED PROTEIN KINASE ACTIVATION AS A STRATEGY FOR PROTECTING VASCULAR ENDOTHELIAL FUNCTION. Clin Exp Pharmacol Physiol 35: 535–545, 2008.

Chapter 2. Cardiac Glutathione Levels Increase in Response to Glucose in Diabetic Rats

Abstract

Diabetic hearts are susceptible to damage from inappropriate activation of the renin angiotensin system (RAS) and hyperglycemic events both of which contribute to increased oxidant production. Inappropriately elevated oxidants impair mitochondrial enzyme function, further contributing to metabolic derangement. Nuclear factor erythriod-2-related factor 2 (Nrf2) induces antioxidant genes including those for glutathione (GSH) synthesis following translocation to the nucleus. We hypothesized that an acute elevation in plasma glucose facilitates Nrf2 nuclear translocation and subsequent expression of Nrf2-associated genes. We used four groups (n = 6-8/group) of 25-week-old rats: 1) LETO (lean strain-control), 2) type II diabetic OLETF, 3) OLETF + angiotensin receptor blocker (ARB; 10 mg olmesartan/kg/d x 8 wks), and 4) ARBM (4 weeks on ARB, 4 weeks off) to study the effects of acutely elevated glucose on cardiac mitochondrial function and Nrf2 activity in the diabetic heart. Animals were gavaged with a glucose bolus (2g/kg) and groups were dissected at T0, T180, and T360 minutes. LETO GSH levels remained stable, while levels increased 125% in OLETF by T360. ARB treatment had no effect over the measurement period. Glutathione cysteine ligase regulatory (GCLM) subunit protein expression increased 78% in OLETF compared to LETO at T180, while ARB treatment lowered expression by 30% despite the elevations in GSH levels. Complex I activity was lowered 32% in OLETF compared to LETO at T0, while ARB treatment had no effect. These data suggest that ARB treatment improves Nrf2-realted gene expression. However, GSH levels increase in diabetic hearts independent of AT1 signaling and mitochondrial function showed no improvement with AT1 antagonism suggesting ARB treatment isn't as beneficial once type II diabetes has manifested.

Introduction

Cardiovascular complications are the most common causes of mortality in type II diabetic (T2DM) patients implicating the diabetic heart as a risk factor [1]. The angiotensin II type 1 (AT1) receptor is inappropriately activated during T2DM contributing to the commonly associated hypertension and increased oxidant production [2]. Furthermore, it is known that hyperglycemia increases oxidant production through elevation in advanced glycation end products and through the polyol pathway [3,4]. Mitochondrial dysfunction occurs during insulin resistance and remains during T2DM reducing the efficiency of energy utilization and increasing oxidant production from aconitase oxidation or improper electron transfer from complex I to II and from II to I [5–7] . Glutathione (GSH), the most abundant non-enzymatic antioxidant in the body, protects the cell from oxidative injury and from xenobiotics. The GSH cycle can tag xenobiotics for degradation through glutathione s-transferase (GST), detoxify hydrogen peroxide through glutathione peroxidase (GPx), and reduce two oxidized GSH molecules (GSSG) through glutathione reductase (GR). GSH's production is regulated by glutamate cysteine ligase which has two subunits, glutamyl cysteine ligase catalytic (GCLC) and modifier (GCLM), which are primarily regulated by transcription Nrf2. Nrf2 is retained in the cytosol through an interaction with Kelch-like ECH-associated protein 1 (Keap1). Oxidation of cysteines on Keap1 frees Nrf2 from Keap1, allowing Nrf2 to translocate into the nucleus where it interacts with small maf proteins and the electrophile response element (EpRE) to initiate transcription of antioxidant genes [8,9]. Transcription of antioxidant proteins mitigates excessive oxidant production through replenishment of NADPH though upregulation of pentose phosphate pathway enzymes [10]. During T2DM, Nrf2's translocation to the nucleus is impaired [11,12], which may contribute to impaired regulation of antioxidants.

Angiotensin receptor blockers (ARB) are prevalent for treatment of hypertension and can decrease p47phox translocation, which reduces the assemblage of NADPH oxidase 2 (Nox2) and superoxide generation [13]. While chronic ARB treatment during insulin resistant conditions improves cardiac mitochondrial function, increases Nrf2 nuclear presence, and subsequent antioxidant activity during an acute glucose challenge, the benefits during a more, frank T2DM condition are not defined. Additionally, the significance of compliance and the cell memory or legacy effect with respect to AT1 signaling during this later stage of impaired insulin signaling has not been examined [14,15]. We hypothesized that an acute elevation in glucose impairs Nrf2-realted gene expression in diabetic hearts, while AT1 antagonism would aid in Nrf2-mediated antioxidant production and energy replenishment (**Figure 1**).

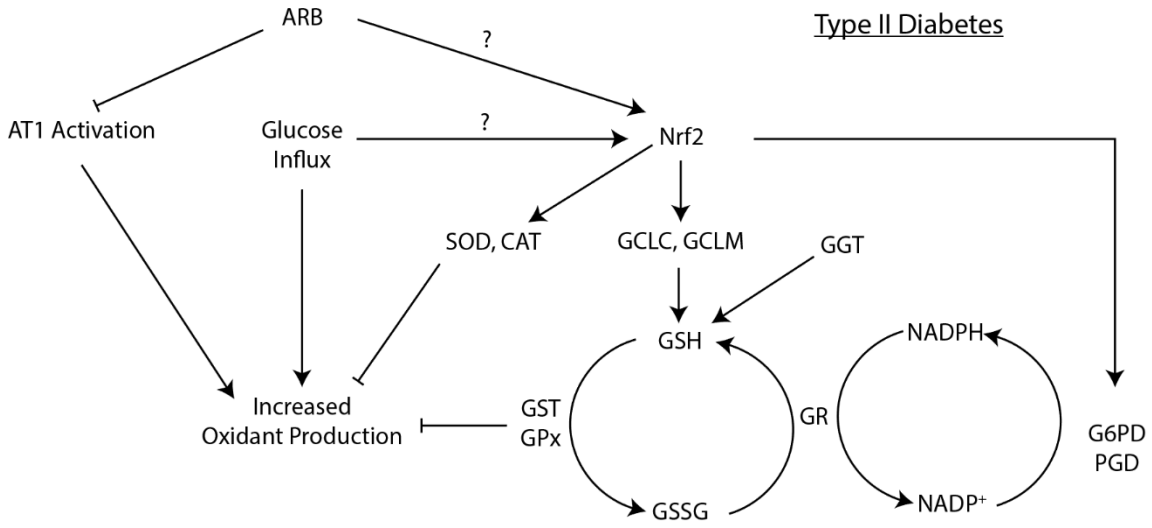

Figure 1: Schematic representation of the proposed connection between the role of Nrf2 mediated antioxidants, oxidant generation from glucose, and inappropriate AT1 activation during Type II diabetes. Abbreviations: ARB = angiotensin receptor blocker, AT1 = angiotensin II type 1 receptor, CAT = catalase, G6PD = glucose 6-phosphate dehydrogenase, GCLC = glutathione cysteine ligase catalytic subunit, GCLM = glutathione cysteine ligase modifier subunit, GGT = gamma-glutamyl transferase, GPx = glutathione peroxidase, GR = glutathione reductase, GSH = reduced glutathione, GSSG = oxidized glutathione, GST = glutathione s-transferase, Nrf2 = Nuclear factor erythriod-2- related factor 2, PGD = phosphogluconate dehydrogenase, and SOD = superoxide dismutase.

Methods

All experimental procedures were reviewed and approved by the institutional animal care and use committees of Kagawa Medical University (Kagawa, Japan), and the University of California, Merced.

Animals

Male, age matched, 17-week-old, lean strain-control Long Evans Tokushima Otsuka (LETO; 428 ± 8g) and obese Otsuka Long Evans Tokushima Fatty (OLETF; 536 ± 6g) rats (Japan SLC Inc., Hamamatsu, Japan) were chosen because OLETF rats have been previously shown to develop insulin resistance and hyperglycemia by 17 weeks of age and frank, T2DM by 24 weeks of age [2]. LETO and OLETF rats were assigned to the following groups (n = 6-8 animals/group/time point): 1) untreated LETO, 2) untreated OLETF, and 3) OLETF + angiotensin receptor blocker (ARB; 10 mg olmesartan/kg/d x 8 wk), and 4) OLETF ± ARB (10 mg olmesartan/kg/d x 4 wks then removed until dissection). This ARB removal group allowed us to assess the impacts of compliance and potential legacy effects [14,15] with respect to AT1 signaling, which has not be studied under T2DM conditions. ARB (Daiichi-Sankyo, Tokyo, Japan) was administered by oral gavage suspended in carboxymethyl cellulose (CMC) to conscious rats [16]. Untreated LETO and

OLETF rats were gavaged with CMC only. All animals were maintained in groups of two to three animals per cage in a specific pathogen-free facility under controlled temperature (23 C) and humidity (55%) with a 12-h light, 12-h dark cycle. All animals were given free access to water and standard laboratory rat chow (MF; Oriental Yeast Corp., Tokyo, Japan).

Body Mass (BM) and Food Consumption

BM and food consumption were measured every other day starting at week 17 through the end of the study to help confirm the diet-induced obesity phenotype typical of the model. BM was also used to determine the appropriate dosage of ARB for treated animals (10mg/kg/d) [16–19]. Food intake was estimated as the average per cage.

Blood Pressure

Systolic blood pressure (SBP) was measured weekly, starting at week 17 until the end of the study (25 weeks) in conscious rats by tail-cuff plethysmography (BP-98A; Softron Co., Tokyo, Japan) to confirm the inappropriate elevation in RAS, which is associated with this model [16–20].

Glucose Tolerance Tests

One week prior to dissections (24 weeks), rats were fasted overnight for 12 hours and gavaged with glucose (2g/kg) to assess the degree of glucose intolerance. Blood was collected for plasma glucose and insulin as previously described [18]. We subsequently calculated area under the curves for glucose and insulin helped confirm the diabetic status of the animals.

Dissections

Animals were dissected at 25 weeks of age because OLETF rats have been shown to be diabetic by 24 weeks [2,21]. Food was removed from the cages at 12 hours before dissection. Cages were staggered to ensure that all rats were fasted for 12 hours ± 15 minutes. Dissections were performed at baseline (T0), and 3 (T180) and 6 hours post-glucose (T360). Oral glucose challenges were also staggered to ensure punctuality for the respected dissection times. Animals were decapitated and trunk blood was collected into chilled vials containing 50 mM EDTA and protease inhibitor cocktail (Sigma, St. Louis, MO) and kept on ice until tubes were centrifuged. Hearts were perfused with saline and rapidly removed, weighed, and snap frozen in liquid nitrogen. The remaining ventricle and plasma were kept at −80 C until analyzed.

GSH Measurements

200mg of heart tissue from the apex of the heart was quickly homogenized in 0.6% sulfosalicylic acid at the time of dissection for deproteination [22]. Samples were then extracted and GSH was measured by electrochemical detection using a Eicom HPLC ECD-300 (Eicom, Kyoto, Japan) as previously described [23].

Western Blot Analyses

A 15-25 mg piece of frozen heart was homogenized in 150uL of sucrose buffer for extraction of mitochondrial, nuclear, and cytosolic fractions [24]. Total protein content of the fractions was measured by the Bradford assay (Bio-Rad Laboratories, Hercules, CA). Five to thirty micrograms of total protein were resolved in 4–15% Tris-HCl SDS gradient gels. Proteins were electroblotted using the Bio-Rad wet transfer onto 0.45-μm polyvinyl difluoride membranes. Membranes were blocked with LI-COR Odyssey blocking buffer and incubated for 16 hours with primary antibodies (diluted 1:100 to 1:4000) against GCLC, GCLM (provided by Dr. Forman), acetylated-Nrf2 (Elabscience, Houston, Tx), and Keap1, Nrf2, GSK3B, NT, Parkin (Santa Cruz Biotechnology, Santa Cruz, CA). Membranes were washed, incubated with IRDye 800CW and/or 700CW donkey anti-goat, donkey anti-mouse, or donkey anti-rabbit (LI-COR Biosciences, Lincoln, NE), and rewashed. Blots were visualized using an Odyssey system (LI-COR Biosciences) and quantified using ImageJ. Nuclear and cytosolic extractions were performed and tested for purity against H3 and GAPDH in both fractions [24]. Mitochondrial extractions were also tested for purity with VDAC1 and GAPDH. In addition to consistently loading the same amount of total protein per well, the densitometry values were further normalized by correcting with the densitometry values by Ponceau S staining [25].

Real-time quantitative PCR analyses

Total RNA was obtained using TRIzol reagent (Invitrogen, Carlsbad, CA). Genomic DNA was degraded on the samples using DNase I enzyme (Roche, Indianapolis, IN). Complementary DNA was reverse transcribed from gDNA-free RNA using the High-Capacity cDNA Reverse Transcription Kit (Applied Biosystems, Foster City, CA) using oligio-dT. Real-time PCR reactions were performed in duplicates, using an equivalent to 100ng of RNA per reaction, using specific primers for Keap1, GSK3B, Nrf2, Bach1, c-Myc, G6PD, PGD, GCLM, GCLC, and normalized with B2M expression. Primer sequences used for qPCR analyses are shown in **Table 2**.

Primer Name	Nucleotide sequence (5’-3’)
Keap1-F	ATGTGATGAACGGGGCAGTC
Keap1-R	AGAACTCCTCCTCCCCGAAG
Gsk3b-F	CTGGCCACCATCCTTATCCC
Gsk3b-R	GAAGCGGCGTTATTGGTCTG
Nrf2-F	ATTTGTAGATGACCATGAGTCGC
Nrf2-R	TGTCCTGCTGTATGCTGCTT
Bach1-F	CACAAAGTGCAAAGACCCCG
Bach1-R	ATCGCCTGACTGCTCGTATG
c-Myc-F	CAGCTCGCCCAAATCCTGTA
c-Myc-R	GCCTCTTGATGGGGATGACC
G6pd-F	GAGGACCAGATCTACCGC
G6pd-R	CAAAATAGCCCCCACGACC

Pgd-F	GCTGACATTGCACTGATTGG
Pgd-R	TCACGAGCAGTATGACCCG
Gclm-F	GTTCATTGTAGGATCG
Gclm-R	GGTGCCTATAGCAACAATCT
Gclc-F	CTGGACTCATCCCCATTC
Gclc-R	GTAGTCAGGATGGTTTGC
B2m-F	ATGGGAAGCCCAACTTCCTC
B2m-R	ATACATCGGTCTCGGTGGGT

Table 1: Primer sequences used for real time PCR.

Biochemical Analyses

Activities of plasma GGT (BIOO Scientific, Austin, TX), nuclear Nrf2 (Active Motif, Carlsbad, CA), and citric acid cycle and antioxidant enzymes (aconitase, CAT, GPx, SOD, GR, and GST) (Cayman Chemical, Ann Arbor, MI) were measured using commercially available kits as previously described [16]. Complex I, Complex II, NADPH ratios, NADH ratios (Abcam, Cambridge, MA), and insulin (Morinaga, Yokohama-Shi, Japan) assays were measured by commercial ELISAs. NADH and NADPH were measured immediately after dissection to avoid sample degradation. All samples were analyzed in duplicate and run in a single assay with intra-assay and percent coefficients of variability of less than 10% for all assays.

Statistics

Means (±SEM) were compared by ANOVA. Means were considered significantly different at $P < 0.05$ using Tukey's HSD. Statistical analyses were performed with SYSTAT 13 software (SYSTAT, San Jose, CA).

Results

AT1 activation increases ventricular hypertrophy

Relative food consumption was 57% higher in OLETF rats compared to LETO (**Table 2**). Treatment had no discernable effect on relative food consumption compared to OLETF. Body mass was 35% higher in OLETF rats compared to LETO with no difference amongst treatment groups (**Table 2**). Absolute ventricular mass increased 15% in OLETF rats compared to LETO (**Table 2**). ARB treatment lowered absolute ventricular mass by 10% while ARBM treatment returned ventricular mass to OLETF levels. Relative ventricular mass was not different between LETO and OLETF, but ARB treatment decreased relative ventricular mass 8% and removal of ARB treatment return levels to OLETF (**Table 2**).

	LETO	**OLETF**	**ARB**	**ARBM**
Food Consumption (g)	20.2 ± 0.6	31.8 ± 1.0 *	30.8 ± 0.7	32.5 ± 0.4
Body Mass (g)	481 ± 7	650 ± 7 *	632 ± 5	631 ± 6

Ventricular Mass (g)	1.34 ± 0.06	1.54 ± 0.02 *	1.39 ± 0.02 †	1.53 ± 0.02 ¥
Relative Ventricular Mass (g/kg)	0.27 ± 0.01	0.25 ± 0.01 *	0.23 ± 0.01 †	0.25 ± 0.01 ¥

Table 2: Mean ± SEM for food consumption, BM, heart mass and relative heart mass in Long Evans Tokushima Otsuka (LETO; n=6), Otsuka Long Evans Tokushima Fatty (OLETF; n=8), OLETF + angiotensin receptor type 1 blocker 8 weeks (ARB; n=8) rats, and OLETF + angiotensin receptor type 1 blocker 4 weeks, then removed (ARBM; n=8) rats. Relative heart mass SEM values are less than 0.01. *Significant difference from LETO (P< 0.05). † Significant difference from OLETF (P< 0.05). ¥Significant difference between OLETF and ARBM (P< 0.05).

ARB effectively blocked the AT1 receptor

Mean SBP increased 42% in OLETF compared to LETO, and while ARB treatment completely ameliorated the elevated arterial pressure, removal of ARB completely restored the hypertension (**Figure 2A**). Plasma angiotensin II was measured to assess the ARB's efficacy. At T0, plasma angiotensin II was 4-fold higher in ARB compared to OLETF. ARBM treatment restored plasma angiotensin II values to OLETF levels (**Figure 2B**).

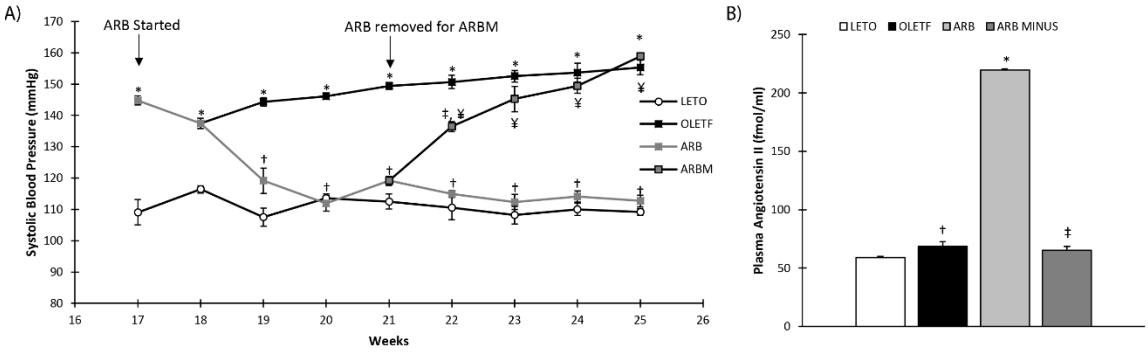

Figure 2: Mean ± SEM values of **A)** Systolic blood pressure starting from 17 weeks until 25 weeks of age, and **B)** plasma angiotensin II levels post glucose challenge in Long Evans Tokushima Otsuka (LETO; n=6), Otsuka Long Evans Tokushima Fatty (OLETF; n=8), OLETF + angiotensin receptor type 1 blocker 8 weeks (ARB; n=8) rats, and OLETF + angiotensin receptor type 1 blocker 4 weeks, then removed (ARBM; n=8) rats. *Significant difference from LETO (P< 0.05). † Significant difference from OLETF (P< 0.05). ‡ Significant difference from ARB (P< 0.05). ¥ Significant difference between OLETF and ARBM (P< 0.05).

ARB treatment improves glucose tolerance and insulin response

Plasma glucose and insulin were measured during the oral glucose tolerance test to assess the degree of glucose intolerance and insulin resistance in type II diabetic rats (**Figure 3A, C**). Plasma glucose area under the curve ($AUC_{glucose}$) was 195% higher in OLETF rats compared to LETO. ARB treatment lowered $AUC_{glucose}$ 19% and ARB removal lowered $AUC_{glucose}$ 21% (**Figure 3B**). Insulin AUC ($AUC_{insulin}$) more than doubled in OLETF rats compared to LETO, and

ARB treatment lowered $AUC_{insulin}$ 30%, while removal of ARB was not different from OLETF or ARB indicative of an intermediary phenotype (but more similar to ARB) (**Figure 3D**).

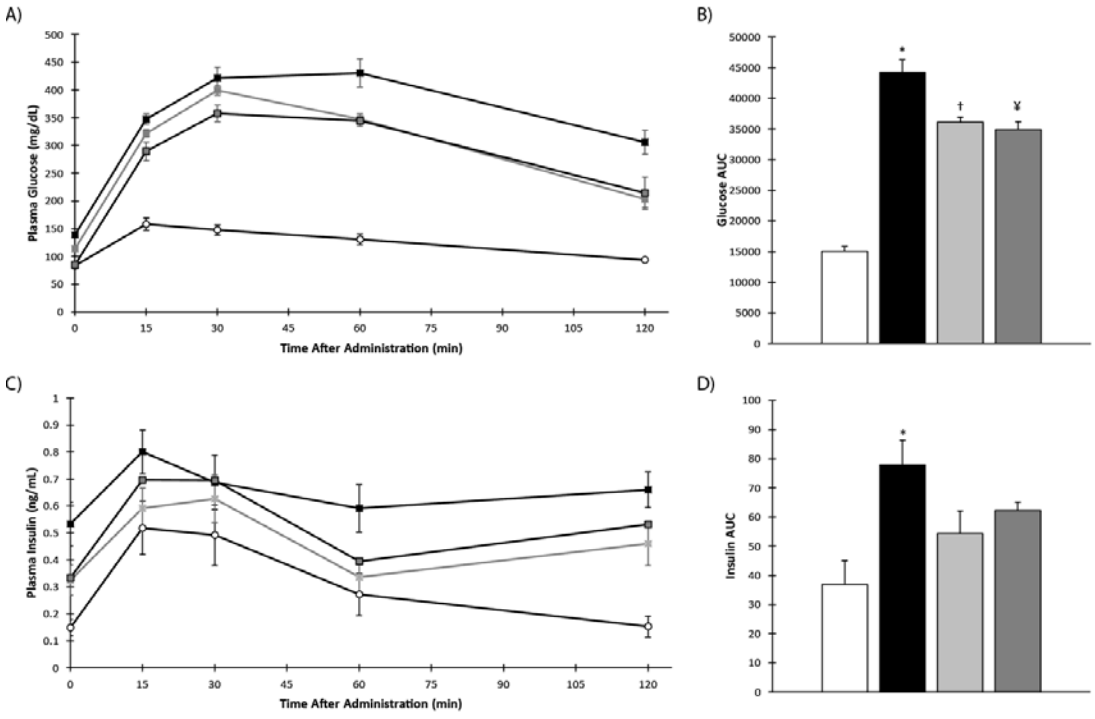

Figure 3: Mean ± SEM values of **A)** plasma glucose levels, **B)** glucose area under the curve values, **C)** plasma insulin levels, and **D)** insulin under the curve values post glucose challenge in Long Evans Tokushima Otsuka (LETO; n=6), Otsuka Long Evans Tokushima Fatty (OLETF; n=8), OLETF + angiotensin receptor type 1 blocker 8 weeks (ARB; n=8) rats, and OLETF + angiotensin receptor type 1 blocker 4 weeks, then removed (ARBM; n=8) rats. *Significant difference from LETO ($P< 0.05$). † Significant difference from OLETF ($P< 0.05$). ¥ Significant difference between OLETF and ARBM ($P< 0.05$).

Diabetes suppresses Nrf2 signaling, but is not profoundly altered with ARB treatment

Nrf2 translocation, acetylation, and several of its regulators were measured to gain a better understanding of an acute glucose challenge on Nrf2 signaling. At T0, Nrf2 mRNA was 32% lower in OLETF rats compared to LETO (**Figure 4A**). Nrf2 mRNA was 27% lower in OLETF compared to LETO rats at T180, while ARB treated animals were 51% lower compared to OLETF. ARBM treatment returned Nrf2 mRNA transcripts to OLETF levels at T180. At T360, Nrf2 transcripts were 41% lower in OLETF compared to LETO rats. At T360, glucose increased Nrf2 transcripts 25% from T0 and T180 in LETO rats. In ARB treated animals, glucose lowered Nrf2 transcripts 56% at T180 compared to T0 (**Figure 4A**). At T0, cytosolic Nrf2 content was 50% lower in OLETF rats compared to LETO (**Figure 4B**). At T0, ARB and ARBM treatments increased cytosolic Nrf2 content 213% and 151%, respectively (**Figure 4B**). At T180, glucose increased cytosolic Nrf2 protein 173% in OLETF rats (**Figure 4B**). No statistical differences were detected in nuclear Nrf2 protein content among the groups (**Figure 4C**). At T0, Nrf2

acetylation increased 30% and 42% in ARB and ARBM treated animals, respectively, compared to OLETF (**Figure 4D**). Glucose increased LETO Nrf2 acetylation 48% and 34% at T180 and T360, respectively, compared to T0. At T0, GSK3β mRNA transcripts were nearly 30-fold higher in ARBM treated animals compared to OLETF and ARB (**Figure 4E**). At T180, GSK3β transcripts increased over 40-fold in ARB animals compared to OLETF, and 75-fold and 83% higher in ARBM compared to OLETF and ARB animals, respectively. At T360, GSK3β transcripts were approximately 36- and 29-fold higher in ARB and ARBM treatment groups, respectively, compared to OLETF. In ARB treated animals, glucose increased GSK3β transcripts approximately 18- and 29-fold at T180 and T360, respectively (**Figure 4E**). At T0, GSK3β protein was 84% higher in OLETF rats compared to LETO (**Figure 4F**). In LETO, GSK3β was 33% higher at T180 compared to T0, and decreased 16% at T360 (**Figure 4F**). At T0, Keap1 mRNA transcripts were 55% and 98% lower in ARB and ARBM treated animals, respectively, compared to OLETF (**Figure 4G**). At T0, Keap1 transcripts were 96% lower in ARBM treatment compared ARB (**Figure 4G**). At T180, Keap1 mRNA decreased 69% in OLETF compared LETO, while ARB treatment increased transcripts by 73%. At T180, Keap1 mRNA was 97% and 99% lower in ARBM treated animals compared to OLETF and ARB treated animals, respectively. At T360, Keap1 transcripts were 94% lower in OLETF compared to LETO. In LETO, Keap1 transcripts were 105% higher at T360 compared to T0. In OLETF, glucose suppressed Keap1 transcripts 29% at T180 and 82% at T360 compared to T0. At T180, Keap1 transcripts in ARB treated animals increased nearly 5-fold compared to T0, but decreased 91% at T360 (**Figure 4G**). At T0, Keap1 protein was 22% lower in ARB treated animals compared to OLETF, while ARBM treatment increased Keap1 protein 42% compared to ARB (**Figure 4H**). At T0, Keap1 protein in ARBM treatment was 41% greater compared to ARB. In ARB treatment, Keap1 protein increased 45% at T180, and deceased 31% and 52% at T360 compared T0 and T180, respectively (**Figure 4H**). At T180, Bach1 mRNA transcripts decreased 64% in OLETF rats compared to LETO (**Figure 4I**). In ARB treated animals, glucose increased Bach1 transcripts at T360 by 64% and 194% compared T0 and T180, respectively (**Figure 4I**). At T0, c-Myc mRNA transcripts was 50% lower in OLETF rats compared to LETO (**Figure 4J**). At T0, c-Myc transcripts were 83% and 84% lower in ARBM treatment compared to OLETF and ARB treatment, respectively. At T180 and T360, transcripts were 48% and 57% lower, respectively, in OLETF compared to LETO (**Figure 4J**). In ARB treated animals, glucose increased c-Myc transcripts over 7- and 5-fold at T180 and T360, respectively, compared to T0 (**Figure 4J**).

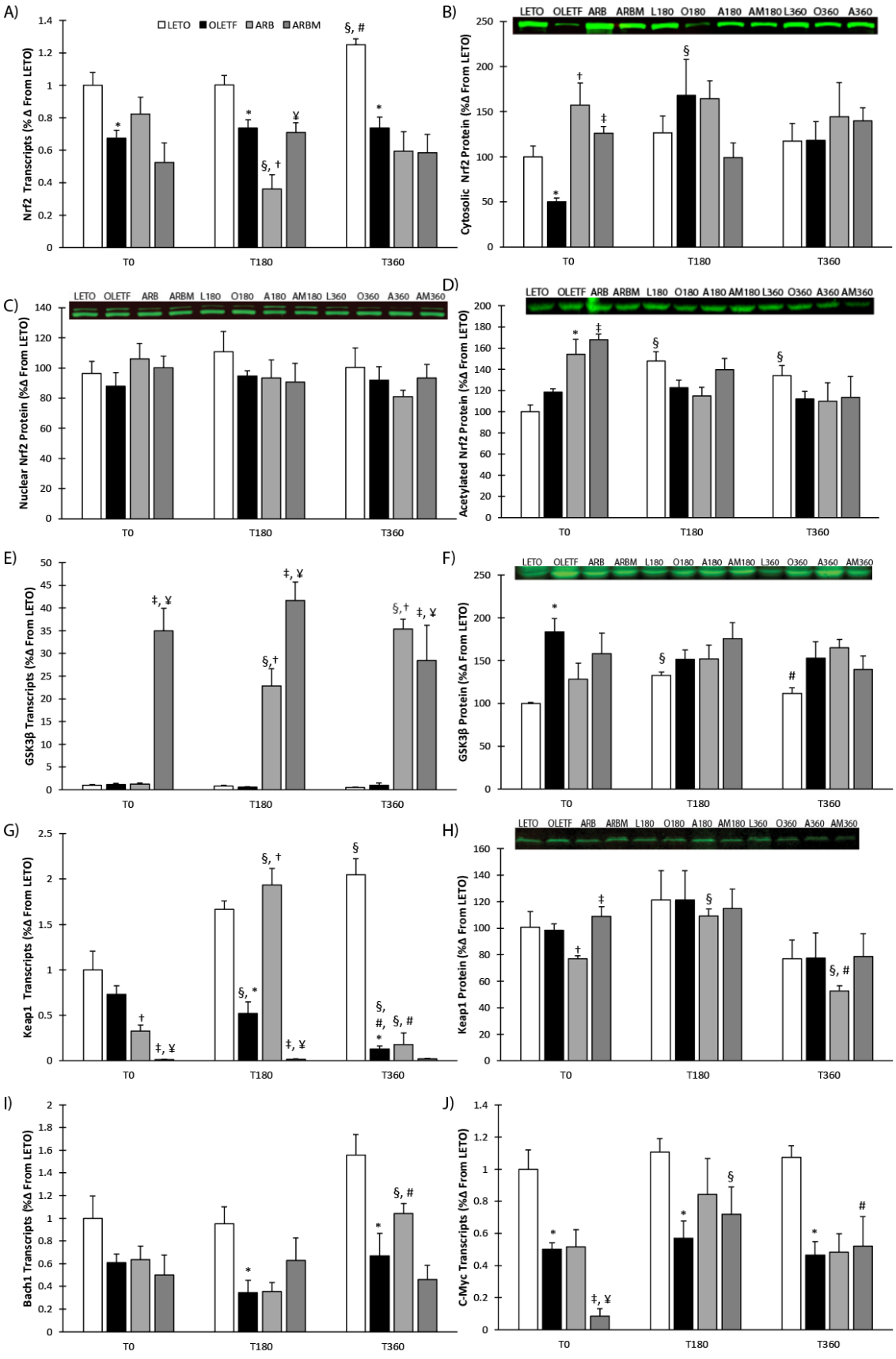
A)
LETO OLETF ARB ARBM
Nrf2 Transcripts (% Δ From LETO)
T0 T180 T360
B)
LETO OLETF ARB ARBM L180 O180 A180 AM180 L360 O360 A360
Cytosolic Nrf2 Protein (%Δ From LETO)
C)
LETO OLETF ARB ARBM L180 O180 A180 AM180 L360 O360 A360 AM360
Nuclear Nrf2 Protein (%Δ From LETO)
D)
Acetylated Nrf2 Protein (%Δ From LETO)
E)
GSK3β Transcripts (%Δ From LETO)
F)
GSK3β Protein (%Δ From LETO)
G)
Keap1 Transcripts (%Δ From LETO)
H)
Keap1 Protein (%Δ From LETO)
I)
Bach1 Transcripts (%Δ From LETO)
J)
C-Myc Transcripts (%Δ From LETO)

Figure 4: Nrf2 signaling pathway. Mean ± SEM values of **A)** nrf2 transcripts, **B)** cytosolic nrf2 protein, **C)** nuclear nrf2 protein, **D)** acetylated-nrf2 protein, **E)** GSK3β mRNA, **F)** GSK3β protein, **G)** keap1 mRNA, **H)** keap1 protein, **I)** bach1 mRNA, and **J)** c-Myc mRNA values post glucose challenge in Long Evans Tokushima Otsuka (LETO; n=6), Otsuka Long Evans Tokushima Fatty (OLETF; n=8), OLETF + angiotensin receptor type 1 blocker 8 weeks (ARB; n=8) rats, and OLETF + angiotensin receptor type 1 blocker 4 weeks, then removed (ARBM; n=8) rats. §Significant difference from respective T0 (P< 0.05). #Significant difference from respective T180 (P< 0.05). *Significant difference from LETO (P< 0.05). † Significant difference from OLETF (P< 0.05). ‡ Significant difference from ARB (P< 0.05). ¥ Significant difference between OLETF and ARBM (P< 0.05).

Diabetic status is associated with impaired response of Nrf2-regulated genes to glucose challenge

At T0, GCLC mRNA transcripts were decreased 39% in OLETF compared to LETO, while ARBM treatment increased transcripts by 49% (**Figure 5A**). In OLETF, GCLC transcripts remained 35% lower than LETO at T180. In LETO, glucose increased GCLC transcripts by 28% and 39% and 35% and 56% in OLETF at T180 and T360, respectively (**Figure 5A**). At T0, GCLM mRNA transcripts were 44% lower in OLETF animals compared to LETO (**Figure 5B**). At T0, ARB treatment increased GCLM transcripts 35% compared to OLETF. At T0, GCLM transcripts were 89% and 92% lower in ARBM treatment compared to OLETF and ARB treated rats, respectively (**Figure 5B**). At T180, glucose increased GCLM transcripts by 90% in ARB treatment compared to OLETF, while GCLM transcripts were 88% and 94% lower in ARBM treatment compared to OLETF and ARB treated rats, respectively (**Figure 5B**). At T360, transcripts were 60% lower in OLETF than LETO, and 70% lower in ARB treated rats than OLETF. In ARBM treatment, GCLM transcripts were 90% and 67% lower than OLETF and ARB treated animals, respectively. At T180, glucose increased GCLM transcripts by 108% in ARB treatment, and decreased 91% at T360 (**Figure 5B**). In LETO, glucose increased GCLM transcripts 24% at T360. In ARB treatment, glucose increased transcripts 108% at T180 and decreased them 91% at T360 (**Figure 5B**). In ARBM treatment, glucose increased GCLM transcripts by 67% at T180 and decreased them 51% at T360 (**Figure 5B**). At T0, G6PD mRNA transcripts in OLETF were 48% lower compared to LETO, and glucose reduced them 56% at T180 compared to LETO (**Figure 5C**). At T0, PGD mRNA transcripts were 41% lower in OLETF rats compared to LETO (**Figure 5D**). In LETO, glucose increased PGD transcripts 53% and 70% at T360 compared T0 and T180, respectively (**Figure 5D**). At T360, PGD mRNA was 68% lower in OLETF rats compared to LETO. At T180, PGD mRNA was 137% higher in ARBM treated animals compared to OLETF (**Figure 5D**).

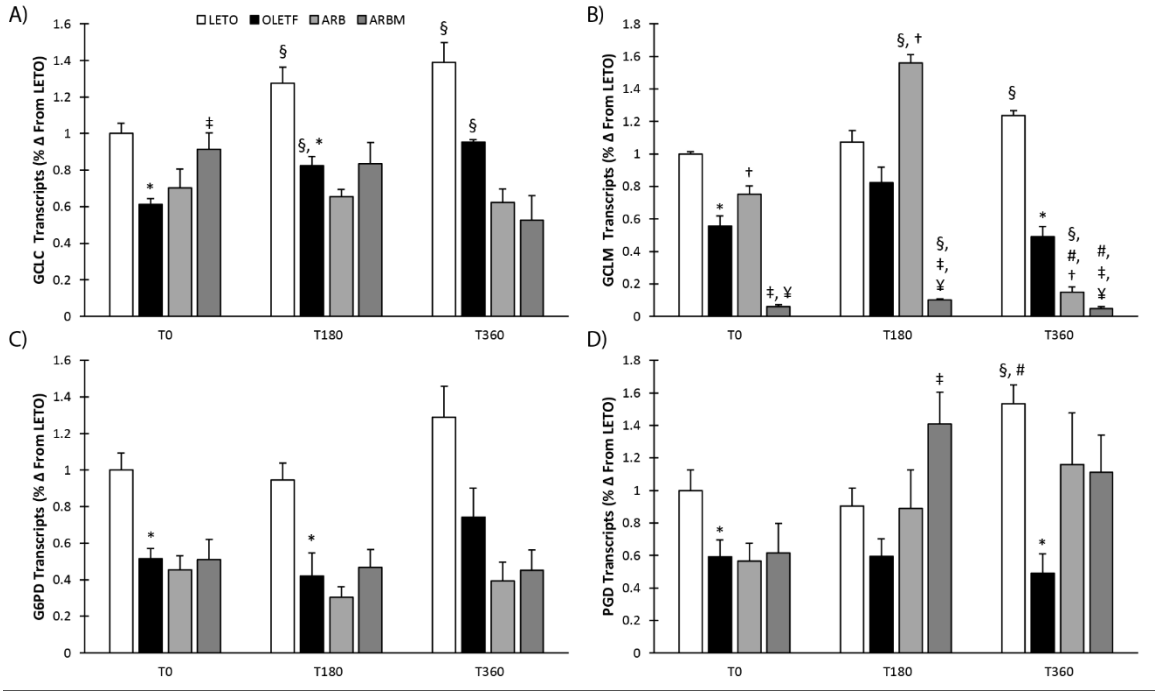

Figure 5: Nrf2 related transcript levels. Mean ± SEM values of **A)** GCLC mRNA, **B)** GCLM mRNA, **C)** G6PD mRNA, and **D)** PGD mRNA values post glucose challenge in Long Evans Tokushima Otsuka (LETO; n=6), Otsuka Long Evans Tokushima Fatty (OLETF; n=8), OLETF + angiotensin receptor type 1 blocker 8 weeks (ARB; n=8) rats, and OLETF + angiotensin receptor type 1 blocker 4 weeks, then removed (ARBM; n=8) rats. §Significant difference from respective T0 (P< 0.05). #Significant difference from respective T180 (P< 0.05). *Significant difference from LETO (P< 0.05). † Significant difference from OLETF (P< 0.05). ‡ Significant difference from ARB (P< 0.05). ¥ Significant difference between OLETF and ARBM (P< 0.05).

GSH synthesis increases in diabetic and ARB treatment groups but not ARBM

At T0, total GSH levels increased 26% in ARB treated rats compared to OLETF (**Figure 6A**). In LETO, glucose suppressed GSH levels 20% and 26% at T180 and T360, respectively, but increased GSH levels 27% and 80% at T180 and T360, respectively, in OLETF. Thus, GSH levels were 68% higher at T180 and 157% higher at T360 in OLETF compared to LETO. At T360, GSH levels were 33% and 31% lower in ARBM treatment compared to OLETF and ARB treated rats, respectively (**Figure 6A**). In ARB treated animals, glucose increased GSH content 39% and 38% at T360 compared to T0 and T180, respectively (**Figure 6A**). At T0, GCLC and GCLM protein levels were 33% and 39% lower, respectively, in OLETF rats compared to LETO, and GCLM levels were restored in ARB treated rats (**Figure 6B and 6C**). In LETO, glucose suppressed GCLM protein levels 24% at T360, and 24% and 35% at T180 and T360, respectively, in ARB treated animals (**Figure 6C**). At T0, plasma GGT activity was 38% lower in OLETF rats compared to LETO, and ARB treatment or removal had no effect (**Figure 6D**). In LETO, glucose increased plasma GGT activity 41% and 35% at T180 and T360, respectively, relative to T0, and 57% and 77% at T180 and T360, respectively, relative to T0 in OLETF. In

ARB treated rats, glucose increased plasma GGT activity 84% and 85% at T180 and T360, respectively, relative to T0, and increased activity 98% at T360 only relative to T0 in ARBM treatment (**Figure 6D**). At T180, plasma GGT activity was 32% lower in OLETF than LETO (**Figure 6D**). At T0, ARB treatment lowered NADP+/NADPH ratios 37% compared to OLETF, but no strain effect was detected (**Figure 6E**). At T360, glucose increased NADP+/NADPH ratios 61% in OLETF compared to LETO and decreased the ratio 18% in ARB treatment and were decreased an additional 34% in ARBM treatment (**Figure 6E**). At T360, glucose increased the ratio of NADP+/NADPH 42% and 86% in OLETF and ARB treated rats, respectively (**Figure 6E**). At T0, ARB treatment increased NAD+/NADH ratios by 33% compared to OLETF, but no strain effect was detected (**Figure 6F**). In LETO, glucose lowered NAD+/NADH ratio 31% at T180, but increased it 97% at T360. At T180, glucose suppressed NAD+/NADH ratio 59% in ARB treated rats compared to OLETF, and ARB removal returned the ratio to OLETF levels. At T360, the ratio was 53% and 37% higher in ARBM treatment than OLETF and ARB treated rats, respectively (**Figure 6F**). At T180, glucose lowered NAD+/NADH ratio 77% in ARB treated rats but increased them nearly 3-fold at T360. At T180, glucose lowered NAD+/NADH ratio 33% in ARBM treated rats but increased them 98% at T360 (**Figure 6F**).

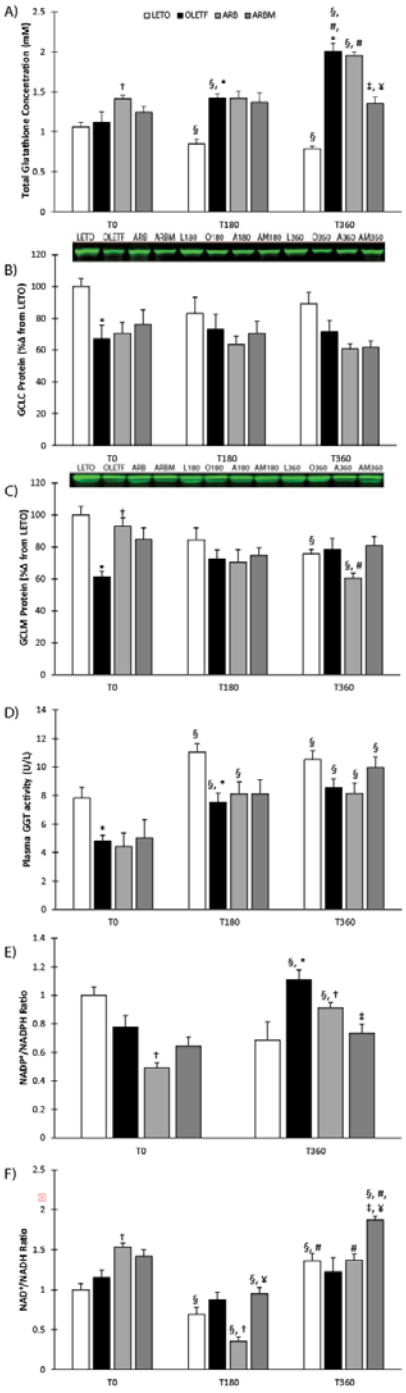

Figure 6: GSH production and cellular redox potential. Mean ± SEM values of **A)** total GSH levels, **B)** GCLM protein, **C)** GCLC protein, **D)** plasma GGT activity **E)** NADP+/NADPH ratio, and **F)** NAD+/NADH ratio values post glucose challenge in Long Evans Tokushima Otsuka (LETO; n=6), Otsuka Long Evans Tokushima Fatty (OLETF; n=8), OLETF + angiotensin receptor type 1 blocker 8 weeks (ARB; n=8) rats, and OLETF + angiotensin receptor type 1 blocker 4 weeks, then removed (ARBM; n=8) rats. §Significant difference from respective T0

(P< 0.05). #Significant difference from respective T180 (P< 0.05). *Significant difference from LETO (P< 0.05). † Significant difference from OLETF (P< 0.05). ‡ Significant difference from ARB (P< 0.05). ¥ Significant difference between OLETF and ARBM (P< 0.05).

Mitochondrial complex I activity decreases and oxidative damage increases in OLETF's

Cardiac mitochondrial function was assessed to determine the impact of ARB treatment on mitochondrial activity. Aconitase activity increased 186% in OLETF rats compared to LETO at T360 (**Figure 7A**). ARB treatment lowered aconitase activity 23% from OLETF at T360. Complex I activity decreased 32% in OLETF rats compared to LETO (**Figure 7B**). OLETF complex I activity continued to decrease 17% and 29% in OLETF rats compared to LETO at T180 and T360 respectively (**Figure 7B**). Glucose suppressed OLETF complex I activity was lower at T360 compared to T180 by 14% (**Figure 7B**). Glucose also suppressed ARB treated rats' complex I activity by 25% at T360 compared to T180 (**Figure 7B**). Glucose increased OLETF complex II activity 47% at T180 and decreased activity 35% by T360 (**Figure 7C**). Total Parkin levels increased 34% in OLETF rats compared to LETO (**Figure 7D**). ARBM treatment increased Parkin levels 27% in OLETF (**Figure 7D**). Total nitrotyrosine levels increased 35% in OLETF rats compared to LETO, while ARB treatment lowered Nitrotyrosine levels 37% (**Figure 7E**).

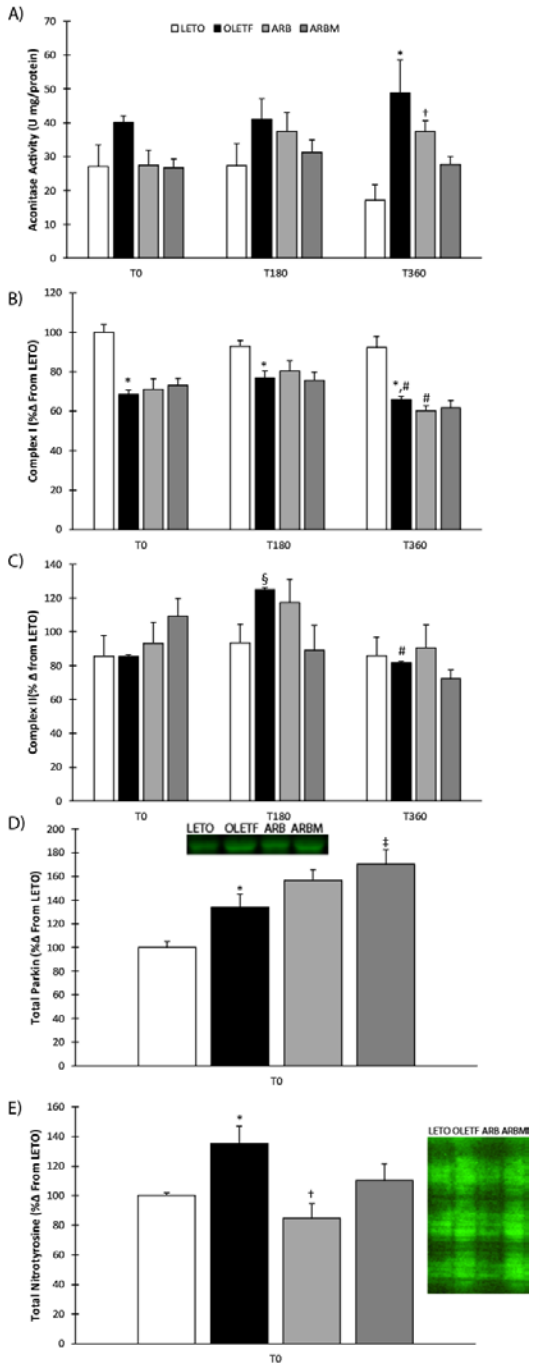

Figure 7: Mitochondrial function and cellular damage. Mean ± SEM values of **A)** aconitase activity, **B)** complex I activity, **C)** complex II activity, **D)** parkin protein levels, and **E)** nitrated protein level values post glucose challenge in Long Evans Tokushima Otsuka (LETO; n=6), Otsuka Long Evans Tokushima Fatty (OLETF; n=8), OLETF + angiotensin receptor type 1 blocker 8 weeks (ARB; n=8) rats, and OLETF + angiotensin receptor type 1 blocker 4 weeks, then removed (ARBM; n=8) rats. §Significant difference from respective T0 (P< 0.05). #Significant difference from respective T180 (P< 0.05). *Significant difference from LETO (P<

0.05). † Significant difference from OLETF (P< 0.05). ‡ Significant difference from ARB (P< 0.05). ¥ Significant difference between OLETF and ARBM (P< 0.05).

Mitochondrial GR activity increases in OLETF and ARB animals in response to glucose

Mitochondrial SOD activity increased with ARB treatment 38% compared to OLETF at T0 (**Figure 8A**). ARBM treatment decreased mitochondrial SOD levels 20% at T0 (**Figure 8A**). Mitochondrial SOD activity increased 34% in OLETF rats compared to LETO at T180 (**Figure 8A**). At T180 ARBM treated animals had 33% lower mitochondrial SOD levels than OLETF and ARB treated rats respectively. Glucose increased LETO mitochondrial SOD activity at T180 20% compared to T0. Glucose increased OLETF mitochondrial SOD levels 42% at T180 and decreased activity at T360 by 19%. Glucose decreased mitochondrial SOD activity 25% at T360 compared to T180 in ARB treated animals (**Figure 8A**). Mitochondrial catalase activity was 85% higher in OLETF rats compared to LETO at T180, while ARB treatment returned activity to control levels (**Figure 8B**). Glucose increased mitochondrial CAT activity 85% at T180 compared to T0. Glucose suppressed mitochondrial CAT levels 49% and 40% respectively in OLETF and ARBM treated animals at T360 compared to T180 (**Figure 8B**). Mitochondrial GPx activity was lower 44% and 49% at T180 in ARBM treated animals compared to OLETF and ARB treated animals (**Figure 8C**). At T360 ARBM animals had 28% lower mitochondrial GPx activity compared to OLETF treatment. Glucose suppressed mitochondrial GPx activity in ARBM treated rats at T180 28% compared to T0 (**Figure 8C**). Mitochondrial GR levels increased in OLETF rats at T180 153% compared to control (**Figure 8D**). ARB treatment further increased mitochondrial GR levels at T180 72% compared to OLETF rats while ARBM lowered activity 70%. Glucose increased LETO mitochondrial GR 90% by T360 compared to T180. Glucose increased mitochondrial GR activity 59% at T180 which then decreased it 54% and 71% by T360 compared to T0 and T180 (**Figure 8D**). Mitochondrial GST was 41% lower in ARBM animals compared to ARB treatment at T0 (**Figure 8E**). Glucose suppressed mitochondrial GST activity in ARB treated animals 44% by T180. LETO mitochondrial GST activities increased 12% at T360 compared to T180 (**Figure 8E**).

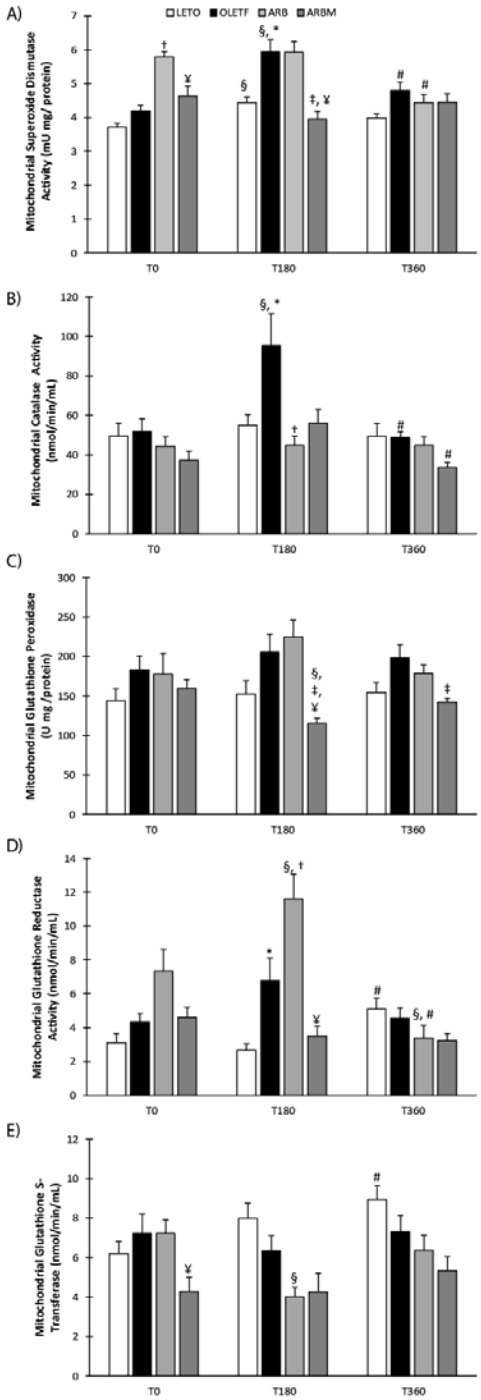

Figure 8: Mitochondrial antioxidant activities. Mean ± SEM values of **A)** superoxide dismutase activity, **B)** catalase activity, **C)** glutathione peroxidase activity, **D)** glutathione reductase activity, **E)** glutathione s-transferase activity values post glucose challenge in Long Evans Tokushima Otsuka (LETO; n=6), Otsuka Long Evans Tokushima Fatty (OLETF; n=8), OLETF + angiotensin receptor type 1 blocker 8 weeks (ARB; n=8) rats, and OLETF + angiotensin receptor type 1 blocker 4 weeks, then removed (ARBM; n=8) rats. §Significant difference from respective T0

(P< 0.05). #Significant difference from respective T180 (P< 0.05). *Significant difference from LETO (P< 0.05). † Significant difference from OLETF (P< 0.05). ‡ Significant difference from ARB (P< 0.05). ¥ Significant difference between OLETF and ARBM (P< 0.05).

Cytosolic antioxidant activities are unchanged in response to glucose

Cytosolic SOD was 25% higher in ARBM treated animals compared to OLETF at T0 (**Figure 9A**). ARB treatment lowered cytosolic SOD activity 17% compared to OLETF rats at T180 while ARBM treatment increased activity 24% (**Figure 9A**). Glucose suppressed cytosolic SOD activity 18% in ARBM treated rats at T360 compared to T0 (**Figure 9A**). No significant changes were observed with cytosolic CAT or GPx activities over the 6-hour time frame (**Figure 9B, C**). Cytosolic GR activity in OLETF rats was 21%, 20%, and 28% lower than LETO rats at T0, T180, and T360 respectively (**Figure 9D**). Glucose increased cytosolic GR activity 16% at T360 compared to T0 and T180 respectively (**Figure 9D**). No significant changes were observed with cytosolic GST activity over the 6-hour time frame (**Figure 9E**).

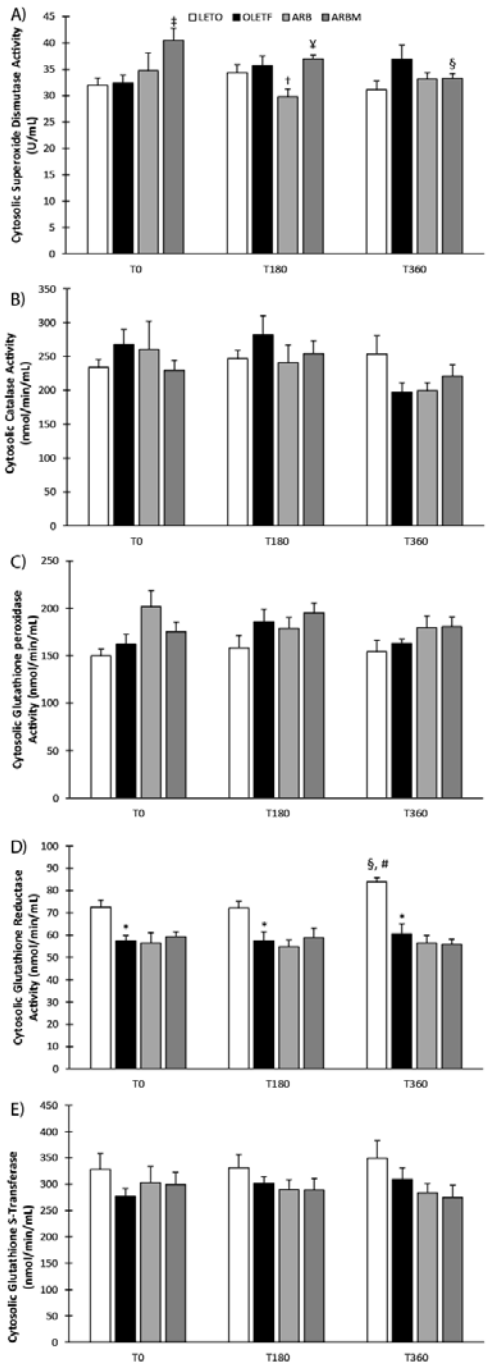

Figure 9: Cytosolic antioxidant activities. Mean ± SEM values of **A)** superoxide dismutase activity, **B)** catalase activity, **C)** glutathione peroxidase activity, **D)** glutathione reductase activity, **E)** glutathione s-transferase activity values post glucose challenge in Long Evans Tokushima Otsuka (LETO; n=6), Otsuka Long Evans Tokushima Fatty (OLETF; n=8), OLETF + angiotensin receptor type 1 blocker 8 weeks (ARB; n=8) rats, and OLETF + angiotensin receptor type 1 blocker 4 weeks, then removed (ARBM; n=8) rats. §Significant difference from respective T0 (P< 0.05). *Significant difference from LETO (P< 0.05). † Significant difference from OLETF

(P< 0.05). ‡ Significant difference from ARB (P< 0.05). ¥ Significant difference between OLETF and ARBM (P< 0.05).

Discussion

The CDC states that T2DM afflicts over 29 million individuals in the United States. The majority of these people experience cardiovascular-related dysfunctions with as many as 70% of individuals with T2DM dying from cardiovascular related complications [26]. During the development of T2DM, endogenous antioxidant production and activity is impaired along with mitochondrial function which is concerning due to the heart's highly oxidative nature [27,28]. The goals of this study were: (1) to elucidate the response of Nrf2-mediated genes to an acute glucose bolus in the diabetic heart, (2) to assess the effects of chronic blockade of AT1 on acutely elevated glucose-induced changes in Nrf2 regulation and mediation, and (3) to evaluate the potential consequences of non-compliance in ARB treatment and potential legacy effects during aforementioned conditions. The latter objective is predicated on some data on "cellular memory" in relation to AT1 antagonism [14,15].

During T2DM, the inappropriate activation of AT1 increases in arterial blood pressure and NADPH oxidase activation, which increases oxidant generation [29,30]. Nrf2 is a transcription factor that controls the expression of a multitude of genes in response to oxidant production, some of which are used for cellular detoxification [31]. We proposed that Nrf2 would be activated and increase several phase II genes in response to glucose because hyperglycemia has been implicated in an increase in oxidant production [4]. No changes in nuclear Nrf2 protein was observed at any timepoint present in the study; however, acetylation of Nrf2 was increased statically in ARB treated animals. Acetylation of Nrf2 has been implicated in initiating gene expression [32,33]. Acetylation rose in the lean strain controls in response to glucose suggesting that, despite the lack of an accumulation of nuclear Nrf2, an increase in transcription likely occurred. Keap1 and GSK3β are two known regulators of Nrf2 in the cytosol and the nucleus. Both repressors had lower levels at T0 indicating that less Nrf2 was being sequestered in the cytosol or degraded in the nucleus as GSK3β has been implicated in nuclear Nrf2 degradation via TrCP [34,35]. Furthermore, Nrf2 binding is regulated by both Bach1 and C-Myc whom act as repressor proteins inhibiting Nrf2's binding to the EpRE in the nucleus [36–38]. Transcripts were lower for both of these repressors in the diabetic animals despite the lack of nuclear accumulation.

GCLC and GCLM are responsible for the formation of GCL which generates γ-glutamyl cysteine from glutamate and cysteine prior to the addition of glutamate by glutathione synthetase to generate GSH [39]. GCLM is the rate limiting subunit to GCL formation and subsequent GSH formation [39]. Glucose-6-phosphate dehydrogenase (G6PD) and 6-Phosphogluconate dehydrogenase (PGD), the two enzymes in the oxidative phase of the pentose phosphate pathway responsible for NADPH replenishment. These four genes were measured because they're under Nrf2's control and have been implicated in other tissues to handle excess glucose during bouts of hyperglycemia to reduce oxidant production [40]. GCLC, GCLM, and PGD all increased in response to glucose in the lean strain controls suggesting that genes under Nrf2's control increase

to aid in GSH production and replenishment of NADPH through the pentose phosphate pathway. Diabetic animals had lower transcript values at all timepoints compared to the lean animals and AT1 antagonism increased only GCLM mRNA transcripts implying that ARB treatment may aid in GSH production but not NADPH replenishment. GCLM mRNA transcripts in animals with ARBM treatment were extremely low were unresponsive after glucose administration indicating that GSH production may be impaired in these animals.

Total GSH is the most abundant non-enzymatic antioxidant in the body and was measuring to gauge the diabetic heart's response to glucose. No differences were observed in GSH prior to glucose administration between lean and diabetic animals. AT1 antagonism increased the amount of GSH at T0. In response to glucose, lean animals had a reduction in glutathione while diabetic animals and ARB treated animals increased glucose after its administration. This suggests that GSH's manufacture is needed during large influxes of glucose. Animals who received ARBM treatment had no alterations in their GSH levels indicating that no response was elicited in response to glucose. GCLC protein was lower in both diabetic and treatment groups while GCLM protein was only increased in ARB treated animals, further supporting the idea that AT1 antagonism may provide some benefit to GSH production during diabetes. Gamma glutamyl transferase is an enzyme responsible for breaking down GSH to allow import of cysteine for intracellular GSH synthesis [41]. Plasma GGT increases in all groups suggesting that cysteine is needed for GSH's production during the glucose challenge.

Ratios of NADPH and NADH were also measured to gain understanding of the diabetic hearts redox potentials during a glucose challenge. NADPH and NADH are important in maintain the cells ability to neutralize oxidants, while NADPH in particular is used replenishment of GSH through GR. ARB treatment lowered the amount of $NADP^+$ at T0, suggesting the cell has more capability of reducing oxidized GSH or producing more. After glucose administration diabetic ARB treated animals groups shifted to a more oxidized state suggesting that NADPH was being utilized despite the influx of glucose. ARBM treated animals were also unresponsive 6 hours later.

The pool of NADH is larger than that of NADPH and is generally kept primarily in the reduced state, however under states where NADPH is low a shift can be seen in from a reduced state to an oxidized state of NADH in which the high energy electrons from NADH are donated to NADPH through nicotinamide nucleotide transhydrogenase [42,43]. NADH levels move to a more reduced state at 3 hours in all groups and become more oxidized at the 6-hour mark in all groups except for the untreated diabetic animals suggesting that NADH may be converted to NADPH during a glucose load which is required GSH reduction via GR.

Mitochondria are susceptible to damage during the transition to T2DM and are known to have impaired function [27]. Previously we demonstrated that in insulin resistant OLETF hearts, mitochondrial function is decreased, while nitrotyrosine and 4-hydroxynonal levels increase [16,19]. While it's still not completely clear, it's believed that changes in mitochondrial oxidant production may cause damage to itself lowering mitochondrial enzyme efficiency and increasing mitophagy [44–46]. Aconitase, is among the most notable due to its high reactivity with oxidants

due to its iron content [5,47]. Aconitase activity increased in response to glucose in the diabetic animals 6 hours later with a reduction in activity in ARB treated animals. This was surprising as we've demonstrated the enzymes reduction in activity in insulin resistance animals [16,19]. Complex I activity was reduced in diabetic animals and in treatment groups while complex II activity did not show any strain effects. It's possible that any changes that occurred in activity occurred prior to the 3-hour mark. Furthermore, complex I and II have been reported to undergo reverse or partial oxidation of oxygen resulting in increased oxidant production [6,48]. Pink1 and Parkin have been reported to initiate mitophagy in the neural tissue [49]. Pink1 accumulates upon the surface of the mitochondria allowing for parkin to translocate into mitochondria to initiate mitophagy of damaged mitochondria [44]. Total parkin levels increased in diabetic animals while AT1 antagonism provided no benefit. Removal of ARB caused parkin levels to be even higher than diabetic animals indicating the reactivation of AT1 plays a role in mitochondrial damage. Hypertension has been thought to play a role in mitochondrial damage through a loss in cardiolipin for electron transport chain complex assembly [50]. This is further corroborated by the increase in mitochondrial nitrotyrosine content and reduction with AT1 antagonism.

We measured the diabetic hearts ability to scavenge oxidants in both the mitochondria and the cytosol. Few notable changes were observed in either organelle, but we observed a reduction in GR in the cytosol with the diabetic animals with no improvement with AT1 antagonism. In the mitochondria ARB treatment increased GR activity after glucose administration. This would indicate that AT1 antagonism aids the mitochondria in reducing GSSG back to GSH which may help protect the mitochondria which houses approximately 10% of the total GSH pool [51].

Here we've demonstrated that during the early stages of type II diabetes, induction of Nrf2 related genes is impaired in diabetic animals in response to glucose, while AT1 antagonism provides some benefit and removing this treatment causes these genes to be lower than diabetic animals. Furthermore, GSH levels increase in response to glucose in diabetic hearts, and while AT1 provides no benefit, removal of this treatment impairs to cell's ability to synthesize GSH, lower's antioxidant activity, increases nitrotyrosine accumulation, high blood pressure and ventricle mass. While ARB treatment has primarily been used to treat hypertension, it is clear that it has beneficial impacts on mitochondrial function and cellular metabolism across a wide variety of tissues. The idea of a cell memory effect from previous ARB treatment may have some benefit, however in this instance it seemed to do more harm than good regarding induction of phase II genes. Here we show that complete removal after four weeks of treatment suggests to be a detriment to the heart in diabetic rat hearts.

REFERENCES

[1] Diabetes Mellitus: A Major Risk Factor for Cardiovascular Disease: A Joint Editorial Statement by the American Diabetes Association; the National Heart, Lung, and Blood Institute; the Juvenile Diabetes Foundation International; the National Institute of Diabetes and Digestive and Kidney Diseases; and the American Heart Association, Circulation. 100 (1999) 1132–1133. doi:10.1161/01.CIR.100.10.1132.

[2] K. Kawano, T. Hirashima, S. Mori, Y. Saitoh, M. Kurosumi, T. Natori, Spontaneous long-term hyperglycemic rat with diabetic complications. Otsuka Long-Evans Tokushima Fatty (OLETF) strain, Diabetes. 41 (1992) 1422–1428.

[3] M. Dunlop, Aldose reductase and the role of the polyol pathway in diabetic nephropathy, Kidney Int. Suppl. 77 (2000) S3-12.

[4] G. Giacchetti, L.A. Sechi, S. Rilli, R.M. Carey, The renin-angiotensin-aldosterone system, glucose metabolism and diabetes, Trends Endocrinol. Metab. TEM. 16 (2005) 120–126. doi:10.1016/j.tem.2005.02.003.

[5] P.R. Gardner, I. Fridovich, Superoxide sensitivity of the Escherichia coli aconitase, J. Biol. Chem. 266 (1991) 19328–19333.

[6] K.R. Pryde, J. Hirst, Superoxide Is Produced by the Reduced Flavin in Mitochondrial Complex I A SINGLE, UNIFIED MECHANISM THAT APPLIES DURING BOTH FORWARD AND REVERSE ELECTRON TRANSFER, J. Biol. Chem. 286 (2011) 18056–18065. doi:10.1074/jbc.M110.186841.

[7] J. Vásquez-Vivar, B. Kalyanaraman, M.C. Kennedy, Mitochondrial Aconitase Is a Source of Hydroxyl Radical AN ELECTRON SPIN RESONANCE INVESTIGATION, J. Biol. Chem. 275 (2000) 14064–14069. doi:10.1074/jbc.275.19.14064.

[8] W. Li, S. Yu, T. Liu, J.-H. Kim, V. Blank, H. Li, A.-N.T. Kong, Heterodimerization with Small Maf Proteins Enhances Nuclear Retention of Nrf2 via Masking the NESzip Motif, Biochim. Biophys. Acta. 1783 (2008) 1847–1856. doi:10.1016/j.bbamcr.2008.05.024.

[9] M.B. Kannan, V. Solovieva, V. Blank, The small MAF transcription factors MAFF, MAFG and MAFK: current knowledge and perspectives, Biochim. Biophys. Acta. 1823 (2012) 1841–1846. doi:10.1016/j.bbamcr.2012.06.012.

[10] M.C. Jaramillo, D.D. Zhang, The emerging role of the Nrf2-Keap1 signaling pathway in cancer, Genes Dev. 27 (2013) 2179–2191. doi:10.1101/gad.225680.113.

[11] G.V. Velmurugan, N.R. Sundaresan, M.P. Gupta, C. White, Defective Nrf2-dependent redox signalling contributes to microvascular dysfunction in type 2 diabetes, Cardiovasc. Res. 100 (2013) 143–150. doi:10.1093/cvr/cvt125.

[12] A.S. Jiménez-Osorio, A. Picazo, S. González-Reyes, D. Barrera-Oviedo, M.E. Rodríguez-Arellano, J. Pedraza-Chaverri, Nrf2 and Redox Status in Prediabetic and Diabetic Patients, Int. J. Mol. Sci. 15 (2014) 20290–20305. doi:10.3390/ijms151120290.

[13] M.L. Onozato, A. Tojo, A. Goto, T. Fujita, C.S. Wilcox, Oxidative stress and nitric oxide synthase in rat diabetic nephropathy: effects of ACEI and ARB, Kidney Int. 61 (2002) 186–194. doi:10.1046/j.1523-1755.2002.00123.x.

[14] H. Sasamura, H. Itoh, 'Memory' and 'legacy' in hypertension and lifestyle-related diseases, Hypertens. Res. (2012). doi:10.1038/hr.2011.222.

[15] H. Sasamura, K. Hayashi, K. Ishiguro, H. Nakaya, T. Saruta, H. Itoh, Prevention and regression of hypertension: role of renal microvascular protection, Hypertens. Res. 32 (2009) 658–664. doi:10.1038/hr.2009.85.

[16] M. Thorwald, R. Rodriguez, A. Lee, B. Martinez, J. Peti-Peterdi, D. Nakano, A. Nishiyama, R.M. Ortiz, Angiotensin receptor blockade improves cardiac mitochondrial activity in response to an acute glucose load in obese insulin resistant rats, Redox Biol. 14 (2018) 371–378. doi:10.1016/j.redox.2017.10.005.

[17] R. Rodriguez, J.N. Minas, J.P. Vazquez-Medina, D. Nakano, D.G. Parkes, A. Nishiyama, R.M. Ortiz, Chronic AT1 blockade improves glucose homeostasis in obese OLETF rats, J. Endocrinol. 237 (2018) 271–284. doi:10.1530/JOE-17-0678.

[18] R. Rodriguez, J.A. Viscarra, J.N. Minas, D. Nakano, A. Nishiyama, R.M. Ortiz, Angiotensin receptor blockade increases pancreatic insulin secretion and decreases glucose intolerance during glucose supplementation in a model of metabolic syndrome, Endocrinology. 153 (2012) 1684–1695. doi:10.1210/en.2011-1885.

[19] J.P. Vázquez-Medina, I. Popovich, M.A. Thorwald, J.A. Viscarra, R. Rodriguez, J.G. Sonanez-Organis, L. Lam, J. Peti-Peterdi, D. Nakano, A. Nishiyama, R.M. Ortiz, Angiotensin receptor-mediated oxidative stress is associated with impaired cardiac redox signaling and mitochondrial function in insulin-resistant rats, Am. J. Physiol. - Heart Circ. Physiol. 305 (2013) H599–H607. doi:10.1152/ajpheart.00101.2013.

[20] P. Montez, J.P. Vázquez-Medina, R. Rodríguez, M.A. Thorwald, J.A. Viscarra, L. Lam, J. Peti-Peterdi, D. Nakano, A. Nishiyama, R.M. Ortiz, Angiotensin Receptor Blockade Recovers Hepatic UCP2 Expression and Aconitase and SDH Activities and Ameliorates Hepatic Oxidative Damage in Insulin Resistant Rats, Endocrinology. 153 (2012) 5746–5759. doi:10.1210/en.2012-1390.

[21] Y.K. Oh, K.W. Joo, J.W. Lee, U.S. Jeon, C.S. Lim, J.S. Han, M.A. Knepper, K.Y. Na, Altered renal sodium transporter expression in an animal model of type 2 diabetes mellitus, J. Korean Med. Sci. 22 (2007) 1034–1041. doi:10.3346/jkms.2007.22.6.1034.

[22] I. Rahman, A. Kode, S.K. Biswas, Assay for quantitative determination of glutathione and glutathione disulfide levels using enzymatic recycling method, Nat. Protoc. 1 (2007) 3159–3165. doi:10.1038/nprot.2006.378.

[23] Y. Hiraku, M. Murata, S. Kawanishi, Determination of intracellular glutathione and thiols by high performance liquid chromatography with a gold electrode at the femtomole level: comparison with a spectroscopic assay, Biochim. Biophys. Acta BBA - Gen. Subj. 1570 (2002) 47–52. doi:10.1016/S0304-4165(02)00152-6.

[24] I. Dimauro, T. Pearson, D. Caporossi, M.J. Jackson, A simple protocol for the subcellular fractionation of skeletal muscle cells and tissue, BMC Res. Notes. 5 (2012) 513. doi:10.1186/1756-0500-5-513.

[25] J.S. Thacker, D.H. Yeung, W.R. Staines, J.G. Mielke, Total protein or high-abundance protein: Which offers the best loading control for Western blotting?, Anal. Biochem. 496 (2016) 76–78. doi:10.1016/j.ab.2015.11.022.

[26] M. Laakso, Cardiovascular Disease in Type 2 Diabetes From Population to Man to Mechanisms, Diabetes Care. 33 (2010) 442–449. doi:10.2337/dc09-0749.

[27] B.B. Lowell, G.I. Shulman, Mitochondrial dysfunction and type 2 diabetes, Science. 307 (2005) 384–387. doi:10.1126/science.1104343.

[28] M.K. Montgomery, N. Turner, Mitochondrial dysfunction and insulin resistance: an update, Endocr. Connect. 4 (2014) R1–R15. doi:10.1530/EC-14-0092.

[29] K.K. Griendling, C.A. Minieri, J.D. Ollerenshaw, R.W. Alexander, Angiotensin II stimulates NADH and NADPH oxidase activity in cultured vascular smooth muscle cells., Circ. Res. 74 (1994) 1141–1148. doi:10.1161/01.RES.74.6.1141.

[30] J.R. Sowers, Diabetes mellitus and vascular disease, Hypertens. Dallas Tex 1979. 61 (2013) 943–947. doi:10.1161/HYPERTENSIONAHA.111.00612.

[31] X.-L. Chen, C. Kunsch, Induction of cytoprotective genes through Nrf2/antioxidant response element pathway: a new therapeutic approach for the treatment of inflammatory diseases, Curr. Pharm. Des. 10 (2004) 879–891.

[32] Y. Kawai, L. Garduño, M. Theodore, J. Yang, I.J. Arinze, Acetylation-Deacetylation of the Transcription Factor Nrf2 (Nuclear Factor Erythroid 2-related Factor 2) Regulates Its Transcriptional Activity and Nucleocytoplasmic Localization, J. Biol. Chem. 286 (2011) 7629–7640. doi:10.1074/jbc.M110.208173.

[33] Z. Sun, Y.E. Chin, D.D. Zhang, Acetylation of Nrf2 by p300/CBP Augments Promoter-Specific DNA Binding of Nrf2 during the Antioxidant Response, Mol. Cell. Biol. 29 (2009) 2658–2672. doi:10.1128/MCB.01639-08.

[34] P. Rada, A.I. Rojo, S. Chowdhry, M. McMahon, J.D. Hayes, A. Cuadrado, SCF/β-TrCP Promotes Glycogen Synthase Kinase 3-Dependent Degradation of the Nrf2 Transcription Factor in a Keap1-Independent Manner, Mol. Cell. Biol. 31 (2011) 1121–1133. doi:10.1128/MCB.01204-10.

[35] S. Chowdhry, Y. Zhang, M. McMahon, C. Sutherland, A. Cuadrado, J.D. Hayes, Nrf2 is controlled by two distinct β-TrCP recognition motifs in its Neh6 domain, one of which can be modulated by GSK-3 activity, Oncogene. 32 (2013) 3765–3781. doi:10.1038/onc.2012.388.

[36] S. Levy, H.J. Forman, C-Myc is a Nrf2-interacting protein that negatively regulates phase II genes through their electrophile responsive elements, IUBMB Life. 62 (2010) 237–246. doi:10.1002/iub.314.

[37] S. Dhakshinamoorthy, A.K. Jain, D.A. Bloom, A.K. Jaiswal, Bach1 competes with Nrf2 leading to negative regulation of the antioxidant response element (ARE)-mediated NAD(P)H:quinone oxidoreductase 1 gene expression and induction in response to antioxidants, J. Biol. Chem. 280 (2005) 16891–16900. doi:10.1074/jbc.M500166200.

[38] L. Zhou, H. Zhang, K.J.A. Davies, H.J. Forman, Aging-related decline in the induction of Nrf2-regulated antioxidant genes in human bronchial epithelial cells, Redox Biol. 14 (2018) 35–40. doi:10.1016/j.redox.2017.08.014.

[39] C.C. Franklin, D.S. Backos, I. Mohar, C.C. White, H.J. Forman, T.J. Kavanagh, Structure, function, and post-translational regulation of the catalytic and modifier subunits of glutamate cysteine ligase, Mol. Aspects Med. 30 (2009) 86–98. doi:10.1016/j.mam.2008.08.009.

[40] S. Takahashi, Y. Izawa, N. Suzuki, Astroglial pentose phosphate pathway rates in response to high-glucose environments, ASN NEURO. 4 (2012). doi:10.1042/AN20120002.

[41] H. Zhang, H.J. Forman, J. Choi, Gamma-glutamyl transpeptidase in glutathione biosynthesis, Methods Enzymol. 401 (2005) 468–483. doi:10.1016/S0076-6879(05)01028-1.

[42] T.S. Blacker, M.R. Duchen, Investigating mitochondrial redox state using NADH and NADPH autofluorescence, Free Radic. Biol. Med. 100 (2016) 53–65. doi:10.1016/j.freeradbiomed.2016.08.010.

[43] D. Ghosh, K.R. Levault, G.J. Brewer, Relative importance of redox buffers GSH and NAD(P)H in age-related neurodegeneration and Alzheimer disease-like mouse neurons, Aging Cell. 13 (2014) 631–640. doi:10.1111/acel.12216.

[44] X. Zheng, T. Hunter, Parkin mitochondrial translocation is achieved through a novel catalytic activity coupled mechanism, Cell Res. 23 (2013) 886–897. doi:10.1038/cr.2013.66.

[45] T. Finkel, Signal Transduction by Mitochondrial Oxidants, J. Biol. Chem. 287 (2012) 4434–4440. doi:10.1074/jbc.R111.271999.

[46] R.S. Balaban, S. Nemoto, T. Finkel, Mitochondria, Oxidants, and Aging, Cell. 120 (2005) 483–495. doi:10.1016/j.cell.2005.02.001.

[47] M.C. Kennedy, M.H. Emptage, J.L. Dreyer, H. Beinert, The role of iron in the activation-inactivation of aconitase., J. Biol. Chem. 258 (1983) 11098–11105.

[48] C.L. Quinlan, A.L. Orr, I.V. Perevoshchikova, J.R. Treberg, B.A. Ackrell, M.D. Brand, Mitochondrial Complex II Can Generate Reactive Oxygen Species at High Rates in Both the Forward and Reverse Reactions, J. Biol. Chem. 287 (2012) 27255–27264. doi:10.1074/jbc.M112.374629.

[49] A.M. Pickrell, R.J. Youle, The roles of PINK1, parkin, and mitochondrial fidelity in Parkinson's disease, Neuron. 85 (2015) 257–273. doi:10.1016/j.neuron.2014.12.007.

[50] A. Eirin, A. Lerman, L.O. Lerman, Mitochondrial injury and dysfunction in hypertension-induced cardiac damage, Eur. Heart J. 35 (2014) 3258–3266. doi:10.1093/eurheartj/ehu436.

[51] M.J. Meredith, D.J. Reed, Status of the mitochondrial pool of glutathione in the isolated hepatocyte, J. Biol. Chem. 257 (1982) 3747–3753.

Chapter 3. Cardiac NF-κB Activation Increases While Nrf2 is Blunted During the Progression of Type II Diabetes in UCD-T2DM Rats

Abstract

The onset of diabetes makes the heart susceptible to oxidative damage because of the associated inflammation and impaired antioxidant response. NF-κB is the primary transcription factor involved in initiating inflammatory cascades while Nrf2 is responsible for increasing genes involved in antioxidant defense. These transcription factors have been suggested to have opposing roles during the manifestation of type II diabetes mellitus (T2DM). Acetylation of these transcription factors enhances their activity; therefore, the objective of this study was to characterize the acetylation of both transcription factors and the subsequent changes in their target genes during the progression of T2DM in the heart. We used UC Davis T2DM (UCD-T2DM) rats at the following ages: 1) lean Sprague Dawley's (SD; n=7), 2) pre-diabetic UCD-T2DM (Pre; n=9), 3) 2-week diabetic UCD-T2DM (2Wk; n=9), 4) 3-month diabetic UCD-T2DM (3Mo; n=13), and 5) 6-month diabetic UCD-T2DM (6Mo; n=9). TNFα mRNA was greater in Pre and 6Mo compared to SD. Nox 2 and 4 proteins were greater from Pre to 6Mo compared to SD. NF-κB acetylation was 45% greater in 2Wk compared to SD and increased further by 97% and 150% in 3Mo and 6Mo compared to SD rats, respectively, while acetylation of Nrf2 was lower in 3Mo compared to SD. In 6Mo, HO1 mRNA and GCLM protein expressions decreased 45% and 32% compared to SD, respectively. These data suggest that during the progression of T2DM, NF-κB activation increases while Nrf2 activation is suppressed, increasing inflammation and oxidant production while impairing the ability of the heart to manage the latter.

Introduction

Type II diabetes (T2DM) is a growing epidemic that is associated with more than 70% of deaths caused by cardiovascular related complications [1]. Insulin resistance and T2DM have been associated with chronic inflammation and impaired nucleophilic tone [2–4]. Nuclear factor kappa-light-chain-enhancer of activated B cells (NF-κB) is a transcription factor that primarily regulates inflammatory cascades by increasing cytokine levels that initiate an immune response, while some cytokines increase oxidant production [5]. Nuclear factor erythroid 2-related factor 2 (Nrf2) opposes NF-κB in that it primarily regulates genes responsible for xenobiotic detoxification, energy replenishment, and neutralizing excess oxidant production [6]. While the mechanisms remain uncertain, downstream targets of NF-κB and Nrf2 negatively regulate the opposing transcription factor, which becomes problematic in diseases associated with increased inflammation and oxidant generation such as T2DM [7,8].

NF-κB is regulated primarily in the cytosol where it's bound to a family of proteins known as NF-κB Inhibitors (IKB). In canonical NF-κB signaling, IKBα is phosphorylated, which allows NF-κB p65 to enter the nucleus where it can initiate a wide array of genes associated with the immune response as well as apoptosis and stress response [5,9]. Tumor necrosis factor alpha (TNFα) is a potent inducer and product of NF-κB and has been implicated in disrupting insulin's

action during periods of hyperglycemia [4]. Among other products associated with NF-κB gene expression are NADPH oxidase 2 (Nox2) and NADPH oxidase 4 (Nox4), both present in cardiac tissue. These Nox proteins are upregulated during the manifestation of T2DM and are also induced in response to TNFα [10–12]. These proteins produce either superoxide and/or hydrogen peroxide both of which are classified as oxidants, and the overexpression of these proteins has been implicated in causing oxidative damage to the cell.

Nrf2 is a transcription factor sequestered in the nucleus by kelch-like ECH-associated protein 1(Keap1) [13]. Canonical activation of Nrf2 occurs when oxidation of Keap1 occurs, causing a conformational shift, liberating Nrf2. Nrf2 translocates to the nucleus where is binds with small maf proteins, which allows binding to the electrophile response element (EpRE) [14,15]. Nrf2 then initiates transcription of genes responsible for xenobiotic and oxidant neutralization and energy replenishment. This process is initiated in response to a rise in oxidant production; however, during T2DM, the translocation of or induction of phase II genes by Nrf2 is impaired, causing increased damage to the cell that is amplified every time the oxidant flux increases. Additionally, the cellular degradation of Nrf2 is mediated by glycogen synthase kinase-3β (GSK3β) through β-TrCP mediated degradation [16]. Thus, the mechanism by which T2DM impairs Nrf2-mediated translation of phase II genes may include increase GSK3β that would further dampen Nrf2's potential.

The mitochondria are recognized as the largest producer of oxidants within the cell [17–19]. The mitochondria generate hydrogen peroxide (H_2O_2) and peroxynitrite ($ONOO^-$) under unstressed conditions. The H_2O_2 is derived from superoxide ($O_2^{\cdot-}$) while $ONOO^-$ is derived from the reaction of nitric oxide (NO) with $O_2^{\cdot-}$. During T2DM oxidant production increases due to the reduction in mitochondrial function [20]. To counter this, an antioxidant pool is present within the mitochondria to aid in detoxification; however, the genes associated with antioxidant production are generally downregulated due to impaired Nrf2 translocation or potentially increased degradation. Increases in oxidant production and decreases in antioxidant defense cause damage to occur to as well as increases in mitophagy by translocation of parkin into the mitochondria [17,21,22].

Traditionally, NF-κB and Nrf2 have been studied independently during various diseases including T2DM. However, several recent reviews have outlined some of their crosstalk [7,23–25], illustrating a counterproductive nature between the two transcription factors. One proposed mechanism is that in the nucleus, NF-κB and Nrf2 compete for CREB, which allows then to bind to their target sequence of DNA [26]. Conversely, some argue that NF-κB is required for Nrf2 nuclear accumulation likely through a signaling event caused by prior activation of NF-κB [27]. Since acetylation of these transcription factors enhances their activity [28–30], our aim was to characterize the acetylation of both transcription factors and the subsequent changes in their target genes during the progression of T2DM in the heart. Furthermore, this rat model of T2DM has demonstrated to more closely represent the pathophysiology of T2DM than other rodent models of the disease [31,32].

Methods

All experimental procedures were reviewed and approved by the institutional animal care and use committees of the University of California, Davis.

Animals

UCD-T2DM rats were generated by crossing obese Sprague Dawley rats with adult-onset obesity and insulin resistance with ZDF Lean rats that have a defect in ß-cell/islet function, but were homozygous wild-type for the leptin receptor [31,33]. The UCD-T2DM Rat model has been characterized and validated in more than 20 subsequent peer-reviewed publications [32]. Lean Sprague Dawley (SD; n=7), pre-diabetic UCD-T2DM (Pre; n=9), 2-week diabetic UCD-T2DM (2Wk; n=9), and 3-month diabetic UCD-T2DM (3Mo; n=13) were all 5.5 months of age at the time of sacrifice. The 6-month diabetic UCD-T2DM (6Mo; n=9) rats were approximately 90 days older than all other rats as described here [33]. Age-matching the animals for their respective stage of diabetes is not possible because the severity of the disease progresses temporally similar to the human condition. All animals were maintained in a specific pathogen-free facility with a 14-h light, 10-h dark cycle. All animals were given ad libitum access to standard laboratory rat chow (Harlan Laboratories, Indianapolis, IN) and water. Prior to dissection animals were fasted for 13 hours and blood was collected via tail vein into EDTA tubes. Then they were given a 200 mg/kg IP injection of pentobarbital sodium and exsanguinated via cardiac puncture. Heart tissue was snap frozen in liquid nitrogen and stored at -80C.

Western Blot Analyses

A 20 mg piece of frozen heart was homogenized in 125uL of sucrose buffer for extraction of the mitochondrial, nuclear, and cytosolic fractions of the cell as previously described [34]. Proteins were assayed as previously described [35] and incubated for 16 hours with primary antibodies (diluted 1:100 to 1:4000) against GCLC, GCLM (Provided by Dr. Forman), acetylated-Nrf2 (Elabscience, Houston, TX), Nox4, Vdac1 (Abcam, Cambridge, MA), NF-κB, acetylated-NFkB, IKBα, p-IKBα, H3, (Cell Signaling, Danvers, MA), Keap1, Nrf2, GSK3B, NT, Parkin, GAPDH (Santa Cruz Biotechnology, Santa Cruz, CA), 4HNE, and Nox2 (EMD Millipore, Burlington, MA). Blots were visualized using an Odyssey system (LI-COR Biosciences) and quantified using ImageJ. Nuclear and cytosolic extractions were performed and tested for purity against H3 and GAPDH in both fractions [34]. Mitochondrial extractions were also tested for purity with Vdac1 and GAPDH. In addition to consistently loading the same amount of total protein per well, the densitometry values were further normalized by correcting with the densitometry values of Ponceau S staining [36].

Real-time quantitative PCR analyses

Total RNA was isolated using TRIzol reagent (Invitrogen, Carlsbad, CA). Genomic DNA was degraded using DNase I enzyme (Roche, Indianapolis, IN). Total RNA purity was confirmed by absorbance at 260/280 and integrity by 1% agarose gel electrophoresis. Complementary DNA was reverse transcribed from genomic DNA-free RNA (2 ug) using the High-Capacity cDNA

Reverse Transcription Kit (Applied Biosystems, Foster City, CA) and oligio-dT. Quantitative PCR reactions were performed in duplicate using an equivalent to 100ng of RNA and specific primers for Keap1, GSK3β, Nrf2, NF-κB, IKBα, Bach1, c-Myc, GCLM, GCLC, HO-1, TNFα, and Nox4. Gene expression was normalized using B2M expression. Data obtained was analyzed using the comparative double delta-CT method. Primer sequences used for this study are shown in **Table 1**.

Primer Name	Nucleotide Sequence (5'-3')	GeneBank Number
Keap1-F	ATGTGATGAACGGGGCAGTC	NM_057152.2
Keap1-R	AGAACTCCTCCTCCCCGAAG	
Gsk3β-F	CTGGCCACCATCCTTATCCC	NM_032080.1
Gsk3β-R	GAAGCGGCGTTATTGGTCTG	
Nrf2-F	ATTTGTAGATGACCATGAGTCGC	NM_031789.2
Nrf2-R	TGTCCTGCTGTATGCTGCTT	
Bach1-F	CACAAAGTGCAAAGACCCCG	NM_001107113.1
Bach1-R	ATCGCCTGACTGCTCGTATG	
C-Myc-F	CAGCTCGCCCAAATCCTGTA	NM_012603.2
C-Myc-R	GCCTCTTGATGGGGATGACC	
Gclm-F	GTTCATTGTAGGATCG	NM_017305.2
Gclm-R	GGTGCCTATAGCAACAATCT	
Gclc-F	CTGGACTCATCCCCATTC	NM_012815.2
Gclc-R	GTAGTCAGGATGGTTTGC	
HO-1-F	GAGCGAAACAAGCAGAACCC	NM_012580.2
HO-1-R	ACCTCGTGGAGACGCTTTAC	
NF-κB-F	GAGCTGGTGGAGGCCCTG	NM_001276711.1
NF-κB-R	GACAGCGGCGTGGAGAC	
IKBα-F	CTCAAGAAGGAGCGGTTGGT	NM_001105720.2
IKBα-R	CCAAGTGCAGGAACGAGTCT	
TNFα -F	TGAGCTCAAGCCCTGGTATG	NM_012675.3
TNFα -R	CCGGACTCCGTGATGTCTAAG	
Nox4-F	AGATGTTGGGCCTAGGATTGTG	NM_053524.1
Nox4-R	TGTGATCCGCGAAGGTAAGC	
B2m-F	ATGGGAAGCCCAACTTCCTC	NM_012512.2
B2m-R	ATACATCGGTCTCGGTGGGT	

Table 1: Primers and GeneBank accession number for real time PCR.

Biochemical Analyses

Aconitase (Cayman Chemical, Ann Arbor, MI) activity was measured using a commercially available kit as previously described [35,37]. Complex I, complex II (Abcam, Cambridge, MA), and TNFα (Meso Scale Discovery, Rockville, MD) assays were measured by ELISA. All samples were analyzed in duplicate and run in a single assay with intra-assay and percent coefficients of variability of less than 10% for all assays.

Statistics

Means (±SEM) were compared by ANOVA. Means were considered significantly different at $P < 0.05$ using Tukey's HSD. Statistical analyses were performed with SYSTAT 13 software (SYSTAT, San Jose, CA).

Results

Cardiac nuclear accumulation and acetylation of NF-κB increases with the progression of diabetes.

Components of NF-κB were measured to gauge the inflammatory response as the animals became more diabetic as chronic low-grade inflammation is a hallmark of T2DM. NF-κB transcripts rose 172% in the hearts of pre-diabetic animals and remained elevated at all stages of T2DM measured. Pre-diabetic animals had 31% more NF-κB transcripts compared to 6-month diabetic animals (**Figure 1A**). Cytosolic NF-κB protein increased 35% in 3-month diabetic rats compared to 2-week diabetic rats (**Figure 1B**). 6-month diabetic rats had 16% lower cytosolic NF-κB protein compared to SD rats and 30% lower NF-κB than 3-month diabetic animals (**Figure 1B**). Nuclear accumulation of NF-κB decreased 15% in pre-diabetic animals compared to SD rats (**Figure 1C**). However, 2-week diabetic rats had 22% and 42% more nuclear NF-κB than SD and pre-diabetic rats respectively. 3-Month diabetic rats had 46% and 71% more Nuclear NF-κB than SD and pre-diabetic rats. Nuclear NF-κB content returned to SD levels in 6-month diabetic animals (**Figure 1C**). Acetylation of NF-κB increased 45% in 2-week diabetic animals compared to SD rats (**Figure 1D**). Acetylation further increased 97% and 150% in 3-month and 6-month rats compared to SD rats, respectively. Acetylation was higher by 86% and 136% in 3-month and 6-month diabetic animals, respectively, compared to prediabetic animals (**Figure 1D**). IKBα mRNA expression increased 160% in 2-week diabetic animals, 173% in 3-month diabetic animals, and 456% in 6-month diabetic animals compared to SD rats (**Figure 1E**). 3-month diabetic rats had 61% more IKBα transcripts than pre-diabetic rats. 6-month diabetic animals had six-fold higher IKBα transcripts compared to SD rats (**Figure 1E**). P- IKBα/IKBα ratio increased 43% in 2-week diabetic rats, while 3 and 6-month diabetic rats increased 76% and 77% compared to SD rats, respectively (**Figure 1F**).

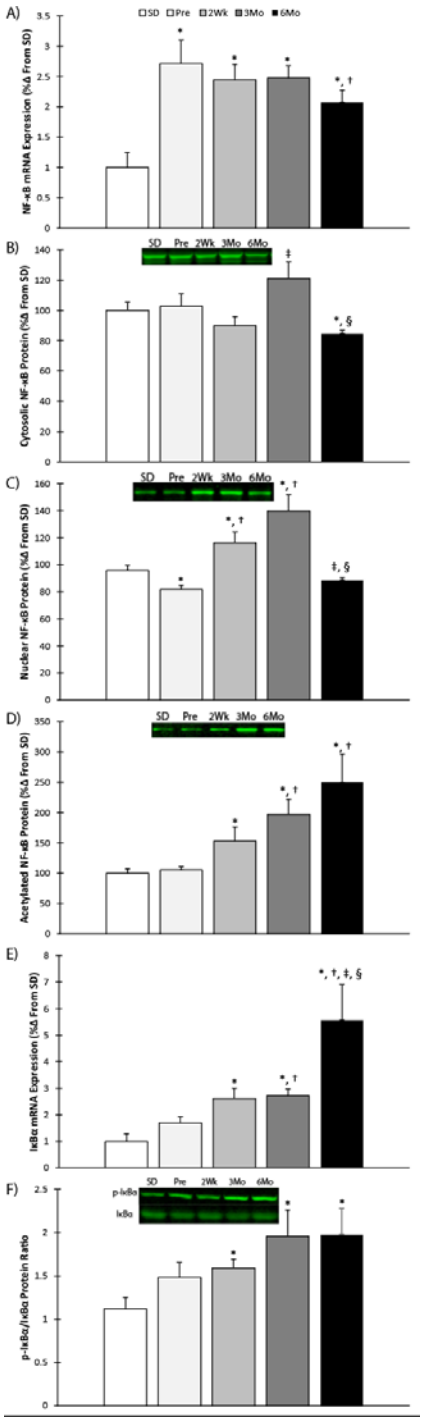

Figure 1: NF-κB signaling during the progression of T2DM. Mean ± SEM values of **A)** NF-κB mRNA, **B)** cytosolic NF-κB protein, **C)** nuclear NF-κB protein, **D)** acetylated-NF-κB protein, **E)** IκBα mRNA, and **F)** p-IκBα/IκBα ratio in Sprague Dawley's (SD; n=7), pre-diabetic UCD-T2DM (Pre; n=9), 2-week diabetic UCD-T2DM (2Wk; n=9), 3-month diabetic UCD-T2DM (3Mo; n=13), and 6-month diabetic UCD-T2DM (6Mo; n=9) rats. * Significant difference from

SD (P< 0.05). † Significant difference from Pre (P< 0.05). ‡ Significant difference from 2Wk (P< 0.05). § Significant difference from 3Mo (P< 0.05).

Cardiac Nrf2 translocation is impaired with the progression of diabetes.

Components of Nrf2 signaling were measured to gauge the cells ability to deal with an oxidative insult as T2DM progression in the heart. Nrf2 mRNA expression decreased 38% and 51% in 2-week diabetic rats compared to SD and pre-diabetic groups, respectively (**Figure 2A**). Nrf2 mRNA was 3-fold higher than all groups in 6-month diabetic animals (**Figure 2A**). Cytosolic Nrf2 protein decreased 55% in pre-diabetic animals compared to SD (**Figure 2B**). 2-week diabetic animals had 130% more cytosolic Nrf2 than pre-diabetic animals. 3-month diabetic animals had 35% and 38% less cytosolic Nrf2 compared to SD and 2-week diabetic rats, respectively. 6-month diabetic rats had 130% and 61% more cytosolic Nrf2 compared to pre-diabetic and 3-month groups respectively (**Figure 2B**). Nuclear Nrf2 was decreased 18% in pre-diabetic animals compared to SD rats and remained lower in 2-week and 3-month diabetic rats (**Figure 2C**). Nuclear Nrf2 content was the same in 6-month diabetic rats compared to SD (**Figure 2C**). Nrf2 acetylation was lower 23% in 3-month rats compared to SD, pre-diabetic, and 2-week diabetic rats (**Figure 2D**). Keap1 mRNA increased 79% in pre-diabetic rats and remained elevated until 6-months were levels returned to SD values (**Figure 2E**). Keap1 mRNA in 6-month diabetic animals was 36%, 40%, and 30% lower than pre-diabetic, 2-month diabetic, and 3-month diabetic animals, respectively (**Figure 2E**). Keap1 protein decreased in 2-week diabetic animals 33% compared to pre-diabetic rats (**Figure 2F**). 6-month diabetic animals had Keap1 protein levels 26% lower than SD and 47% lower than 3-month diabetic rats (**Figure 2F**). GSK3β mRNA increased in pre-diabetic animals 119% and remained elevated throughout the disease progression (**Figure 2G**). 3-month diabetic animals had 17% lower GSK3β than 2-week diabetic animals. Nuclear GSK3β protein rose steadily starting in pre-diabetic animals and continuing to 6-month diabetic animals 25% compared to SD (**Figure 2H)**. Bach1 mRNA decreased in 2-week and 3-month diabetic animals 47% and 41% compared to pre-diabetic animals (**Figure 2I**). 6-month diabetic animals had 3.5-fold more Bach1 transcripts compared to SD, 2-week, and 3-month diabetic animals and 2-fold more than pre-diabetic animals (**Figure 2I**). C-Myc mRNA expression decreased in pre-diabetic and 2-week diabetic animals 30% and 40%, respectively, compared to SD rats (**Figure 2J**). C-Myc mRNA further decreased by 53% in 6-month diabetic animals compared to SD rats and was 47% lower than 3-month diabetic rats (**Figure 2J**).

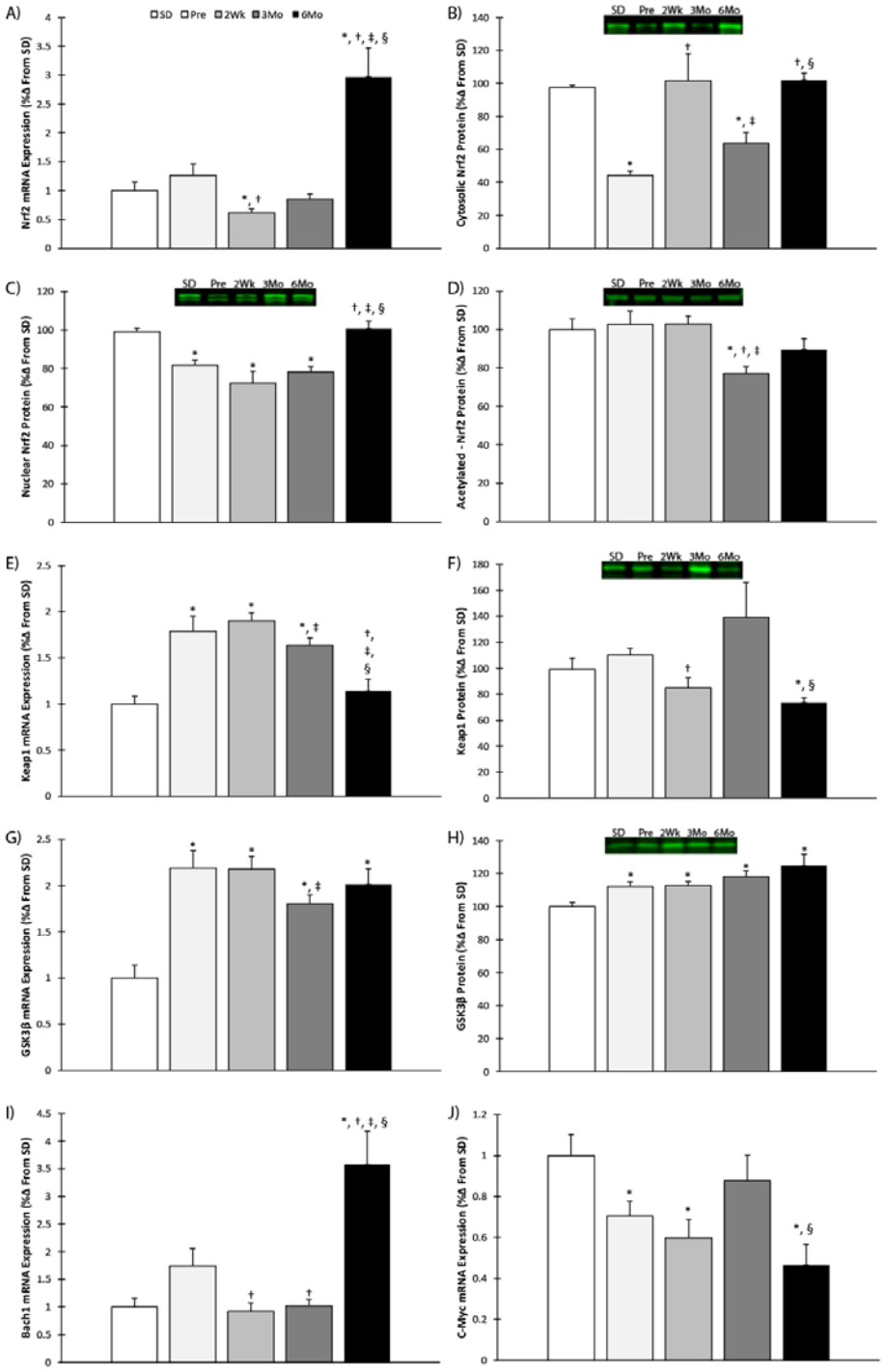

Figure 2: Nrf2 signaling during the progression of T2DM. Mean ± SEM values of **A)** Nrf2 mRNA, **B)** cytosolic Nrf2 protein, **C)** nuclear Nrf2 protein, **D)** acetylated-Nrf2 protein, **E)** Keap1 mRNA, **F)** Keap1 protein, **G)** GSK3β mRNA, **H)** GSK3β protein, **I)** C-Myc mRNA, and **J)** Bach1 mRNA in Sprague Dawley's (SD; n=7), pre-diabetic UCD-T2DM (Pre; n=9), 2-week diabetic UCD (2Wk; n=9), 3-month diabetic UCD-T2DM (3Mo; n=13), and 6-month diabetic UCD-T2DM (6Mo; n=9) rats. * Significant difference from SD ($P< 0.05$). † Significant

difference from Pre (P< 0.05). ‡ Significant difference from 2Wk (P< 0.05). § Significant difference from 3Mo (P< 0.05).

Activation of NF-κB increases in the heart as diabetes progresses.

TNFα and Nox proteins were measured to gauge the inflammatory response and increase in oxidant production during the progression of T2DM in the heart.TNFα mRNA expression increased 169% in pre-diabetic animals compared to SD rats (**Figure 3A**). TNFα transcripts decreased 52% and 56% in 2-week and 3-month diabetic animals compared to pre-diabetic (**Figure 3A**). 6-month diabetic animals had 234% and 184% more TNFα transcripts compared to SD and 3-month diabetic animals (**Figure 3A**). Plasma TNFα levels increased 84% and 100% in 3-month and 6-month diabetic animals compared to SD rats (**Figure 3B**). 6-month diabetic animals also had 71% more plasma TNFα levels than pre-diabetic animals. Nox4 mRNA expression increased in pre-diabetic animals 476% and remained elevated through the disease progression (**Figure 3C**). Nox4 protein expression increased in pre-diabetic animals and continued to increase in 6-month animals 278% from SD (**Figure 3D**). 6-month animals were also 78% and 83% higher than pre-diabetic and 2-week diabetic rats (**Figure 3D**). Nox2 protein increased in pre-diabetic animals through 6-month diabetic animals 146% compared to SD rats (**Figure 3E**).

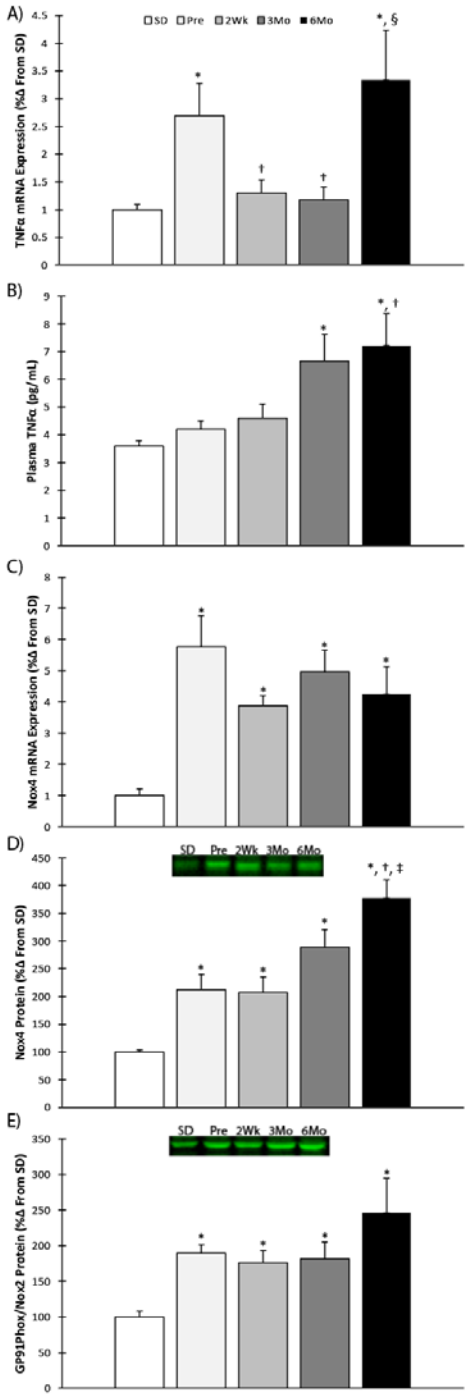

Figure 3: Downstream targets of NF-κB activation. Mean ± SEM values of **A)** TNFα mRNA, **B)** TNFα plasma levels, **C)** Nox4 mRNA, **D)** Nox4 protein, and **E)** Nox2 protein in Sprague Dawley's (SD; n=7), pre-diabetic UCD-T2DM (Pre; n=9), 2-week diabetic UCD (2Wk; n=9), 3-month diabetic UCD-T2DM (3Mo; n=13), and 6-month diabetic UCD-T2DM (6Mo; n=9) rats. * Significant difference from SD ($P< 0.05$). † Significant difference from Pre ($P< 0.05$). ‡ Significant difference from 2Wk ($P< 0.05$). § Significant difference from 3Mo ($P< 0.05$).

Manifestation of diabetes blunts Nrf2 response in the heart.

Several genes were measured under Nrf2's control to ascertain the activation of Nrf2 during the progression of T2DM. HO-1 mRNA expression decreased in pre-diabetic animals 30% compared to SD (**Figure 4A**). HO-1 mRNA expression was 45% and 40% lower than SD and 2-week diabetic rats, respectively, at 6 months (**Figure 4A**). GCLC mRNA expression increased 42% in pre-diabetic animals compared to SD rats (**Figure 4B**). GCLC transcripts were lower in 2-week, 3-month, and 6-month diabetic animals by 46%, 28%, and 60%, respectively, compared to pre-diabetic rats. GCLC transcripts were also 43% lower in 6-Month diabetic animals than SD and 3-month rats (**Figure 4B**). GCLC protein increased in pre-diabetic to 6-month diabetic animals by 66% compared to SD rats (**Figure 4C**). GCLM mRNA expression decreased 35% in 6-month diabetic animals compared to 3-month diabetic animals (**Figure 4D**). GCLM protein decreased in 3-month and 6-month diabetic animals compared to SD, pre-diabetic, and 2-week diabetic rats respectively (**Figure 4E**).

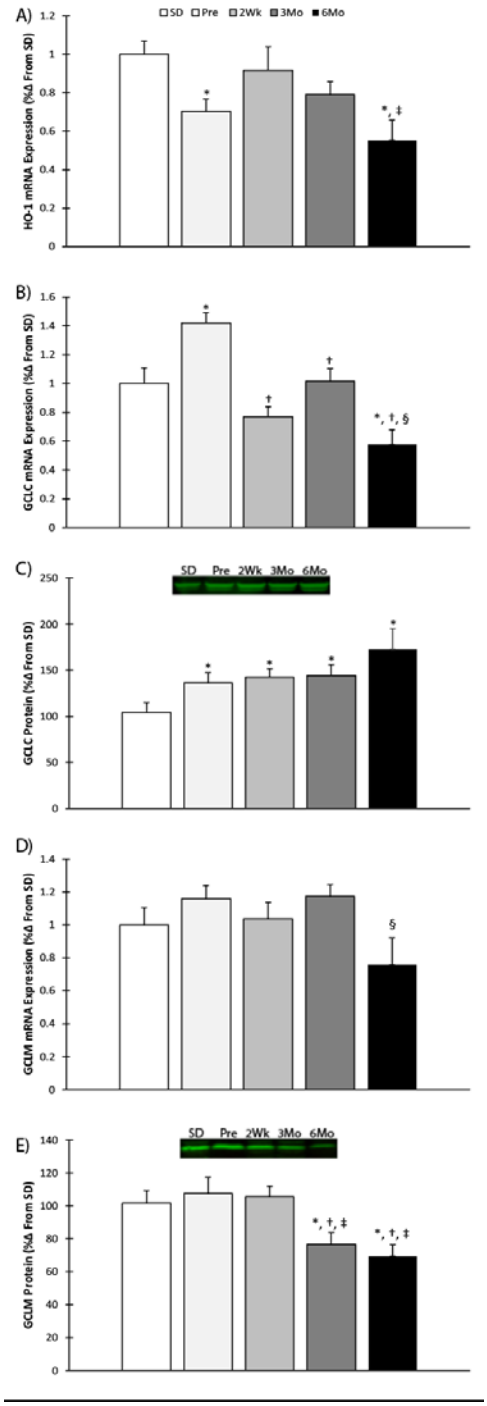

Figure 4: Downstream targets of Nrf2 activation. Mean ± SEM values of **A)** HO-1 mRNA, **B)** GCLC mRNA, **C)** GCLC protein, **D)** GCLM mRNA, and **E)** GCLM protein, in Sprague Dawley's (SD; n=7), pre-diabetic UCD-T2DM (Pre; n=9), 2-week diabetic UCD (2Wk; n=9), 3-month diabetic UCD-T2DM (3Mo; n=13), and 6-month diabetic UCD-T2DM (6Mo; n=9) rats. * Significant difference from SD ($P < 0.05$). † Significant difference from Pre ($P < 0.05$). ‡ Significant difference from 2Wk ($P < 0.05$). § Significant difference from 3Mo ($P < 0.05$).

Mitochondrial mitophagy and damage increases in the heart during the manifestation of diabetes.

Mitochondrial function and damage were measured to gain insight in the state of mitochondrial enzyes during the progression of T2DM. No changes were observed in aconitase with the progression of diabetes (**Figure 5A**). Complex I decreased 47% in the 2-week diabetic rats and remained lower in 3-month and 6-month diabetic rats compared to SD (**Figure 5B**). Complex II activity was decreased in pre-diabetic diabetic animals 50% and also remained lower at 2 weeks, 3, and 6 months diabetic compared to SD rats (**Figure 5C**). At 6 months of T2DM, complex II activity was 31% lower than the pre-diabetic rats (**Figure 5C**). Parkin translocation to the mitochondria increased 61% in Pre-diabetic animals, 74% in 3-month diabetic animals, and 62% in 6-month diabetic animals compared to SD (**Figure 5D**). Mitochondrial 4-HNE formation was 55% higher in pre-diabetic animals and remained elevated as T2DM progressed compared to SD rats (**Figure 5E**).

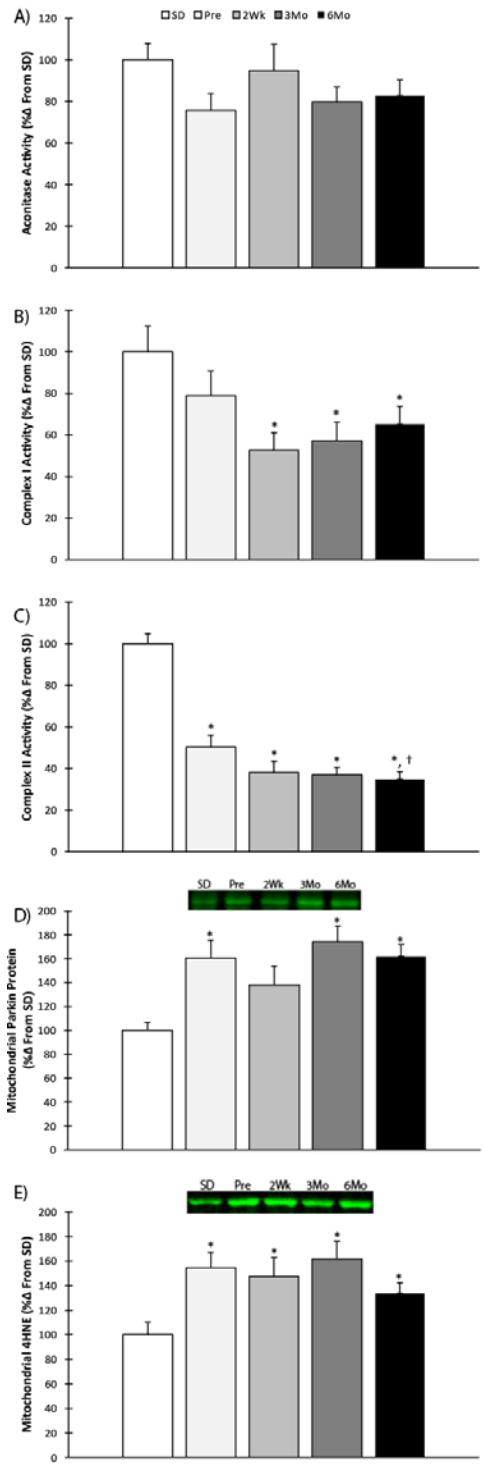

Figure 5: Mitochondrial Function during the progression of T2DM. Mean ± SEM values of **A)** aconitase activity, **B)** complex I activity, **C)** complex II activity, **D)** mitochondrial Parkin content, and **E)** mitochondrial 4HNE adducts in Sprague Dawley's (SD; n=7), pre-diabetic UCD-T2DM (Pre; n=9), 2-week diabetic UCD (2Wk; n=9), 3-month diabetic UCD-T2DM (3Mo; n=13), and

6-month diabetic UCD-T2DM (6Mo; n=9) rats. * Significant difference from SD ($P< 0.05$). † Significant difference from Pre ($P< 0.05$).

Discussion

NF-κB activation during T2DM has long been known as obesity is associated with chronic low-grade inflammation. Here we demonstrate that NF-κB translocation increases in the hearts of UCD-T2DM rats with the progression of T2DM. Furthermore, acetylation of nuclear NF-κB increases as the disease progresses further corroborating the evidence for increased inflammation. Meanwhile Nrf2, which is responsible for initiating transcription of genes involved in reducing excess oxidants, and energy replenishment decreases with the progression of T2DM. Acetylated-Nrf2 does not change or is lowered in some cases as T2DM progresses indicating a likely reduction in detoxification gene induction.

NF-κB is tethered in the cytosol by IKBα which requires phosphorylation to liberate NF-κB. Here we demonstrate that as the animals age, IKBα phosphorylation increases indicating that less NF-κB is being sequestered in the cytosol. An increase in nuclear NF-κB protein is also observed in the 2Wk and 3Mo group indicating that more NF-κB has translocated. Interestingly, there's a reduction in nuclear accumulation by the 6Mo timeframe in both nuclear and cytosolic content, but a higher presence of acetylated NF-κB is present, eliciting a more pronounced inflammatory effect. This is further suggested by corresponding increases in plasma TNFα levels and nox both of which promote inflammation and apoptosis or increases in oxidant generation. TNFα is both a target gene and inducer of NF-κB and subsequently Nox assemblage [5,11,36]. Here we demonstrate that these three entities are upregulated as diabetes progresses suggesting chronic inflammation during the manifestation of T2DM.

Nrf2 behaves in a similar manner as NF-κB and is sequestered in the cytosol by Keap1. Keap1 protein decreased as T2DM progressed, yet nuclear translocation never increased more than the control animals. Furthermore, acetylation is one of the modifications done to both NF-κB and Nrf2 to enhance their gene induction[27,28]. Here we show that acetylation of Nrf2 is unchanged, or lower in the case of the 3Mo diabetic animals. GSK3β is also a regulator of Nrf2 and is found in both the cytosol and the nucleus. In this study, we saw an increase in nuclear GSK3β as the animals became more diabetic indicating that an increase in nuclear export or degradation of Nrf2 via β-TrCP would likely occur [37,38]. Bach1 and c-Myc, both known suppressors of Nrf2 in the nucleus [39,40] were measured and decreased as diabetes progressed, however in 6Mo animals Bach1 transcripts increased dramatically indicating that if Nrf2 would enter the nucleus, its ability to bind to the EpRE may be impaired. Overall, an increase in nuclear content and increased Nrf2 mRNA at 6Mo coupled with increased nuclear GSK3β and Bach1 resulted in no change in Nrf2 genes implying that many conflicting signals are being presented suggesting that Nrf2 signaling is perturbed during T2DM.

HO-1 which has been implicated as a negative regulator of NF-κB due to its production of carbon monoxide which is considered anti-inflammatory [7,41]. HO-1, a Nrf2 target gene is downregulated in 6Mo animals, further supporting Nrf2's impaired induction. During stressful events, GSH is increased to handle an increase in oxidants. While in the 6Mo state where

NADPH oxidases are in higher concentration, we see an increase in GCLC protein but a reduction in GCLM protein. GCLC and GCLM dimerize to produce glutathione cysteine ligase. GCLC catalyzes the production of gamma-glutamylcycteine, while GCLM modulates the activity of GCLC [42] and therefore the rate of GSH, for which GCLC activity is rate limiting. Thus, downregulation of GCLM during the progression of diabetes suggest that the cell's ability to handle increases in oxidant generation may be impaired.

Mitochondrial function was assessed to track mitochondrial dysfunction as diabetes progressed. No changes were observed in aconitase activity, which is surprising because aconitase is easily oxidized and has been shown to be impaired during mitochondrial dysfunction [35,43–45]. Activity of both complex I and complex II decreased as the animals became more diabetic suggesting an impairment in mitochondrial electron transport in T2DM. Furthermore, mitochondrial parkin protein increases as a function of diabetes progression. Parkin has been reported to accumulate within the mitochondria that have accrued damage initiating mitophagy [20,21]. Mitochondrial 4-hydroxynonenal (4-HNE) adducts increased in the pre-diabetic animals and remained elevated as the disease progressed. Previously we've demonstrated increases in mitochondrial 4-HNE in Otsuka Long Evans Tokushima Fatty rats during insulin resistance [34]. The increase of mitochondrial parkin, 4HNE accumulation, and the dampened activity of complex I and II primarily during the insulin resistance phase and during the progression of diabetes suggest that UCD-T2DM rats exhibit mitochondrial dysfunction early in their disease progression.

Together these data illustrate that the inflammatory response propagated by NF-κB increases as T2DM progresses while the antioxidant response by Nrf2 is blunted. Furthermore, acetylation of NF-κB increases as the animals become more diabetic while Nrf2 acetylation is unchanged with corresponding increases in Nox proteins and TNFα and reductions in Nrf2 related antioxidant gene expression. This proves to be problematic because diabetic hearts are at increased risk of oxidative and nitrosative damage especially under the periods of increased glucose loads.

References

[1] M. Laakso, Cardiovascular Disease in Type 2 Diabetes From Population to Man to Mechanisms, Diabetes Care. 33 (2010) 442–449. doi:10.2337/dc09-0749.

[2] G.V. Velmurugan, N.R. Sundaresan, M.P. Gupta, C. White, Defective Nrf2-dependent redox signaling contributes to microvascular dysfunction in type 2 diabetes, Cardiovasc. Res. 100 (2013) 143–150. doi:10.1093/cvr/cvt125.

[3] X. Cheng, R.C.M. Siow, G.E. Mann, Impaired redox signaling and antioxidant gene expression in endothelial cells in diabetes: a role for mitochondria and the nuclear factor-E2-related factor 2-Kelch-like ECH-associated protein 1 defense pathway, Antioxid. Redox Signal. 14 (2011) 469–487. doi:10.1089/ars.2010.3283.

[4] G.S. Hotamisligil, N.S. Shargill, B.M. Spiegelman, Adipose expression of tumor necrosis factor-alpha: direct role in obesity-linked insulin resistance, Science. 259 (1993) 87–91.

[5] M.S. Hayden, S. Ghosh, NF-κB, the first quarter-century: remarkable progress and outstanding questions, Genes Dev. 26 (2012) 203–234. doi:10.1101/gad.183434.111.

[6] M.C. Jaramillo, D.D. Zhang, The emerging role of the Nrf2-Keap1 signaling pathway in cancer, Genes Dev. 27 (2013) 2179–2191. doi:10.1101/gad.225680.113.

[7] J.D. Wardyn, A.H. Ponsford, C.M. Sanderson, Dissecting molecular cross-talk between Nrf2 and NF-κB response pathways, Biochem. Soc. Trans. 43 (2015) 621–626. doi:10.1042/BST20150014.

[8] M.P. Soares, M.P. Seldon, I.P. Gregoire, T. Vassilevskaia, P.O. Berberat, J. Yu, T.-Y. Tsui, F.H. Bach, Heme Oxygenase-1 Modulates the Expression of Adhesion Molecules Associated with Endothelial Cell Activation, J. Immunol. 172 (2004) 3553–3563. doi:10.4049/jimmunol.172.6.3553.

[9] K. Brown, S. Gerstberger, L. Carlson, G. Franzoso, U. Siebenlist, Control of I kappa B-alpha proteolysis by site-specific, signal-induced phosphorylation, Science. 267 (1995) 1485–1488.

[10] S.-A. Manea, A. Constantin, G. Manda, S. Sasson, A. Manea, Regulation of Nox enzymes expression in vascular pathophysiology: Focusing on transcription factors and epigenetic mechanisms, Redox Biol. 5 (2015) 358–366. doi:10.1016/j.redox.2015.06.012.

[11] A. Manea, L.I. Tanase, M. Raicu, M. Simionescu, Transcriptional regulation of NADPH oxidase isoforms, Nox1 and Nox4, by nuclear factor-κB in human aortic smooth muscle cells, Biochem. Biophys. Res. Commun. 396 (2010) 901–907. doi:10.1016/j.bbrc.2010.05.019.

[12] J. Kuroda, T. Ago, S. Matsushima, P. Zhai, M.D. Schneider, J. Sadoshima, NADPH oxidase 4 (Nox4) is a major source of oxidative stress in the failing heart, Proc. Natl. Acad. Sci. 107 (2010) 15565–15570. doi:10.1073/pnas.1002178107.

[13] K. Itoh, P. Ye, T. Matsumiya, K. Tanji, T. Ozaki, Emerging functional cross-talk between the Keap1-Nrf2 system and mitochondria, J. Clin. Biochem. Nutr. 56 (2015) 91–97. doi:10.3164/jcbn.14-134.

[14] H. Sasaki, H. Sato, K. Kuriyama-Matsumura, K. Sato, K. Maebara, H. Wang, M. Tamba, K. Itoh, M. Yamamoto, S. Bannai, Electrophile response element-mediated induction of the cystine/glutamate exchange transporter gene expression, J. Biol. Chem. 277 (2002) 44765–44771. doi:10.1074/jbc.M208704200.

[15] M.B. Kannan, V. Solovieva, V. Blank, The small MAF transcription factors MAFF, MAFG and MAFK: current knowledge and perspectives, Biochim. Biophys. Acta. 1823 (2012) 1841–1846. doi:10.1016/j.bbamcr.2012.06.012.

[16] H. Van Remmen, A. Richardson, Oxidative damage to mitochondria and aging, Exp. Gerontol. 36 (2001) 957–968.

[17] P. Newsholme, E.P. Haber, S.M. Hirabara, E.L.O. Rebelato, J. Procopio, D. Morgan, H.C. Oliveira-Emilio, A.R. Carpinelli, R. Curi, Diabetes associated cell stress and dysfunction: role of mitochondrial and non-mitochondrial ROS production and activity, J. Physiol. 583 (2007) 9–24. doi:10.1113/jphysiol.2007.135871.

[18] S.S. Korshunov, V.P. Skulachev, A.A. Starkov, High protonic potential actuates a mechanism of production of reactive oxygen species in mitochondria, FEBS Lett. 416 (1997) 15–18.

[19] B.B. Lowell, G.I. Shulman, Mitochondrial dysfunction and type 2 diabetes, Science. 307 (2005) 384–387. doi:10.1126/science.1104343.

[20] A.M. Pickrell, R.J. Youle, The roles of PINK1, parkin, and mitochondrial fidelity in Parkinson's disease, Neuron. 85 (2015) 257–273. doi:10.1016/j.neuron.2014.12.007.

[21] X. Zheng, T. Hunter, Parkin mitochondrial translocation is achieved through a novel catalytic activity coupled mechanism, Cell Res. 23 (2013) 886–897. doi:10.1038/cr.2013.66.

[22] W. Li, T.O. Khor, C. Xu, G. Shen, W.-S. Jeong, S. Yu, A.-N. Kong, Activation of Nrf2-antioxidant signaling attenuates NF-κB-inflammatory response and elicits apoptosis, Biochem. Pharmacol. 76 (2008) 1485–1489. doi:10.1016/j.bcp.2008.07.017.

[23] H. Chen, Y. Fang, W. Li, R.C. Orlando, N. Shaheen, X.L. Chen, NFkB and Nrf2 in esophageal epithelial barrier function, Tissue Barriers. 1 (2013) e27463. doi:10.4161/tisb.27463.

[24] N. Wakabayashi, S.L. Slocum, J.J. Skoko, S. Shin, T.W. Kensler, When NRF2 talks, who's listening?, Antioxid. Redox Signal. 13 (2010) 1649–1663. doi:10.1089/ars.2010.3216.

[25] G.-H. Liu, J. Qu, X. Shen, NF-kappaB/p65 antagonizes Nrf2-ARE pathway by depriving CBP from Nrf2 and facilitating recruitment of HDAC3 to MafK, Biochim. Biophys. Acta. 1783 (2008) 713–727. doi:10.1016/j.bbamcr.2008.01.002.

[26] H. Zhang, L. Zhou, J. Yuen, N. Birkner, V. Leppert, P.A. O'Day, H.J. Forman, Delayed Nrf2-regulated antioxidant gene induction in response to silica nanoparticles, Free Radic. Biol. Med. 108 (2017) 311–319. doi:10.1016/j.freeradbiomed.2017.04.002.

[27] A. Lanzillotta, I. Sarnico, R. Ingrassia, F. Boroni, C. Branca, M. Benarese, G. Faraco, F. Blasi, A. Chiarugi, P. Spano, M. Pizzi, The acetylation of RelA in Lys310 dictates the NF-κB-dependent response in post-ischemic injury, Cell Death Dis. 1 (2010) e96. doi:10.1038/cddis.2010.76.

[28] Z. Sun, Y.E. Chin, D.D. Zhang, Acetylation of Nrf2 by p300/CBP Augments Promoter-Specific DNA Binding of Nrf2 during the Antioxidant Response, Mol. Cell. Biol. 29 (2009) 2658–2672. doi:10.1128/MCB.01639-08.

[29] Y. Kawai, L. Garduño, M. Theodore, J. Yang, I.J. Arinze, Acetylation-Deacetylation of the Transcription Factor Nrf2 (Nuclear Factor Erythroid 2-related Factor 2) Regulates Its Transcriptional Activity and Nucleocytoplasmic Localization, J. Biol. Chem. 286 (2011) 7629–7640. doi:10.1074/jbc.M110.208173.

[30] B.P. Cummings, E.K. Digitale, K.L. Stanhope, J.L. Graham, D.G. Baskin, B.J. Reed, I.R. Sweet, S.C. Griffen, P.J. Havel, Development and characterization of a novel rat model of type 2 diabetes mellitus: the UC Davis type 2 diabetes mellitus UCD-T2DM rat, Am. J. Physiol. Regul. Integr. Comp. Physiol. 295 (2008) R1782-1793. doi:10.1152/ajpregu.90635.2008.

[31] B.D. Piccolo, J.L. Graham, K.L. Stanhope, O. Fiehn, P.J. Havel, S.H. Adams, Plasma amino acid and metabolite signatures tracking diabetes progression in the UCD-T2DM rat model, Am. J. Physiol. Endocrinol. Metab. 310 (2016) E958-969. doi:10.1152/ajpendo.00052.2016.

[32] I. Dimauro, T. Pearson, D. Caporossi, M.J. Jackson, A simple protocol for the subcellular fractionation of skeletal muscle cells and tissue, BMC Res. Notes. 5 (2012) 513. doi:10.1186/1756-0500-5-513.

[33] M. Thorwald, R. Rodriguez, A. Lee, B. Martinez, J. Peti-Peterdi, D. Nakano, A. Nishiyama, R.M. Ortiz, Angiotensin receptor blockade improves cardiac mitochondrial activity in response to an acute glucose load in obese insulin resistant rats, Redox Biol. 14 (2018) 371–378. doi:10.1016/j.redox.2017.10.005.

[34] J.S. Thacker, D.H. Yeung, W.R. Staines, J.G. Mielke, Total protein or high-abundance protein: Which offers the best loading control for Western blotting?, Anal. Biochem. 496 (2016) 76–78. doi:10.1016/j.ab.2015.11.022.

[35] J.P. Vázquez-Medina, I. Popovich, M.A. Thorwald, J.A. Viscarra, R. Rodriguez, J.G. Sonanez-Organis, L. Lam, J. Peti-Peterdi, D. Nakano, A. Nishiyama, R.M. Ortiz, Angiotensin receptor-mediated oxidative stress is associated with impaired cardiac redox signaling and mitochondrial function in insulin-resistant rats, Am. J. Physiol. - Heart Circ. Physiol. 305 (2013) H599–H607. doi:10.1152/ajpheart.00101.2013.

[36] J. Dong, E. Jimi, C. Zeiss, M.S. Hayden, S. Ghosh, Constitutively active NF-kappaB triggers systemic TNFalpha-dependent inflammation and localized TNFalpha-independent inflammatory disease, Genes Dev. 24 (2010) 1709–1717. doi:10.1101/gad.1958410.

[37] P. Rada, A.I. Rojo, S. Chowdhry, M. McMahon, J.D. Hayes, A. Cuadrado, SCF/β-TrCP Promotes Glycogen Synthase Kinase 3-Dependent Degradation of the Nrf2 Transcription Factor in a Keap1-Independent Manner, Mol. Cell. Biol. 31 (2011) 1121–1133. doi:10.1128/MCB.01204-10.

[38] S. Chowdhry, Y. Zhang, M. McMahon, C. Sutherland, A. Cuadrado, J.D. Hayes, Nrf2 is controlled by two distinct β-TrCP recognition motifs in its Neh6 domain, one of which can be modulated by GSK-3 activity, Oncogene. 32 (2013) 3765–3781. doi:10.1038/onc.2012.388.

[39] S. Levy, H.J. Forman, C-Myc is a Nrf2-interacting protein that negatively regulates phase II genes through their electrophile responsive elements, IUBMB Life. 62 (2010) 237–246. doi:10.1002/iub.314.

[40] H. Zhang, H. Liu, K.J.A. Davies, C. Sioutas, C.E. Finch, T.E. Morgan, H.J. Forman, Nrf2-regulated phase II enzymes are induced by chronic ambient nanoparticle exposure in young mice with age-related impairments, Free Radic. Biol. Med. 52 (2012) 2038–2046. doi:10.1016/j.freeradbiomed.2012.02.042.

[41] M.-H. Li, J.-H. Jang, H.-K. Na, Y.-N. Cha, Y.-J. Surh, Carbon Monoxide Produced by Heme Oxygenase-1 in Response to Nitrosative Stress Induces Expression of Glutamate-Cysteine Ligase in PC12 Cells via Activation of Phosphatidylinositol 3-Kinase and Nrf2 Signaling, J. Biol. Chem. 282 (2007) 28577–28586. doi:10.1074/jbc.M701916200.

[42] C.C. Franklin, D.S. Backos, I. Mohar, C.C. White, H.J. Forman, T.J. Kavanagh, Structure, function, and post-translational regulation of the catalytic and modifier subunits of glutamate cysteine ligase, Mol. Aspects Med. 30 (2009) 86–98. doi:10.1016/j.mam.2008.08.009.

[43] P.R. Gardner, I. Fridovich, Superoxide sensitivity of the Escherichia coli aconitase, J. Biol. Chem. 266 (1991) 19328–19333.

[44] M.C. Kennedy, M.H. Emptage, J.L. Dreyer, H. Beinert, The role of iron in the activation-inactivation of aconitase., J. Biol. Chem. 258 (1983) 11098–11105.

[45] P. Montez, J.P. Vázquez-Medina, R. Rodríguez, M.A. Thorwald, J.A. Viscarra, L. Lam, J. Peti-Peterdi, D. Nakano, A. Nishiyama, R.M. Ortiz, Angiotensin Receptor Blockade Recovers Hepatic UCP2 Expression and Aconitase and SDH Activities and Ameliorates Hepatic Oxidative Damage in Insulin Resistant Rats, Endocrinology. 153 (2012) 5746–5759. doi:10.1210/en.2012-1390.

Conclusions and Future Directions

The heart in diabetic individuals undergoes constant stress during the progression and development of type II diabetes from the chronic elevation in AT1 activation. Higher systolic blood pressure has been termed the silent killer and causes cellular damage slowly that accumulates over a prolonged period of time. However, during type II diabetes, this stress is amplified when high levels are glucose are ingested generating oxidants which render enzymes inactive, disrupt cellular structures through chemical modification, or initiate inflammatory cascades to perpetuate their formation. The studies present here examined the consequences on mitochondrial function and Nrf2 activation during the progression and manifestation of type II diabetes.

Previous studies have demonstrated the effectiveness of AT1 receptor antagonism through angiotensin receptor blockers (ARB) during the development of insulin resistance in a wide variety of tissues, however these studies were limited to static changes. Our data shows that ARB treatment during a glucose challenge in insulin resistant and type II diabetes improves mitochondrial function and Nrf2-related gene expression or protein while untreated hearts exhibited lower mitochondrial function and less viable antioxidant defense. These studies illustrate that the normal physiological responses to counter increased oxidant production are perturbed during acute glucose challenges and that lowering systolic blood pressure improves the antioxidant response primarily in insulin resistant hearts. While we have demonstrated that ARB treatment is beneficial to both insulin resistant and type II diabetic hearts, the reason why still remains. ARB treatment lowers systolic blood pressure and ventricular mass. Some argue that the increase in systolic blood pressure contributes to the mitochondrial dysfunction while others claim that the lowering of AT1 mediated NADPH oxidase formation is the cause.

Chronic low-grade inflammation has long been understood as a component of the progression of type II diabetes. NF-κB a transcription factor responsible for initiating inflammatory cascades has also been known to have an opposing role on Nrf2. These studies demonstrate that as animals become more diabetic the inflammatory response increases while the antioxidant response remains unchanged or is blunted. While its thought that NF-κB and Nrf2 compete for the same molecular machinery for initiation of their target genes, this still remains to be elucidated. Since AT1 has been reported to increase inflammatory cascades as well during diabetes through a TNFα mediated process indicating that the benefits of ARB treatment may extend farther than a reduction in systolic blood pressure, an increase in mitochondrial function, and that this blockade may be the reason why Nrf2 related genes have an increased response in ARB treated hearts.

While, the use of animals for the glucose challenges was novel, these studies could be supported by the use of cell lines to elucidate the mechanisms involved in mitochondrial dysfunction and the interaction between Nrf2 and NF-κB in the nucleus to ascertain the mechanisms behind their complex interaction. Doing so could prove to be beneficial for individuals who currently have diabetes or are in the early stages of its development since the failing heart is the leading cause of mortality in diabetes patients.